Ste20-like kinases and regulator proteins in the cytoskeleton of *Dictyostelium discoideum*

Dissertation
der Fakultät für Biologie der
Ludwig-Maximilians-Universität München
zur Erlangung des akademischen Grades
„Doktor der Naturwissenschaften“
(Dr. rer. nat.)

vorgelegt von

Christoph Gallinger

aus München

München, 2014

Eidesstattliche Erklärung

Ich versichere hiermit an Eides statt, dass die vorgelegte Dissertation von mir selbständig und ohne unerlaubte Hilfe angefertigt ist.

München, den 23. Juni 2014
Christoph Gallinger

Ort der Durchführung

Der experimentelle Teil dieser Dissertation wurde von Januar 2010 bis Juni 2014 im Labor von Prof. Dr. Michael Schleicher am Institut für Anatomie und Zellbiologie der Ludwig-Maximilians-Universität München ausgeführt.

Place of realisation

The experimental part of this work was carried out from January 2010 to June 2014 in the laboratory of Prof. Dr. Michael Schleicher at the institute for Anatomy and Cell Biology, Ludwig-Maximilians-University, Munich

1. Gutachter: Prof. Dr. Michael Schleicher

2. Gutachter: Prof. Dr. Barbara Conradt

Datum der Einreichung: Mittwoch, den 16.07.2014
Datum der mündlichen Prüfung: Montag, den 01.12.2014

Publications

Journal

In preparation. **Gallinger C**, Köhler S, Schleicher M, Rohlfs M (2014) Mo25 in *Dictyostelium discoideum* interacts with the Ste20-like kinase SvkA and controls cell division, development and slug motility

2014 Glöckner G, Hülsmann N, Schleicher M, Noegel AA, Eichinger L, **Gallinger C**, Pawlowski J, Sierra R, Euteneuer U, Pillet L, Moustafa A, Platzer M, Groth M, Szafranski K, Schliwa M (2014) The genome of the foraminiferan *Reticulomyxa filosa Current Biology* 24: 11–18

2013 Müller R, Herr C, Sukumaran SK, Omosigho NN, Plomann M, Riyahi TY, Stumpf M, Swaminathan K, Tsangarides M, Yiannakou K, Blau-Wasser R, **Gallinger C**, Schleicher M, Kolanus W, Noegel AA (2013) The cytohesin paralog Sec7 of *Dictyostelium discoideum* is required for phagocytosis and cell motility *Cell Communication and Signaling* 11: 54-71

Talk

07/2012 Annual International Dictyostelium Conference, 2012, Madrid, Spain
Title: The role of Mo25 for cytokinesis in *Dictyostelium discoideum*.

Poster Presentations

03/2014 Sanftenberg L, Gallinger J, **Gallinger C**, Joseph JM, Rieger D,Henze F, Müller-Taubenberger A, Schleicher M, Actin variants in *Dictyostelium* amoebae, Annual Meeting of the German Society for Cell Biology, 2014, Regensburg, Eur. J. Cell Biol. 93, A85

12/2013 Sanftenberg L, Gallinger J, **Gallinger C**, Joseph JM, Rieger D, Henze F, Müller-Taubenberger A, Schleicher M, Actin Variants in *Dictyostelium disoideum*, ASCB 53rd international meeting, 2013, New Orleans, LA, U.S.A. Mol Biol Cell 24, 164, (321)

12/2012 **Gallinger C**, Köhler S, Wachowius M, Rohlfs M, Schleicher M, The role of Mo25 for cytokinesis in *Dictyostelium discoideum*, ASCB 52nd international meeting, 2012, San Francisco, CA, U.S.A., Mol Biol Cell 23, 157, (260)

03/2012 **Gallinger C**, Köhler S, Wachowius M, Rohlfs M, Schleicher M, The role of Mo25 for cytokinesis in *Dictyostelium discoideum*, Annual Meeting of the German Society for Cell Biology, 2012, Dresden, Germany, Eur. J. Cell Biol. 91, S10-12

04/2011 **Gallinger C**, Rohlfs M, Köhler S, Batsios P, Schleicher M, Ste20-like kinases in *Dictyostelium discoideum*, Annual Meeting of the German Society for Cell Biology, 2011, Bonn, Germany, Eur. J. Cell Biol. 90, PS-02

Table of content

Figures

Tables

Abbreviations

General:

3’/5’	Three prime/five prime
°C	Degree celsius
µl	Microliters
µm	Micrometer
aa	Amino acid
ADP	Adenosine-di-phosphate
Amp	Ampiciline
ATP	Adenosine-tri-phosphate
BLAST	Basic local alignment search tool
BSA	Bovine serum albumin
C-terminal	Carboxy terminal
cAMP	Cyclic adenosine monophosphate
cDNA	Complementary deoxyribonucleic acid
DAPI	4',6-diamidino-2-phenylindole
dd	Double distilled
DDB	*Dictyostelium discoideum* base (Dictybase)
DNA	Deoxyribonucleic acid
DTT	Dithiothreitol
EDTA	Ethylenediaminetetraacetic acid
EGTA	Ethylene glycol tetraacetic acid
EST	Expressed sequence tag
G418	Genetecine
g	Gram
GFP	Green flourescent protein
GST	Glutathione S-transferase
GTP	Guanosine triphosphate
h	Hour

HEPES	4-(2-Hydroxyethyl)-1-piperazineethanesulfonic acid
IPTG	Isopropyl beta-D-1-thiogalactopyranoside
kDa	Kilo Dalton
LB	Lysogeny broth
LSM	Laser scanning microscope
LysB	Lysis buffer
M	Molar concentration
mM	Millimolar concentration
m	Molarity
M-phase	Mitosis-phase
MALDI-TOF	Matrix-assisted laser desorption/ionization-time of flight
mg	Milligram
min	Minute
ml	Milliliter
mm	Millimeter
mRNA	Messenger ribonucleic acid
MUSCLE	Multiple Sequence Comparison by Log- Expectation
N-terminal	amino-terminal
NCP	Nucleus/chromatin preparation
ng	Nanogram
nm	Nanometer
OD	Optical density
PBG	Phosphate buffered fish gelatine
PBS	Phosphate buffered saline
PCR	Polymerase chain reaction
PDB	Protein database
pH	Power of hydrogen
PMSF	Phenylmethylsulfonyl fluoride
RNA	Ribonucleic acid
Rpm	Revolutions per minute
S-Phase	Synthesis-phase

SDS-PAGE	Sodium dodecyl sulfate-polyacrylamide gel electrophoresis
TEDAB	Triethylenediamine buffer
TO-PRO	Quinolinium, 4-[3-(3-methyl-2(3H)-benzothiazolylidene)-1-propenyl]-1-[3-(trimethylammonio)propyl]-, diiodide/ 157199-63-8
TRIS	Tris(hydroxymethyl)aminomethane

Organisms:

Ce	*Caenorhabditis elegans*
Dd	*Dictyostelium discoideum*
Dm	*Drosophila melanogaster*
Hs	*Homo sapiens*
Nc	*Neurospora crassa*
Rf	*Reticulomyxa filosa*
Sc	*Saccharomyces cerevisiae*
Sp	*Schizosaccharomyces pombe*

Proteins:

Abi2	Similar to Abelson tyrosine kinase Interacting protein 2
Abp1	Actin binding protein 1
Ace2p	Activator of CUP1 expression 2p
AMPK	5‘ Adenosine mono phosphate-activated protein kinase
CAB39	Calcium binding protein 39
Cbk1	Cell wall biosynthesis kinase 1
CBS	Cystathionine beta synthase
CDC42	Cell division control protein 42 homolog
DstC	*Dictyostelium* serine threonine kinase C
Fray 1/2	Frayed kinase 1/2
FRIP	Fray interacting protein
GCK	Germinal centre kinase
GTPase	Guanosine triphosphate hydrolase
Hippo	“Hippopotamus”-like phenotype

Hym1	Hypha-like metulae 1
HymA	Hypha-like metulae A
JNK	c-Jun N-terminal kinases
Kic1p	Kinase that interacts with Cdc31p
KrsA/B	Kinase responsive to stress
Lats1	Large tumour suppressor 1
LKB1	Liver kinase B1
MARK3	Microtubule affinity regulating kinase 3
MAPK	Mitogen-activated protein kinases
Mo25	Morula protein 25
Mst1/2/3/4	Mammalian Ste20-like kinase 1/2/3/4
mTor	Mammalian target of rapamycin
Nak1	PAK-related kinase Nak1
Ndr	Nuclear dbf2-related kinase
Orb6	Serine/threonine protein kinase Orb6
OSR1	Oxidative stress response kinase 1
p21	p21 / WAF1 / CIP1, cyclin-dependent kinase inhibitor 1
p38	p38 mitogen-activated protein kinases
p53	Tumour protein p53
PAK	p21 activated kinase
Par1	Partitioning defective 1
Pmo25	Mo25 family protein Pmo25
Ppk11	PAK-related kinase Ppk11
Rac	Similar to RAs-related-C3 botulinum toxin substrate
Raf-1	Rapidly accelerated fibrosarcoma 1
Salvador	Salvador
Sok1	Suppressor of kinase 1
SPAK	STE20/SPS1-related proline-alanine-rich protein kinase
Ste7/11/20	Sterile 7/11/20
STRAD	Ste20-related adaptor protein
SvkA	Severin kinase A

Tao2	Thousand-and-one amino acids 2
TSC1/2	Tuberous sclerosis 1/2
Warts	Warts
Wnt	Wingless-related integration site
Ysk1	Yeast Sps1/Ste20-related Kinase 1

1 Summary

The cytoskeleton in most eukaryotes consists of actin filaments, intermediate filaments, microtubules and specific associated proteins. It determines the shape and the polarity of a cell and is inevitable for the coordination of cell movement. The regulation of this complex structure requires a highly organised and specialised signalling network. Ste20-like kinases and the regulator protein Mo25 (Morula protein 25) are part of this signalling network. The main objective of this work was the functional characterisation of the regulator protein Mo25 and the Ste20-like kinases Fray1, Fray2 (Frayed kinase 1/2) and DstC (*Dictyostelium* serine threonine kinase C) in the amoeba *Dictyostelium discoideum* (*D. discoideum*). An additional project was to map and characterise the actin and actin related genes in the genome of the fresh water foraminifer *Reticulomyxa filosa* (*R. filosa*).

Mo25 is a highly conserved 40 kDa scaffolding protein with a 60% identity from amoeba to man. The disruption of the *mo25* gene in *D. discoideum* results in very large, multinucleated cells which are unable to complete cytokinesis. Growth as well as development is severely delayed in the Mo25-minus strain. Furthermore, in phototaxis assays performed with multicellular aggregates (slugs), the Mo25-minus slugs were unable to migrate towards the light source. These findings imply that Mo25 plays an important role in cytokinesis, growth and cell polarity. We could link the Ste 20-like kinase SvkA (severin kinase), a homolog of the human Mst3, Mst4 (Mammalian Ste20-like kinase 3/4) and Ysk1/Sok1 (Yeast Sps1/Ste20-related kinase 1, Suppressor of Kinase 1) kinases to Mo25 as a binding partner. To further elucidate the interaction of Mo25 with SvkA as well as their role in cytokinesis or polarity signalling, we generated a series of GFP–Mo25 rescue constructs with distinct point mutations in protein-protein interaction surfaces and transformed these into the Mo25-minus background.

The kinase domains of the Ste20-like kinases, Fray1 and Fray2 in *D. discoideum* are highly homologous to the catalytic domains of OSR1 (Oxidative stress response kinase 1) and SPAK (Ste20/SPS1-related proline-alanine-rich protein kinase) in humans and Frayed in fruit fly. Here, we generated the knockout clones Fray1-minus, Fray2-minus, and the double knockout Fray2Fray1-minus in *D. discoideum*. In developmental studies, Fray2-minus did not show an altered phenotype, whereas Fray1-minus and Fray2Fray1-minus

developed slightly slower into fruiting bodies. When grown in shaking culture, Fray1-minus and Fray2Fray1-minus showed a reduced growth rate compared to Fray2-minus and the wild type. In addition, by using a GFP-Trap resin we identified a binding partner of Fray1, a yet unknown protein that we named FRIP (Fray Interacting Protein). FRIP mainly consists of a CBS (Cystathionine beta synthase) domain pair and is 30% identical to the gamma subunit of the AMPK (5‘ adenosine mono phosphate-activated protein kinase) complex in *D. discoideum*. The Ste20-like kinase DstC has been described to be a regulator of the actin driven process of phagocytosis. The catalytic domain of DstC is most similar to the mammalian kinase Mst2 (Mammalian Ste20-like kinase 2) and Hippo (“Hippopotamus”-like phenotype) of *D. melanogaster*. We could map the sorting signal that localises DstC to phagocytic cups and acidic vesicles to about 90 amino acids. Here we present an array of distinct point mutations for the identification of the exact localisation signal.

R. filosa is a fresh water protist which belongs to the the group of Foraminifera within the Rhizaria. The *R. filosa* genome is the first foraminiferal and only the second rhizarian genome to be deciphered. In this bioinformatics project, we could identify, map and characterise four new actin genes in addition to the already known actin and about 40 genes that code for potential actin related proteins of seven different protein classes.

2 Zusammenfassung

Das eukaryotische Zytoskelett besteht in der Regel aus Aktinfilamenten, Intermediärfilamenten, Mikrotubuli und spezifischen assoziierten Bindeproteinen. Es bestimmt Form und Polarität einer Zelle und ist damit maßgeblich an der Koordination der Zellbewegung beteiligt. Die Regulation dieser komplexen Vorgänge erfordert ein hoch spezialisiertes und organisiertes Signalsystem. Ein Teil dieses Signalsystems sind die Ste20-ähnlichen Kinasen und Mo25 (Morula protein 25), ein struktureller Organisator von Kinasen im Zytoskelett. Das Hauptziel dieser Arbeit war die funktionelle Charakterisierung des Proteins Mo25 und der Ste20-ähnlichen Kinasen Fray1, Fray2 (Frayed kinase 1/2) und DstC (*Dictyostelium* serine threonine kinase C) der sozialen Amöbe *Dictyostelium discoideum* (*D. discoideum*). Ein weiteres Projekt war die Kartierung und Charakterisierung der Aktine und Aktin verwandten Gene im Genom des Süßwasser Foraminiferen *Reticulomyxa filosa* (*R. filosa*).

Das hoch konservierte, 40 kDa große Regulatorprotein Mo25 der Amöbe *D. discoideum* ist zu 60% identisch zu seinem Homolog im Menschen. Durch die Disruption des *mo25*-Gens in *D. discoideum* bilden sich sehr große, mehrkernige Zellen, welche sich nicht mehr normal teilen können. Das Wachstum, wie auch die Vollendung des Entwicklungszyklus sind in der Mo25-minus Mutante stark eingeschränkt. Ferner können sich die mehrzelligen Aggregate, die sogenannten „slugs“, in Phototaxis Experimenten nicht in Richtung einer Lichtquelle bewegen. Diese Ergebnisse weisen darauf hin, dass Mo25 eine wichtige Rolle bei Zellteilung, Wachstum und Zellpolarität spielt. Wir konnten die Ste20-ähnliche Kinase SvkA (Severin kinase), ein Homolog der menschlichen Kinasen Mst3, Mst4 (Mammalian Ste20-like kinase 3/4) und Ysk1/Sok1 (Yeast Sps1/Ste20-related kinase 1, Suppressor of Kinase 1), als einen Bindepartner von Mo25 verifizieren. Um die Wechselwirkung von Mo25 mit SvkA näher zu untersuchen, erzeugten wir eine Reihe von GFP-Mo25 Konstrukten mit verschiedenen Punktmutationen in den Protein-Protein Interaktionsflächen und brachten diese in die Mo25-minus Zelllinie ein. Daraufhin untersuchten wir die verschieden Auswirkungen der Punktmutationskonstrukte auf Zellteilung und Zellpolarität.

Die Kinase-Domänen der Ste20-like-Kinasen, Fray1 und Fray2 der Amöbe *D. discoideum* weisen eine hohe Ähnlichkeit zu den katalytischen Domänen von OSR1 (Oxidative stress response kinase 1) und SPAK (Ste20/SPS1-related proline-alanine-rich protein kinase) im Menschen und zu Frayed in der Fruchtfliege *Drosophila melanogaster* (*D. melanogaster*) auf. Die Disruption der Gene *fray1*, *fray2* einzeln und *fray2* und *fray1* zusammen ergab keine Veränderung im Phänotyp von *D. discoideum*. Auch der Entwicklungszyklus verlief im Vergleich zum Wildtyp nahezu unverändert. Lediglich beim Wachstum in Schüttelkultur zeigten die Fray1-minus und Fray2Fray1-minus Mutanten eine leicht verringerte Wachstumsrate im Vergleich zum Fray2-minus Stamm und dem Wildtyp. Zusätzlich konnte ein bisher unbekanntes Protein als Bindungspartner von Fray1 identifiziert werden, welches wir FRIP (Fray interacting protein) genannt haben. FRIP besteht hauptsächlich aus zwei CBS (Cystathionine beta synthase)-Domänen Paaren und ist zu 30% identisch zu der gamma-Untereinheit des AMPK (5‘ adenosine mono phosphate-activated protein kinase)-Komplexes in *D. discoideum*. Die Ste20-ähnliche Kinase DstC wurde als Regulatorprotein des Aktin-gesteuerten Prozesses der Phagozytose beschrieben. Die katalytische Domäne von DstC ist der homologen Domäne der Säugerkinase Mst2 (Mammalian Ste20-like kinase 2) und der Kinase Hippo (“Hippopotamus”-like phenotype) aus der Fruchtfliege sehr ähnlich. Wir konnten das Signal, welches DstC an den Zellmund und an angesäuerte Vesikel in *D. discoideum* lokalisiert, auf etwa 90 Aminosäuren eingrenzen. Hier präsentieren wir eine Zusammenstellung verschiedener Punktmutationen zur Veränderung der Aminosäuren, welche potentiell für die subzelluläre Lokalisierung des Proteins wichtig sind.

R. filosa ist ein einzelliger Frischwasser Protist aus der Gruppe der Foraminiferen innerhalb der Rhizarien. Das *R. filosa* Genom ist das erste vollständig sequenzierte Genom der Foraminiferengruppe und erst das zweite der Rhizarien. In diesem bioinformatischen Projekt war es die Aufgabe, Aktin und Aktin-ähnliche Gene im Genom von *R. filosa* zu finden und zu kartieren.

3 Introduction

3.1 Proteins

Proteins are an object of investigation since the 18th century and were described in various essays by several early chemists amongst them De Frumento Beccari, Henri Braconnot and Albrecht Kossel (Beccari, 1745, Braconnot, 1820, Kossel, 1898). They examined extracts from specimen such as plant grains, blood and egg white and the main observations were the ability to flocculate and coagulate upon the treatment with heat or acid. The word protein was coined 1839 by the dutch chemist Gerardus Johannes Mulder in a publication on the composition of animal substances (Mulder, 1839). Insulin was the first protein that got sequenced by Frederick Sanger in 1949 and John Kendrew and Max Perutz solved the first protein structures myoglobin and hemoglobin respectively in the late 1950's (Sanger, 1949, Kendrew et al., 1958, Perutz et al., 1960). In 1955 the information carrier DNA could be connected to protein synthesis due to the findings of Mahlon Hoagland and Paul Zamecnik together with Francis Crick (Hoagland, 1955, Hoagland et al., 1956, Crick, 1957). It was shown that the polypeptide chains of proteins are synthesised according to the nucleotide sequence of the DNA. 20 different amino acids are the building blocks that can be integrated to become a protein. The information encoded in the genes, already determines the size, folding and by that the function and field of application of the protein. Furthermore, the characteristics of proteins can be altered by post-translational modifications. Thereby, different functional groups such as amino acids, acetate, phosphate, lipids or carbohydrates can get attached onto or removed from the polypeptide (Burnett and Kennedy, 1954, Sadoul et al., 2008). This addition or removal, the so called post-translational modifications, deviates the chemical nature of certain amino acids or induces structural changes and primes the protein for its purpose. One of the first post-translational modifications is the removal of the N-terminal methionine of newly synthesised proteins (Giglione et al., 2004). Other common modifications include glycosylation, ubiquitination, nitrosylation, methylation, acetylation, lipidation and proteolysis (Walsh, 2006). One frequent and most important post-translational modification is the protein phosphorylation. It represents a key tool for

activating or inactivating enzymes for the regulation of cellular processes.

3.2 Kinases, crucial regulators of cellular processes

Kinases are critical regulation tools in metabolism, cell signalling, protein regulation, cellular transport, secretory processes and fundamental cellular pathways such as the cell cycle, apoptosis, stress responses, cellular volume sensing and regulation, osmotic homeostasis and link cell cycle activities with cell volume. All these meticulous regulations are achieved by the precise interplay of phosphorylation and dephosphorylation of proteins. Phosphorylated proteins have first been described by the chemist Phoebus Levene and his colleague in 1902 (Levene and Alsberg, 1906), but the actual mechanism of enzymatic phosphorylation of casein was discovered in 1954 by George Burnett and Eugene P. Kennedy (Burnett and Kennedy, 1954).

Phosphorylation is one of the most important reversible post-translational modifications of life. The addition of a phosphate group from the donor molecule ATP or ADP (adenosine-tri-phosphate, adenosine-di-phosphate) onto substrates is mediated by kinases whereas dephosphorylation is handled by phosphatases (Krebs and Fischer, 1956). Thereby the phosphate is transferred onto a serine, threonine or tyrosine, in some cases also histidine, arginine, lysine and other residues of an acceptor molecule (Cozzone, 1988). This often results in a conformational change of the target molecule which then alters its activity and function. Hence, kinases are an inevitable element of the complex signalling cascades in prokaryotes, eukaryotes and archaea (Kyriakis, 2014). The human genome comprises about 530 protein kinase genes, which constitutes about 2% of all human genes (Manning et al., 2002b). It is thought that up to 30% of all human proteins are modified by kinase activity (Cohen, 2002). Furthermore, there are additional kinase groups that phosphorylate other substrate classes. This heterogeneous group can be classified into three major subgroups, indicating their substrate: carbohydrate kinases, lipid kinases and protein kinases. Carbohydrate kinases organise the breakdown of carbohydrates to monosaccharides for example in the glycolysis of mammals (Holzer and Duntze, 1971). Lipid kinases phosphorylate lipids on the plasma membrane of cells, as well as on the membranes of the organelles. Those phosphorylated lipids can change their reactivity and localisation in the cell and can as well be used in signal transduction

such as in the insulin signalling pathway (Cantley, 2002). The third class constitutes the biggest and most diverse kinase subgroup, the protein kinases. Protein kinases phosphorylate proteins to modify their function within a signalling cascade. Phosphorylation can increase or decrease the activity of a protein, stabilise it or mark it for destruction, localise it within a specific cellular compartment, and it can initiate or disrupt its interaction with other proteins (Adams, 2001). The protein kinases can be further subdivided into at least eight major groups based on their phylogenetic relations (Manning et al., 2002b).

3.3 Ste20-like kinases

One subgroup of the protein kinases are the Ste (from "sterile") kinases. The *ste*-genes were first discovered during a genetic analysis in the budding yeast *Saccharomyces cerevisiae (S. cerevisiae)*. The Ste group is further subcategorised into Ste7, Ste11 and Ste20 kinases. Ste20 in particular was identified as a suppressor of mating defects and as a dominant activator of the mating response (Ramer and Davis, 1993). Further biochemical characterisation demonstrated that *ste20* encodes a serine/threonine kinase. Hence Ste20 was the prime forerunner of a kinase superfamily. In human, respectively amoebae, the Ste20-like kinases comprise 10% and 15% of the kinome and employ a broad variety of functions (Manning et al., 2002b).

Ste20-like kinases exist in two different types according to their domain architecture. In the p21 (cyclin-dependent kinase inhibitor 1)-activated kinases (PAKs) the kinase domain is located at the C-terminus of the enzyme. Additionally, at the C-terminus a CDC42 (Cell division control protein 42)/Rac (similar to RAs-related-C3 botulinum toxin substrate)-interactive-binding (CRIB) domain is placed that mediates binding to small GTPases for activation. The structure of the germinal centre kinases (GCKs) in contrast is characterised by the catalytic domain being located more mid to N-terminal and a variable C-terminus which is mostly tailored according to the field of application of the kinase. While PAKs are grouped into group I and group II (Jaffer and Chernoff, 2002), the GCKs are a much bigger and more diverse group that is subdivided into groups GCK-I-VIII (Dan et al., 2001). The denominator of all Ste20-like kinases is the highly conserved catalytic domain pattern

consisting of the subdomains I-XI (Hanks and Hunter, 1995b). The subdomain VIII with the signature amino acid sequence –xGTPxWMAPEx- (x indicates variable amino acids) plays a major role in recognition of peptide substrates.

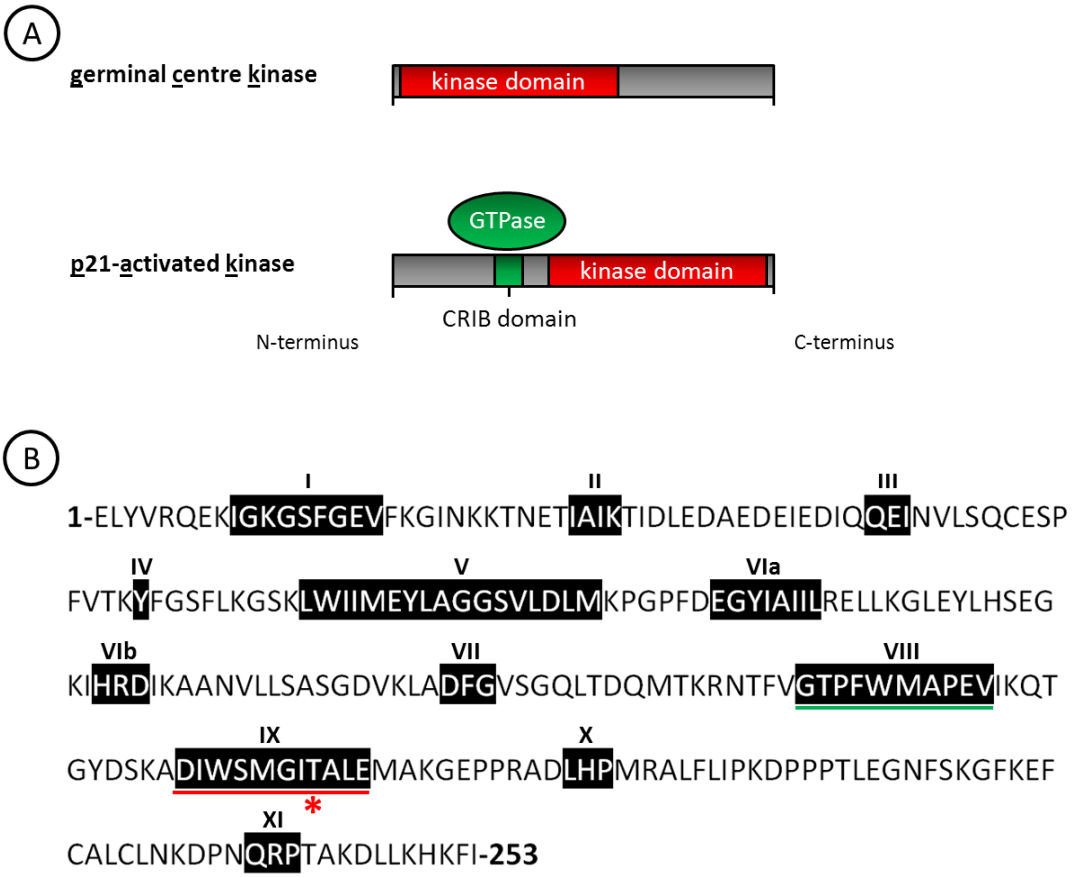

Figure 1: Structure of germinal centre kinases and p21-activated kinases
(A) The structure of the germinal centre kinases (GCKs) compared to the p21-activated kinases. GCKs are characterised by their N-terminal catalytic domain. The catalytic domain of the PAKs is located at the C-terminus of the protein. Additionally, PAKs possess a CRIB domain which binds small GTPases. (B) Amino acid sequence of the catalytic domain of the Ste20-like severin kinase (SvkA). Roman numerals above the sequence mark the 12 conserved subdomains of the Ste20-kinase group as described (Hanks and Hunter, 1995a). The green bar indicates the signature motif of the protein kinases which is implicated in the recognition of peptide substrates. The red bar indicates the subdomain in which the Threonine (red asterisk) needs to be phosphorylated to activate the kinase.

Maximal kinase activity requires the phosphorylation of threonine 197 in subdomain IX. Pseudokinases, although members of the Ste20-group, lack these important residues that are necessary for activation (Kannan and Taylor, 2008). With the crystallisation of the kinase domains of Tao2 (Thousand-and-one amino acids 2) (Zhou et al., 2004), OSR1 (Oxidative stress response kinase 1) (Lee et al., 2009), Mst1 (Mammalian Ste20-like kinase

1) (Hwang et al., 2007) and Mst2 (Mammalian Ste20-like kinase 2) (Liu et al., 2014) the structures, binding and activation mechanisms have been revealed. The kinase domains consist of α-helices and β-sheets that provide the framework for the conserved kinase fold with an ATP-binding cleft and the catalytic loop. The switch from an inactive to an active kinase conformation involves the transfer of a phosphate group onto the activation site. Pseudokinases however, are not activated by the addition of a phosphate group, but upon the binding to a regulator protein like Mo25 (Morula protein 25) (Rajakulendran and Sicheri, 2010). The activation modulates and enables the kinase to act on downstream targets (Zhou et al., 2004). Ste20-like kinases of groups GCK-I, IV, V, VII and VIII have been reported to be key players in the MAP (mitogen-activated protein)-kinase signalling pathway, regulating the JNK (c-Jun N-terminal kinases) pathway and the p38 (p38 mitogen-activated protein kinases)-mediated pathway (Piechotta et al., 2003). GCK-III group kinases Mst3 (Mammalian Ste20-like kinase 3), Mst4 (Mammalian Ste20-like kinase 4) and Ysk1/Sok1 (Yeast Sps1/Ste20-related Kinase 1, Suppressor of Kinase 1), act as regulators of apoptosis in human (Radu and Chernoff, 2009). Just recently Mst3 (Mehellou et al., 2013) and Mst4 (Shi et al., 2013) have been crystallised together with the regulator protein Mo25. The direct interaction of the scaffolding protein Mo25 and the Ste20-like kinase can amplify kinase activity up to 100-fold (Filippi et al., 2011).

The genome of *D. discoideum* harbours about 285 kinase genes, which is around 50% of the amount of kinase genes in *Homo sapiens* (*H. sapiens*). The Ste20-like kinase group of *D. discoideum* with 17 members is almost as big as in human (24 members). About half of the Ste20-like kinases in *D. discoideum* have homologues in the other eukaryotes whereas the other half seems to be social amoebae specific (Goldberg et al., 2006). The generation of minus mutants is very simple (Faix et al., 2004) and, in contrast to higher eukaryotes, alternative splicing variants are very limited in *D. discoideum* (Yu et al., 2011). Thus *D. discoideum* proves to be a simple yet effective model organism to study pathways and functions of kinases. For example, the GCK-III group kinase SvkA (severin kinase A) of *D. discoideum* has been reported to be essential for the late stages of cytokinesis. SvkA-minus mutants form big multinucleated cells, sometimes containing more than 30 nuclei (Rohlfs et al., 2007). SvkA is also the first Ste20-like kinase that has been discovered in *D. discoideum* due to its ability to phosphorylate the F-actin severing protein severin *in*

vitro (Eichinger et al., 1998). In addition the GCK-II group member KrsA (Kinase responsive to stress A) has been described to phosphorylate severin as well, (Arasada et al., 2006) and further to be essential for normal development and cAMP relay (Muramoto et al., 2007). The second Krs kinase, KrsB (Kinase responsive to stress B), possesses four calpain-III domains and is crucial for establishing cell polarity during chemotaxis in *D. discoideum* (Artemenko et al., 2012). Altogether, twelve Ste20-like germinal centre kinase and four p21 activated kinase genes have been detected in in the genome of *D. discoideum* (Goldberg et al., 2006).

Amongst them are Fray1 (Frayed kinase 1) and Fray2 (Frayed kinase 2), which are members of the GCK-VI group. Their kinase domain is 45% and 54% identical to the Ste20-like kinase Frayed in *Drosophila melanogaster* (*D. melanogaster*). Frayed is reported to be essential for the normal axonal ensheathment (Leiserson et al., 2000a). Frayed-minus mutants in *D. melanogaster* die early in larval development and have nerves with severe swelling and axonal defasciculation. In addition, Frayed in conjunction with Mo25 is described to be crucial for asymmetric divisions during neuroblast development (Yamamoto et al., 2008). *Frayed*-minus as well as *mo25*-minus *D. melanogaster* mutants exhibit an indistinguishable defect in the localisation of cell fate determinant Miranda to the basal cortex. In human the closest homologue to Fray1 and Fray2 is the Ste20-like kinase OSR1 which together with kinase SPAK (STE20/SPS1-related proline-alanine-rich protein kinase) jointly modulates homeostasis (Delpire and Gagnon, 2008).

The kinase domain of Ste20-like kinase DstC (*Dictyostelium* Ste20-like kinase C) of the GCK-II group from *D. discoideum* is 49% identical to Hippo ("hippopotamus"-like phenotype) in *D. melanogaster* and 51% identical to Mst2 in humans. In the fruit fly the Ste20-like kinase Hippo together with the kinases Salvador and Warts plays a fundamental role in connecting the regulation of organ size during eye development (Edgar, 2006, Zhao et al., 2008). Hippo-minus mutants display increased rates of cell proliferation and cancer. In human Mst2 is known as regulator of various tumour suppressors like serine/threonine protein kinases Lats1 (Large Tumour Suppressor 1) and Raf-1 (Rapidly Accelerated Fibrosarcoma 1) (Chan et al., 2005, O'Neill et al., 2005) and as key player in the Hippo pathway (Avruch et al., 2011). The extensive characterisations of Fray1, Fray2 and DstC of *D. discoideum* are part of this work.

3.4 Mo25, the master regulator

Mo25 is a highly conserved 40 kDa scaffolding protein with 60% identity from amoeba to man. It facilitates and activates a complex of a Ste20-like kinase with downstream kinases (ten Klooster et al., 2009). In yeast Mo25 is described as essential for cytokinesis and polarity and consequently, minus-mutants are not viable (Nozaki et al., 1996). In humans Mo25 is part of a complex with the pseudokinase STRAD (Ste20-related adaptor protein) and the Ste20-like kinase LKB1 (Liver kinase B1) (Figure 2c) (Zeqiraj et al., 2009a). Disruption of this complex causes the inherited disease Peutz-Jeghers-syndrome (Spicer et al., 2003).

Mo25 has first been described as cDNA clone 25 enriched in the mouse morula (Mo) during a library screen in 1993 by Hiroshi Miyamoto and his colleagues (Miyamoto et al., 1993). At first glance, due to its amino acid sequence, it was thought to be a calcium-binding protein. It turned out that Mo25 is in fact a regulator protein which is highly conserved throughout the eukaryotes (Karos and Fischer, 1999, Filippi et al., 2011). Crystallisation of the human Mo25 revealed a structure of six α-helical repeats (R1-R6) (Figure 2a). Each repeat consists of three α-helices of varying length. Juxtaposed, these six triplets form a right-handed helix that exhibits a clamp-like structure with a concave and a convex side (Milburn et al., 2004). The N-terminus of the protein begins with two anti-parallel helices and is not as thoroughly conserved as the C-terminus. At the convex side of the protein, a repeat 6 extends a dilated loop caused by the amino acid sequence 284-NPNKT-288 with the positively charged lysine. This, on the one hand forms the cleft which functions as hydrophobic binding pocket (Figure 2b) (M260) for the amino acids 429-WEF-431 (Trp-Glu-Phe) which represent the binding motif of STRAD. On the other hand, it forces further hydrophobic regions of the other five helices at the concave side to the protein surface (Figure 2b) (R227), which can thus interact with the N-terminal amino acids of STRAD via hydrogen bonds (Zeqiraj et al., 2009b). STRAD is a pseudokinase of the Ste20-like kinase family (Ling et al., 2008). As pseudokinases lack the catalytic residues in the kinase core, they are catalytically inactive (Kannan and Taylor, 2008). The third very important binding site is also located on the concave side of Mo25 (Figure 2b) (R240). There the binding of the kinase LKB1 to the Mo25/STRAD-complex occurs and completes the trimeric complex (Boudeau et al., 2004).

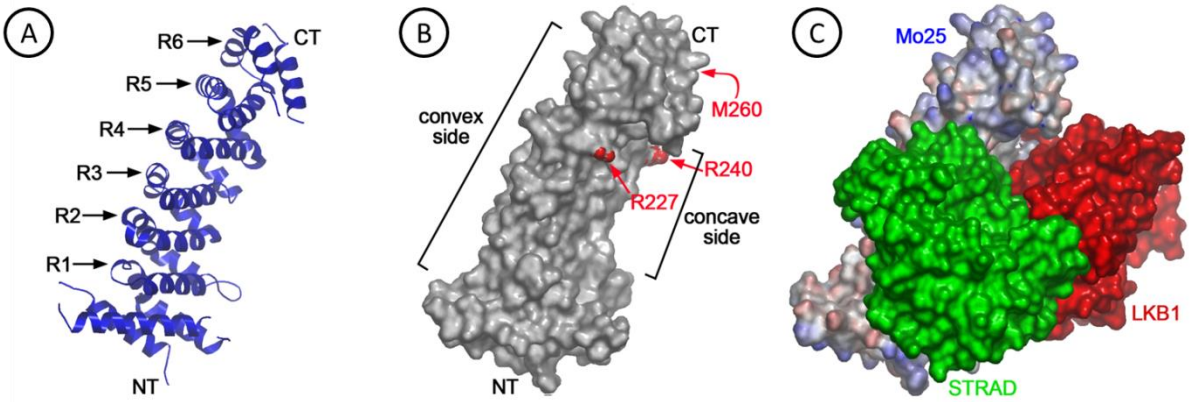

Figure 2: The scaffolding protein Mo25 (CAB39) from *H. sapiens*
(A) The ribbon model of human Mo25 (CAB39: calcium binding protein 39) (PDB: 2wtkA) displays the N-terminal antiparallel helices that transition into six α-helical repeats (R1-R6). (B) The surface model depicts the clamp-like scaffolding structure with the convex and the concave sides. The known binding sites of STRAD and LKB1 are marked in red. (C) The scaffolding protein Mo25 (CAB39) in complex with the pseudokinase STRAD (green) and the serine/threonine kinase LKB1 (red). Only upon formation of this trimeric complex LKB1 gets converted into an active kinase state and is translocated from the nucleus into the cytosol.

The serine/threonine kinase LKB1 is a tumour suppressor. Unlike other kinases LKB1 is not activated by phosphorylation in its activation loop. The scaffolding protein Mo25 together with STRAD and ATP bind LKB1-like a “substrate” and thereby induce the active kinase fold in LKB1 leading to the phosphorylation of downstream targets (Zeqiraj et al., 2009a). Only in the complex with Mo25 and STRAD, LKB1 is exported from the nucleus to the cytoplasm and can exert its kinase activity (Baas et al., 2003). The targets regulated by the Mo25/STRAD/LKB1-complex are manifold. For example, cell cycle arrest of cells is regulated by inducing the cell cycle progression regulator p21 through a p53 (Tumour protein 53)-dependent mechanism (Tiainen et al., 2002). Mutations that disrupt the Mo25/STRAD/LKB1-complex cause uncontrolled cell proliferation. This leads to an autosomal dominant disease called Peutz-Jeghers-syndrome (Boudeau et al., 2003, Baas et al., 2003) with a high disposition to develop intestinal cancer very early on in life (Jansen et al., 2009). The Mo25/STRAD/LKB1-complex is also responsible for maintaining cell polarity in intestinal cells by inducing the remodelling of the actin cytoskeleton in order to form apical brush borders (Baas et al., 2004b, Baas et al., 2004a). Furthermore, the energy sensor AMP-kinase and at least 12 more kinases of the AMPK (5' Adenosine monophosphate-activated protein kinase) subfamily are direct downstream targets

regulated by the trimeric complex (Lizcano et al., 2004, Jaleel et al., 2005). The AMPK related kinase Par1 (Partitioning defective 1)/MARK3 (Microtubule affinity regulating kinase 3) which plays a key role in the Wnt (Wingless-related integration site) signalling pathway for polarity is directly phosphorylated by the Mo25/STRAD/LKB1-complex (Brajenovic et al., 2004). Additionally, the trimeric complex also regulates the mammalian target of rapamycin through the AMPK-TSC2:TSC1 (Tuberous sclerosis 1:2)-complex (Orlova et al., 2010) and hence further proves to be a key player in the mTor (Mammalian target of rapamycin) pathway. Another example for the control by the Mo25/STRAD/LKB1-complex is the regulation of axiogenesis in neurodevelopment. Disruption of the trimeric complex prevents the formation of projection axons in the cerebral cortex (Veleva-Rotse et al., 2014). In addition, Mo25 does not bind and therefore regulates LKB1 exclusively. The Ste20-like kinases SPAK, OSR1, Mst3, Mst4 and Ysk1/Sok1 (Yeast Sps1/Ste20-related Kinase 1, Suppressor of Kinase 1) are reported to bind to the same hydrophobic binding pocket of Mo25 similar to STRAD (Filippi et al., 2011, Mehellou et al., 2013). Upon binding to Mo25, Mst4 rotates the αC helix toward its catalytic core and, thus allows the Mst4 kinase domain to form a specific homodimer that is required for trans-autophosphorylation (Shi et al., 2013). This interaction with Mo25 induces an up to 100-fold activation of the kinases, enhancing their ability to phosphorylate downstream targets (Filippi et al., 2011).

In simpler eukaryotic organisms such as *Aspergillus nidulans (A. nidulans)* for example, the disruption of the *mo25* homologue gene (*hymA*, Hypha-like metulae A) leads to a developmental phenotype noticeable in hypha-like metulae (Karos and Fischer, 1996). In *S. cerevisiae* the corresponding gene (*hym1*, Hypha-like metulae 1) is involved in cell separation (Dorland et al., 2000), formation of mating projections and apical bud growth and facilitates the localisation of the Ndr (Nuclear dbf2-related kinase) family kinase Cbk1 (Cell wall biosynthesis kinase 1) to the bud neck (Bidlingmaier et al., 2001). Hym1 is part of the RAM network where it interacts with the Ste20-like kinase Kic1p (Kinase that interacts with Cdc31p) to regulate the transcription factor Ace2p (Activator of CUP1 expression 2p) -dependent polarised morphogenesis (Nelson et al., 2003). In *Schizocaccharomyces pombe* (*S. pombe*) a similar complex of Pmo25 (Mo25 family protein Pmo25) and the Ste20-like kinase Nak1 (PAK-related kinase Nak1) regulates the

localisation and activity of the Ndr-family kinase Orb6 (Serine/threonine protein kinase Orb6) that regulates cell polarity and cell division (Kanai et al., 2005, Mendoza et al., 2005). In addition, another Ste20-like kinase, Ppk11 together with Pmo25, was shown to play a supporting role for cell division (Goshima et al., 2010). Mo25 has evolved as a key regulator of a certain group of Ste20 kinases and also represents an ancestral mechanism of regulating the conformational change of pseudokinases to activate catalytically competent protein kinases (Filippi et al., 2011).

Mo25 of the social amoeba *D. discoideum* is 60% identical to its homologues in yeast and human. Potential downstream targets of Mo25 could be the Ste20-like severin kinase (SvkA) which is highly similar to kinases Nak1 (*S. pombe*), Kic1p (*S. cerevisiae*) and Mst4 (*H.sapiens*) (Eichinger et al., 1998). As there is no solid data on the occurrence of pseudokinases and no direct homologue of STRAD exists in *D. discoideum*, sequence comparisons revealed that the kinases Fray1 and Fray2 and SvkA are the closest relatives to STRAD. Interestingly, SvkA, Fray1 and Fray2 also contain a WEF (Trp-Glu-Phe), WSF (Trp-Ser-Phe) or WIF (Trp-Ile-Phe) sequence motif, respectively, which is implicated in facilitating the binding of the pseudokinase STRAD to Mo25 at a similar distance to the catalytic domain as in STRAD (Boudeau et al., 2003). This renders them as putative interacting partners of Mo25. A deeper insight into the conducts of Mo25 in *D. discoideum* is an integral part of this work.

3.5 Cell division

Cell division combines the processes of mitosis and cytokinesis. The fundamental functions of the reproduction cycle are the duplication of chromosomes and cytoplasmic components, the separation of chromosomes during mitosis and the division into two independent daughter cells during cytokinesis (Cooper and Hausman, 2013). The duplication of the DNA and cytoplasmic components happens during S-phase (Maya-Mendoza et al., 2009). Mitosis and cytokinesis take place during the so called M-phase which can be subdivided into five steps (Blow and Tanaka, 2005). During prophase the duplicated nuclear DNA starts to condensate to form a homologous set of chromosomes while the spindle apparatus is formed. Additionally the nuclear membrane dissolves in

higher eukaryotes (De Souza and Osmani, 2007). Subsequently in metaphase the chromosomes are most densely packed and the mitotic spindle is fully formed (Mahmoudi et al., 2011). In anaphase, each set of homologous chromosomes gets transferred to one of the two spindle poles by microtubules. With the entry into telophase the nuclear membrane is re-established around the decondensing chromosomes and two new nuclei are set up. Cytokinesis is the final step of cell division by which the mother cell is physically divided into two independent daughter cells (Eggert et al., 2006). Important insights into the molecular mechanisms of cell division emerged from the research with model organisms such as *S. cerevisiae* (budding yeast) (Sobel, 1997), *S. pombe* (fission yeast) (Hayles and Nurse, 1989) and the amoeba *D. discoideum* (Robinson et al., 2002).

Mechanics of cell division in *D. discoideum* consist of four distinguishable steps (Wolf et al., 1999). During the first step a cleavage plane is established by the orientation of the intra nuclear mitotic spindle and the chromosomes are segregated while the nuclear membrane stays intact during closed mitosis (Effler et al., 2006). In the second step the centrosomes move towards the incipient daughter cells powered by motor proteins on microtubules that are linked to the cell cortex (Neujahr et al., 1997). Additionally, actin is assembled in an inner ring at the plasma membrane where the cleavage furrow will form. This is followed by the localisation of myosin II which will generate the force of contraction. After rounding up, the cells elongate in the third step and through the contraction of the ring structure the cleavage furrow occurs (Glotzer, 2001). In the final fourth step, membrane fusion mediated by the ring structure separates the two daughter cells (Robinson and Spudich, 2004). Two unconventional but sometimes frequent ways of cell division should be mentioned here as well: the traction mediated cell division and the cell division by midwife cells which are attracted chemotactically to the cleavage furrow to divide the two daughter cells mechanically by force (Nagasaki et al., 2009). An orchestrated array of cytoskeletal proteins is required for successfully completing mitosis and cytokinesis (Gerisch et al., 2004, Surcel et al., 2010). For the late stages of cytokinesis in *D. discoideum*, the Ste20-like kinase severin (SvkA) has been described to be essential. SvkA-minus cells are unable to separate after mitosis and form big multinucleated cells (Rohlfs et al., 2007). The Ste20-like kinase Hippo in *D. melanogaster*, to which DstC of

D. discoideum is very similar, has extensively been described as regulator of organ size during eye development (Wu et al., 2003). Hippo-minus mutants exhibit increased rates of cell proliferation and cancer (Zhao et al., 2008). In ascomycote *A. nidulans* the Mo25 homologue HymA of has been reported to be involved in the production of asexual non motile spores. In HymA-minus mutants conidiophore development is blocked, resulting in a reproduction defect and indicating a disturbance in mitosis (Karos and Fischer, 1999). Also in budding and fission yeast, the minus mutants of the respective Mo25 homologue Hym1 have severe problems in forming apical buds and mating projections due to a halt in mitosis (Bogomolnaya et al., 2004). All these previous findings strongly suggest that the herein investigated kinases Fray1, Fray2 and DstC together with SvkA and the scaffolding protein Mo25 of *D. discoideum* are implicated in cell division.

3.6 The model organism *D. discoideum*

The amoeboid organism *D. discoideum* (Figure 3) now has a scientific history of nearly 150 years since it was first discovered by Julius Oscar Brefeld in the late 60's of the 19th century (Brefeld, 1869). Brefeld already described some of the most fundamental features of *D. discoideum*, including the switch from single cell to multicellular aggregates that are formed upon starvation. Over the years further descriptive essays on nutrient uptake by Vuillemin (Vuillemin, 1903) and development by Harper (Harper, 1926, Harper, 1932) were published. But it was not until Kenneth Brian Raper, who discovered the progenitor of the *D. discoideum* strains used in laboratories all over the world today (Raper, 1935) transferred *D. discoideum* as model organism into modern day cell science.

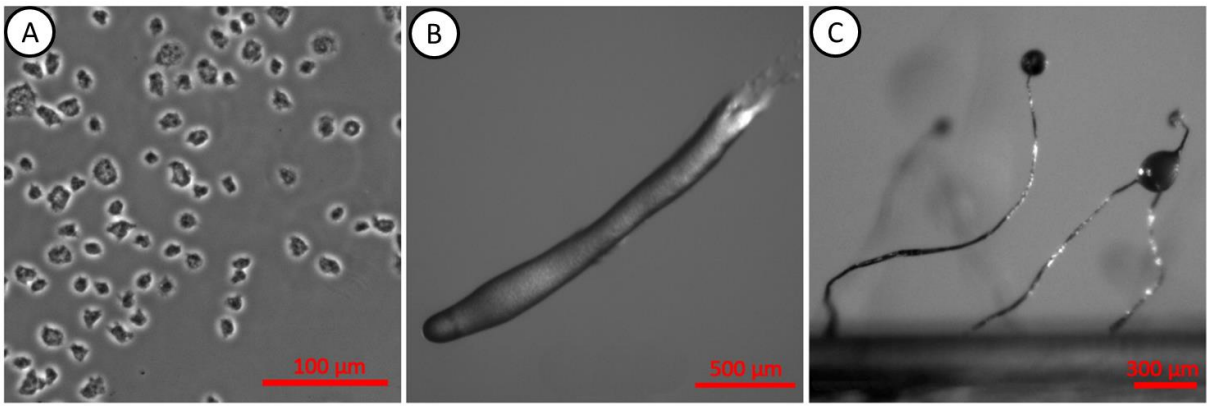

Figure 3: Different life cycle stages of *D. discoideum*
(A) Single amoebae (B) Upon starvation approximately 1 x 10^5 cells form a motile pseudoplasmodium, the multicellular slug. Slugs are able to migrate photo- and thermotactically. (C) In the last stage of the developmental cycle the multicellular organism differentiates into a fruiting body.

Phylogenetically, *D. discoideum* belongs to the social amoebae and is positioned right between the fungi and plants, but is more distant from plants (Baldauf et al., 2000). Social amoebae are characterised by their unique life cycle which proceeds from autonomously living amoebae to a multicellular organism with well differentiated tissues (Chisholm and Firtel, 2004). With 5-10 microns in diameter, *D. discoideum* cells are relatively small, but still easily accessible by microscope. The common reproduction type of the normally haploid *D. discoideum* is asexual. Nevertheless, a sexual reproduction mode exists where two amoebae of different mating types fuse. This fused cell then engulfs all the other cells and encapsulates the whole aggregate into the so called macrocyst. The macrocyst is a

protective shell consisting of cellulose. Inside the macrocyst, the large diploid cell divides first through meiosis, then continues through mitosis. Finally, the new amoebae are released (Filosa and Dengler, 1972). Whilst sexual reproduction can be induced under laboratory conditions, a successful germination of a *D. discoideum* macrocyst is very rare. High yields of *D. discoideum* can be obtained by keeping the amoebae on a bacterial lawn or in axenic medium (HL5) under constant shaking (Ashworth and Watts, 1970). At temperatures between 18 and 22°C, the duplication rate is 8-15 hours. In its natural environment *D. discoideum* thrives on forest soil, decaying leaves and dung and feeds mostly on bacteria via phagocytosis (Weijer, 2004).

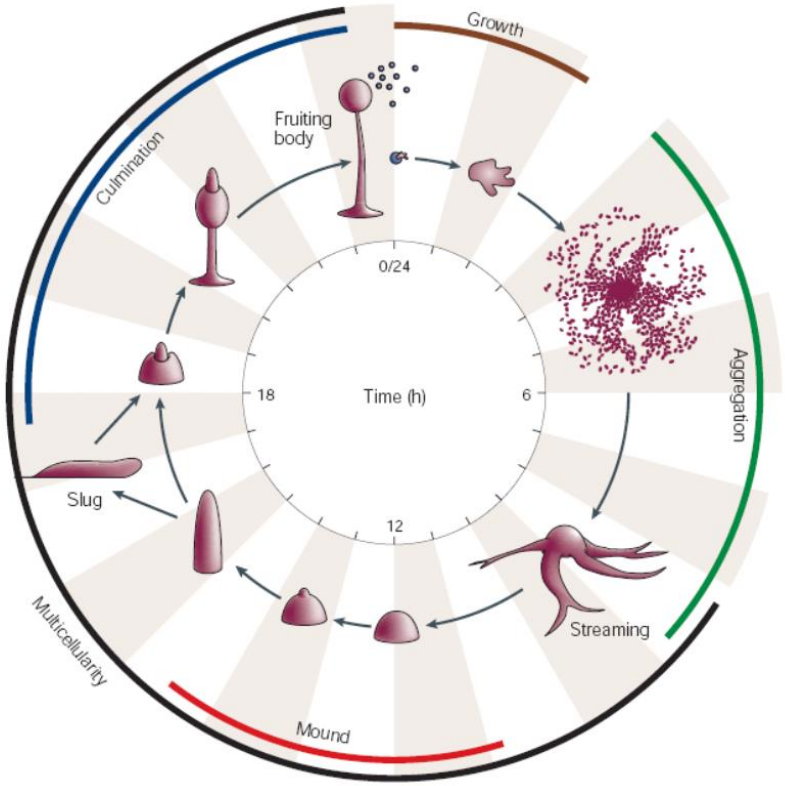

Figure 4: The life cycle of *D. discoideum*
The life cycle of *D. discoideum* starts with individual, vegetative amoebae that hatch from spores. Upon starvation the amoebae aggregate mediated by the chemotaxis towards a cyclic AMP gradient. During this process, cells stream towards the central aggregation centre. The aggregation results in the formation of a multicellular organism, known as mound. Already in this phase cells sort into so called prestalk and prespore cells with an approximate 20%:80% ratio and form a tipped aggregate. As development proceeds, the tip extends and an anterior–posterior axis forms, which is maintained through the slug and early culminant stages. Culmination, the formation of the fruiting body, completes the *D. discoideum* life cycle. The prestalk cells develop into vacuolated stalk cells and form the stalk and a disc at the basis. The prespore cells migrate onto the top of the stalk and form the sorus consisting of several thousand spores. Picture taken from (Chisholm and Firtel, 2004).

Upon deprivation of nutrients, *D. discoideum* enters its unique life cycle that is characterised by the developmental switch from single cells to multicellular aggregate by cAMP-mediated chemotaxis (Figure 4). During this multicellular phase *D. discoideum* can form a mobile intermediate, the so called slug. This intermediate is susceptible to light and heat and able to migrate towards the respective source. Further on, during culmination the slug rises from the substrate and forms a fruiting body consisting of a stalk anchored in a flattened cellular disc and crowned with a globose-to-slightly-citriform spore mass (Raper, 1984). 80% of the cells migrate into the sorus and transform into spores, whereas the remaining 20% are sacrificed to build the stalk. Completion of one entire developmental cycle takes under laboratory conditions about 24 hours from start to end. The genome has a size of 33.8 megabases, is organised in 6 chromosomes (Urushihara, 2008) and codes for approximately 12.500 proteins (Eichinger et al., 2005). Thus, *D. discoideum* possesses almost as many genes as *D. melanogaster* and more than twice as many as yeast, but only half as many as human (Goldberg et al., 2006). Furthermore, due to its haploidity the genome is easily accessible for manipulation by recombinative methods (Faix et al., 2004). Regarding all these advantages, *D. discoideum* proves to be a suitable and versatile model organism for regulation of cellular dynamics, cell adhesion, phagocytosis, cell polarity, mitosis, cell division and morphogenesis.

The control of all these processes requires a sophisticated underlying control and signalling system. The genome of *D. discoideum* encodes approximately 285 kinases. About half of them have analogues in other eukaryotes and the other half are probably social amoeba specific (Goldberg et al., 2006). This relatively large signal network and the unique switch from single cell to multicellular organism provides the perfect framework for studying the regulation of cell division and cell polarity.

3.7 The fresh water foraminifer *R. filosa*

The phylum Foraminifera belongs to the eukaryote branch of the Rhizaria. It is one of the most diverse groups of amoeboid protists, comprising roughly 5000 living species. For the greater part they live in salt water and tens of thousands of fossil taxa exist (Flakowski et al., 2005) The test of a foraminifer was first mentioned in a letter to a friend by Antony van Leeuwenhoek in 1700 (Dobell, 1932), but it was not until about 130 years later when Alcide d'Orbigny first described and named the taxon in 1826, respectively 1840 (d'Orbigny, 1826, d'Orbigny, 1840). Almost all works on Foraminifera to date dealt with their taxonomy and due to the lack of cultivability almost no molecular data were available. Therefore, the total sequencing of the genome of the fresh water foraminifer *R. filosa* represents one the first insights into the molecular world of the Rhizaria. *R. filosa* was discovered in a puddle during a walk through New York's central park by Ruth N. Nauss in 1937 (Nauss, 1949). In its natural habitat *R. filosa* is growing in the detritus of fresh water and feeds on cyanobacteria, bacteria, rotifers, green algae and ciliates. The clear advantages, in contrast to most other foraminifers, is the cultivability in fresh water, even if only in its plasmodial state (Glöckner et al., 2014), and the fact that *R. filosa* is not encapsulated. Under laboratory conditions *R. filosa* exists as a large syncytium (diameter up to 3 cm) with thousands of haploid nuclei. The phenotype is characterised by a central area from which hundreds of filamentous reticulopodia protrude into the surroundings (Figure 5a). This corona of reticulopodia is responsible for the uptake of nutrients and their transport to the cell body via rapid plasma streaming (Travis and Bowser, 1991). Facing unfavourable conditions, the plasmodia are set to encystation. In nature, *R. filosa* grows to giant net-like plasmodia with up to 10 cm or more in diameter, consisting of numerous central areas that are connected by thick veins and extending slender reticulopodia in the periphery. Easily accessible for microscopy due to its transparent appearance, the transport of nutrients and organelles in the pseudopodial network can be observed. The cargo transport in *R. filosa* is one of the fastest particle movements through cytoplasm within a cell in eukaryotes. Velocities of up to 12.5 microns per second have been measured (Ashkin et al., 1990). This feature made *R. filosa* a first-rate research object for the mechanisms of bidirectional cargo transport.

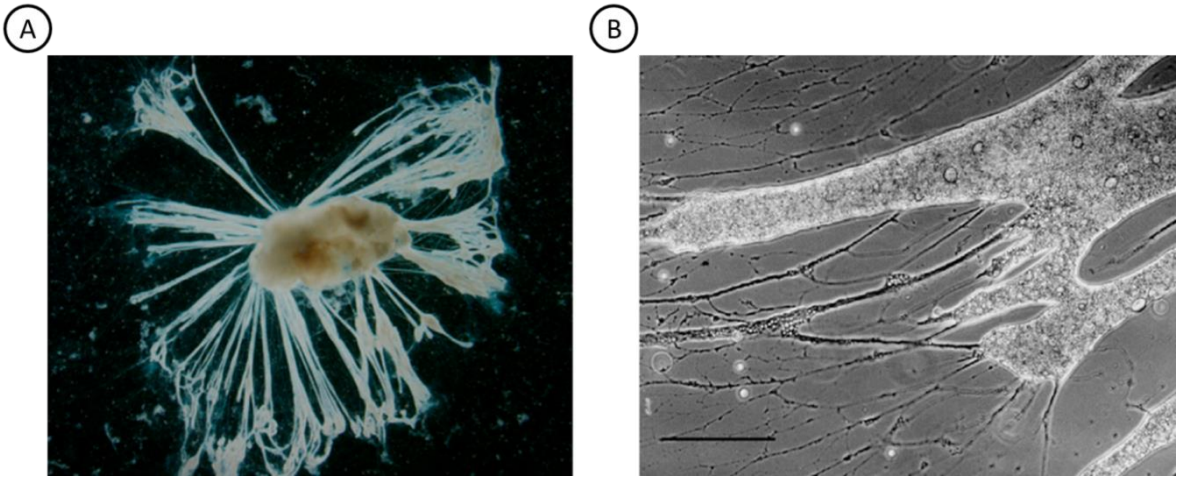

Figure 5: The rhizarian foraminifer *R. filosa*
(A) A 1-3cm big syncytium with thousands of nuclei. Rapid plasma streams transport nutrients to the cell body. (B) Periphery of the central area with thicker strands and filose anastomosing reticulopodia. Bar = 50 microns. Picture taken from (Glöckner et al., 2014)

Also the assembly and disassembly of microtubules happens with remarkably high speed, with elongations of up to 6.5 microns per second versus degradation rates of 19.5 microns per second (Schliwa et al., 1991). The cytoskeleton consists mainly of microtubules, whereas the concentration of actin is relatively low compared to other eukaryotes. Also a centrosome is missing as well as the conventional organisation of the microtubules (Orokos et al., 2000). Even though there are clear indications for sexual reproduction in the genome of *R. filosa*, only reproduction by a very unique way of cell division is known to date. During growth, the nuclear divisions occur synchronised and correlate with the mass increase of cytoplasm. The nuclear envelope stays intact during the whole process and is only permeable to the spindle microtubules. Also the nucleoli attached at the nuclear envelope do not get resolved but being split between the resulting daughter nuclei. Next, *R. filosa* discontinues the bidirectional transport and starts to transport degradation products and expendable nutrients unidirectionally to the cell surface to get rid of them via exocytosis. Afterwards, all of the cytoplasm, including the central area, migrates towards the outer tips of the reticulopodia. There, three to four new central areas emerge, that after some growth will merge their filamentous plasmodia and so create the net-like appearance (Hülsmann, 2006). The genome of *R. filosa* is extremely repetitive. The large amount of identical sequences is a mechanism to provide

more gene copies probably for higher transcriptional activity. Furthermore, this also helps to enhance gene diversification in certain gene families, that code for essential key proteins, such as the kinesin family for example (Glöckner et al., 2014). The recently sequenced genome of *R. filosa* is only the second rhizarian genome, the other available whole genome is from *Bigelowiella natans* (Curtis et al., 2012). Keeping in mind that the supergroup Rhizaria constitutes one of the six, respectively eight major branches of the eukaryotes (Adl et al., 2013), the availability of only two whole genomes is rather scarce. The *R. filosa* genome is, therefore, an important step into a better understanding of the evolution of the eukaryotes.

3.8 Goals of this project

Cell division, mitosis, cytokinesis and cell polarity are key points of the reproduction cycle. Disturbances of these fundamental processes cause chromosomal aberrations, uncontrolled growth and cell division and thus direct contribution to an irate development of the cell.

Ste20-like kinases and their signalling partners have been shown to be regulatory elements of cell division, mitosis and cytokinesis (Manning et al., 2002b). Additionally, they also control a multitude of different other cellular processes. The removal of these regulator proteins should lead to a drastically altered phenotype of the cell.

The genome of *D. discoideum* comprises 17 Ste20-like kinases and encodes the regulator protein Mo25. It has been reported that Mo25 is a master regulator of a number of cellular processes and an avid modulator of kinase activity (Filippi et al., 2011).

The major aim of this thesis was to investigate Mo25, its interactions and regulatory pathways.

A second goal was the functional characterisation of the Ste20-like kinases Fray1, Fray2 and DstC of *D. discoideum* which all have homologues in higher eukaryotes.

The third endeavour of this thesis was to map and characterise the actin and actin related genes in the genome of the recently sequenced fresh water foraminifer *R. filosa.*

4 Materials and Methods

4.1 Materials

4.1.1 Instruments

Balances	Sartorius
BioDocAnalyze	Biometra
Fluorescence spectrometer	LS 55 Perkin Elmer
Gene pulse electroporator Xcell	BioRad
Gelsystem MiniPROTEAN	BioRad
PCR-thermocycler Tpersonal	Biometra
pH-meter pH720	Inolab WTW series
Power supplies	BioRad, Biometra, Consort
Protein transfer Transblot Semi-Dry	BioRad
Protein transfer TF 77XP	Serva
Real time PCR Opticon III instrument	MJ Research
Shaker Orbital Incubator SI500	Stuart
Shaking incubator with temperature control	Memmert
Shakers for *D. discoideum* cultures	Kühner
Sonficator Sonifier250	Banson
Thermomixer	Eppendorf
Tabletop film processor Curix 60	Agfa
Vortex Genie 2	Bender & Hobein
Waterbath	GFL, Kühner

Microscopes

Axiovert 25	Carl Zeiss
Axiovert 200M	Carl Zeiss
LSM 510 Meta confocal microscope	Carl Zeiss

Objectives

10x A-Plan 0.25 Ph1	Carl Zeiss
20x LD A-Plan 0.30 Ph1	Carl Zeiss
40x LD A-Plan 0.50 Ph2	Carl Zeiss
63x Neofluar 1.4 oil immersion objective	Carl Zeiss
100x Neofluar 1.3 oil immersion objective	Carl Zeiss

Centrifuges

GS-6KR	Beckman
J2-21M/E	Beckman
J6-HC	Beckman
Microcentrifuge 5415 D, 5417 R	Eppendorf
Optima LE-80K	Beckman
Optima TL ultracentrifuge	Beckman

Rotors

JA-10, JA-14, JA-20	Beckman
Ti35, Ti45, Ti70	Beckman
TLA 100.3	Beckman

4.1.2 Computer Programs

Adobe CS2	Adobe Systems
Adobe Acrobat Pro Extended	Adobe Sytems
ApE plasmid editor v1.10.4	M. Wayne Davis
AxioVision	Carl Zeiss
BioDoc Analyze	Biometra
BioEdit 7.0.9.0	Tom Hall
ClustalX2	Des Higgins
CorelDraw 12	Corel Corporation
EndNote X7	Thomson Reuters

ImageJ 1.44p	Wayne Rasband
LSM 5, 4.2 SP1	Carl Zeiss
Microsoft Office	Microsoft Corporation
OpenAstexViewer 3.0	Mike Hartshorn
TreeView 1.6.6	Roderic D. M. Page
ZEN	Carl Zeiss

4.1.3 Online Programs

DictyBase	www.dictybase.org
ExPASy	www.expasy.org
MUSCLE	www.ebi.ac.uk
NCBI	www.ncbi.nlm.nih.gov
NetPhosK	www.cbs.dtu.dk/services/NetPhosK/
NEB-tools	www. tools.neb.com
RCSB-PDB	www.rcsb.org
Reticulomyxa BLAST Server	www.genome.imb-jena.de/reti_blast/BlastReti.cgi
SMART	www. smart.embl-heidelberg.de

4.1.4 Laboratory consumables

1.5 ml centrifuge tubes	Sarstedt
Amersham Hyperfilm ECL	GE Healthcare
Cell culture plates, 24 wells	Starlab Int.
Cell culture dishes, Ø 100 mm x 20 mm	Greiner bio-one
Dialysis tubings Type 8, 20, 27	Biomol
Gel-blotting paper 3MM Chr	Whatman
GFP-Nano-Trap	Chromotek
High Pure Plasmid Isolation Kit	Roche
High Pure PCR Product Purification Kit	Roche
High precision cuvettes 10mm	Hellma
Nitrocellulose transfer membrane Protran BA85	Whatman

PCR tubes Thermo Tube 0.2 ml	Peqlab
PCR product cloning kit	Qiagen
Phusion High-Fidelity DNA polymerase	New England Biolabs
Petri dishes Ø 92 mm x 16 mm	Sarstedt
Pipettes 10 ml, 25 ml	Sarstedt
Pipet tips	Biozym, Gilson, Starlab
Plasmid DNA Purification Maxi Kit	Macherey Nagel
Quantitect SYBR1 green PCR Kit	Qiagen
Restriction Enzymes	New England Biolabs
RNeasy Mini Kit	Qiagen
Sterile filter, Filtropur S 0.2	Sarstedt
Transcriptor High Fidelity cDNA Synthesis Kit	Roche
Tubes 15 ml, 50 ml	Sarstedt
Ultracentrifuge tubes 1.5 ml	Beckman

4.1.5 Reagents

Standard laboratory chemicals were mainly purchased from Biomol, Biorad, Fluka, Invitrogen, Merck, Peqlab, Roche, Roth, Serva and Sigma-Aldrich and had the degree of purity 'p.a.' unless otherwise mentioned. Media and buffers used in this study were prepared with de-ionised water (Millipore), sterilised either by autoclaving or passing through a micro-filter (pore size 0.2 µm).

4.1.6 Antibodies

Primary antibodies used in this study

Actin, *D. discoideum* (Act-1)	monoclonal	Simpson et al (1984)
GFP (K3-184-2)	monoclonal	Noegel et al (2004)
GST (268-44-6)	monoclonal	Faix et al (1998)
Fray1	polyclonal	Andreas Batsios
Mo25	polyclonal	Susanne Köhler
SvkA	polyclonal	Ludwig Eichinger

Secondary antibodies used in this study

Goat-anti-mouse IgG Cy3-conjugated	Invitrogen
Anti-mouse IgG horseradish peroxidase-linked (ECL)	GE Healthcare

4.1.7 Vectors

pDEX-GFP(g418)-N1	Meino Rohlfs
pDEX-GFP(g418)-N2	Meino Rohlfs
pDEX-GFP(g418)-C2	Meino Rohlfs
pDRIVE	Qiagen
pGEX-6P-1	GE Healthcare
pLPBLP	Faix et al (2004)

Constructs generated

pDEX-GFP(g418)-C2 + Mo25 K17A	present study
pDEX-GFP(g418)-C2 + Mo25 K34A	present study
pDEX-GFP(g418)-C2 + Mo25 K34A+K38Q	present study
pDEX-GFP(g418)-C2 + Mo25 K132A	present study
pDEX-GFP(g418)-C2 + Mo25 R227A	present study
pDEX-GFP(g418)-C2 + Mo25 R240A	present study
pDEX-GFP(g418)-C2 + Mo25 R240A+F243A	present study
pDEX-GFP(g418)-C2 + Mo25 F258A+M259A	present study
pDEX-GFP(g418)-C2 + Mo25 M260A	present study
pGEX-6P-1 + Mo25 K17A	present study
pGEX-6P-1 + Mo25 K34A	present study
pGEX-6P-1 + Mo25 K34A+K38Q	present study
pGEX-6P-1 + Mo25 K132A	present study
pGEX-6P-1 + Mo25 R227A	present study
pGEX-6P-1 + Mo25 R240A	present study
pGEX-6P-1 + Mo25 R240A+F243A	present study
pGEX-6P-1 + Mo25 F258A+M259A	present study
pGEX-6P-1 + Mo25 M260A	present study

pGEX-6P-1 + Mo25 Mo25 cDNA	present study
pGEX-6P-1 + Mo25 Dr FISH	present study
pGEX-6P-1 + Mo25 Hs HUMAN	present study
pLPBLP Fray1 KO B	present study
pLPBLP Fray2 KO	present study
CreLox Fray2	present study
pDEX-GFP-N1 Fray1	present study
pLPBLP FRIP	present study
pDEX-GFP(g418)-N2 DstC S411/T414/S418	present study
pDEX-GFP(g418)-N2 DstC S411D/T414E/S418D	present study
pDEX-GFP(g418)-N2 DstC S411A/T414A/S418A	present study
pDEX-GFP(g418)-N2 DstC Y404	present study
pDEX-GFP(g418)-N2 DstC Y404E	present study
pDEX-GFP(g418)-N2 DstC Y404F	present study
pDEX-GFP(g418)-N2 DstC Y404_s	present study
pDEX-GFP(g418)-N2 DstC Y404E_s	present study
pDEX-GFP(g418)-N2 DstC Y404F_s	present study

4.1.8 Bacterial strains

Klebsiella aerogenes

E. coli DH5α	Invitrogen
E. coli DH10Bac	Invitrogen
E. coli BL21 RIL	Stratagene
E. coli ArcticExpress RIL	Stratagene

4.1.9 *D. discoideum* strains

Designation	Resistance	Constructed by/for
Ax2 (laboratory wild-type)		
Ax2 GFP	G 10	Meino Rohlfs
Ax2 + Fray1	G 10	Meino Rohlfs
Fray1 KO	B 5	present study
Fray2 KO	B 5	present study
Fray2 KO Cre/Lox	-	present study
Fray2Fray1 KO	B 5	present study
FRIP KO	B 5	present study
Mo25 KO	B 5	Susanne Köhler
Mo25 KO + GFP Mo25	G 10	Susanne Köhler
Mo25 KO + Mo25 GFP	G 10	Susanne Köhler
Mo25 KO + Mo25 K17A	G 10	present study
Mo25 KO + Mo25 K34A	G 10	present study
Mo25 KO + Mo25 K34A+K38Q	G 10	present study
Mo25 KO + Mo25 K132A	G 10	present study
Mo25 KO + Mo25 R227A	G 10	present study
Mo25 KO + Mo25 R240A	G 10	present study
Mo25 KO + Mo25 R240A+F243A	G 10	present study
Mo25 KO + Mo25 F258A+M259A	G 10	present study
Mo25 KO + Mo25 M260A	G 10	present study

4.2 Methods

4.2.1 Molecular methods

Standard molecular biology protocols were performed essentially as described (Sambrook and Russel, 2001). Genomic DNA from *D. discoideum* strains was isolated using the LysB buffer (10 mM Tris pH 8.0, 50 mM KCl, 2.5 mM $MgCl_2$, 0.45% NP40, 0.45% Tween20, 0.5 µg/µl Proteinase K) (Charette and Cosson, 2004). Total RNA from *D. discoideum*

strains was purified using the RNeasy Mini Kit (Qiagen), and cDNA was subsequently synthesised using the Transcriptor High Fidelity cDNA Synthesis Kit (Roche). Polymerase chain reactions (PCRs) were performed with either Taq-Polymerase or Phusion High-Fidelity DNA Polymerase (New England Biolabs) according to the manufacturer's manual. PCR products were cloned into expression vectors using standard restriction enzyme mediated cloning or via the PCR product cloning kit (Qiagen). Plasmid DNA was obtained from *E. coli* by using standard alkaline lysis miniprep or by using the silica-based mini and maxiprep kits (Roche, Macherey Nagel). Chemically competent *E. coli* cells were prepared according to the $CaCl_2$ method (Dagert and Ehrlich, 1979). The accuracy of the DNA sequences inserted into the respective expression vectors was controlled by sequencing using specific primers (Eurofins MWG Operon, Ebersberg). The real time PCR was performed essentially as described (Farbrother et al., 2006).

4.2.2 Biochemical Methods

4.2.2.1 SDS-Polyacrylamide Gel Electrophoresis

Protein mixtures were separated by standard discontinuous SDS-PAGE (Laemmli, 1970) and either stained with Coomassie Brilliant Blue R 250 or transferred onto a nitrocellulose membrane via semi-dry Western blotting using a transfer buffer (25 mM Tris pH 8.5, 190 mM glycine, 20% methanol, 0.02% SDS) essentially as described (Towbin et al., 1979). The membranes were blocked with nonfat milk powder in NCP buffer (10 mM Tris pH 7.3, 150 mM NaCl, 0.05% Tween20), incubated with the particular primary and secondary antibodies and developed using the Enhanced Chemiluminescence System.

4.2.2.2 GST-tagged protein expression, purification and pull-down assay

Constructs in pGEX vectors, inducibly expressing the protein of interest with an N-terminal GST-tag, were transformed into BL21 RIL or BL21 RIL ArcticExpress *E. coli* strains. Cultures were inoculated and grown overnight in LB medium containing the particular antibiotics at 37°C, then diluted 1:20 and grown at 37 °C to an OD_{600} of 0.4 – 0.8. Expression was induced by adding 0.5 mM IPTG to the culture and cells were grown at

37°C for 2 hours or at 16°C or 20°C overnight. The bacteria were pelleted and resuspended in PBS (137 mM NaCl, 2.7 mM KCl, 8.1 mM Na_2HPO_4, 1.5 mM KH_2PO_4, pH 7.4) containing 2 mM DTT, 1 mM EDTA, 5 mM benzamidine, 100 µM PMSF and one Complete Protease Inhibitor cocktail tablet (Roche) per 50 ml lysis buffer. The cells were opened by sonification in the presence of 0.5 mg/ml lysozyme, the lysates were centrifuged (35,000 g for 20-30 minutes at 4°C) and the supernatant was incubated with the glutathione-sepharose 4B resin at 4°C for 2-3 hours under slight agitation. The matrix was washed with 10-20 column volumes of lysis buffer and either kept on ice for following protein interaction pull-down assays with *D. discoideum* cell lysates or eluted with TEDAB buffer pH 7.4 containing 30 mM reduced glutathione. The purity and quality of the protein in the appropriate fractions were analysed by SDS-PAGE.

In case a pull-down assay was performed, 5 x 10^7 – 1 x 10^8 *D. discoideum* cells were opened in 1 ml homogenisation buffer (30 mM Tris pH 8.0, 4 mM EGTA, 2 mM EDTA, 2 mM DTT, 30% sucrose, 5 mM benzamidine, 100 µM PMSF, 0.2 mM ATP Na_2 salt, one Complete Protease Inhibitor cocktail tablet (Roche) per 20 ml buffer) by freezing and thawing or by the addition of 1% Triton X-100 to the homogenisation buffer. The whole cell lysate was centrifuged at 10,000 g and 4°C for 15-30 minutes and the supernatant was used for incubation with the GST-tagged purified protein bound to the sepharose. After an incubation of about 90 minutes, the beads were washed with 10-100 column volumes of homogenisation buffer and boiled in SDS sample buffer. The interaction of proteins was subsequently analysed by SDS-PAGE and Western blotting.

4.2.2.3 Immunoprecipitation

For the identification of interacting proteins the GFP-Nano-Trap (Chromotek) technique was used (Rothbauer et al., 2008). 5 x 10^7 – 1 x 10^8 *D. discoideum* cells overexpressing a recombinant GFP-tagged protein were harvested and opened in lysisbuffer (25 mM HEPES pH 7.4, 50 mM NaCl, 1 mM EDTA, 1 mM EGTA, 1 mM DTT, 5 mM benzamidine, 1 µM PMSF, one Complete Protease Inhibitor cocktail tablet (Roche) per 20 ml buffer, 5% Glycerol, 1% Triton X-100). The lysate was centrifuged for 15-30 minutes at 10,000 g and 4°C and subsequently the supernatant was incubated with 15 – 20 µl GFP-Trap agarose beads equilibrated in lysis buffer. After about 60 – 90 minutes incubation at 4°C under

gentle end-over-end mixing the beads were washed according to the manufacturer's protocol and the GFP-tagged protein and additional bound proteins were eluted by boiling in SDS-sample buffer. Proteins were separated by SDS-PAGE and stained with Coomassie Brillant Blue R 250 or with silver stain (O'Connell and Stults, 1997). Bands of interest were cut out from the gel and analyzed and identified by MALDI-TOF or Orbitrap mass spectrometry (ZfP, LMU Munich).

4.2.2.4 Live-cell microscopy

Cells were transferred into an open glass-bottomed chamber, and washed twice with phosphate buffer (PB, 14.6 mM KH_2PO_4, 2 mM Na_2HPO_4, pH 6.1). Confocal images were taken using an inverted LSM 510 Meta confocal microscope (Zeiss) equipped with a 63x Neofluar 1.4 or a 100x Neofluar 1.3 oil immersion objective. For excitation, the 488-nm argon ion laser line, the 543-nm and the 633-nm helium neon laser lines were used, and emission was collected using 510-525 nm band-pass, 585-615 nm band-pass or a 650 nm long pass filter.

4.2.2.5 Immunoflourescence microscopy

For immunolabeling, Ax2 wild-type or mutant cells settled onto glass coverslips, previously washed with 5% HCl, or cells grown on coverslips were fixed in ice-cold methanol for 10 min or with paraformaldehyde/picric acid (2% paraformaldehyde, 10 mM Pipes, 15% saturated picric acid, pH 6.0) for 20 min and post-fixed with 70% ethanol for 10 min, followed by PBS/glycine and PBG (0.5% BSA, 0.05% fish gelatine, 1xPBS, passed through 0.5 µm filter) followed by three washing steps. Fixed preparations were incubated with monoclonal or polyclonal antibodies, washed three times with PBG and labelled by fluorescence dye-coupled secondary antibodies. F-actin was stained with TRITC-labelled phalloidin. Nuclei were detected with either TO-PRO-3 iodide or DAPI. After staining, coverslips were embedded in Gelvatol and analysed via the microscope.

4.2.2.6 Confocal microscopy

Confocal microscopy data were acquired as described (Weber et al., 1999). All pictures were taken on an inverted Axiovert LSM 510 Meta confocal microscope (Zeiss) with a 63x or 100x oil immersion objective with a numerical aperture of 1.4 and 1.3, respectively. Excitation of fluorophores was achieved with the 488 nm argon ion laser line, the 543 nm and 633 nm helium neon laser lines, and emission was collected using 510-525 nm band-pass, 585-615 nm band-pass or 650 nm long-pass filters. When imaging fluorescent *D. discoideum* mutants, cells were transferred into an open glass-bottomed chamber and recorded at 10-seconds intervals.

4.2.3 Cell biological methods

4.2.3.1 *D. discoideum* cell culture and transformation

D. discoideum Ax2 (laboratory strain wild-type) and mutant cells derived from Ax2 were cultivated axenically (Urushihara, 2006) in sterile HL5 medium (Formedium), either in cell culture dishes, in shaking culture at 150 rpm or on lawns of *K. aerogenes*. For long term storage, cells were frozen in *D. discoideum* storage medium (82% AX-medium, 9% Horse Serum, 9% DMSO) or spores were obtained from phosphate agar plates and frozen in Soerensen buffer pH 6.0 (14.6 mM KH_2PO_4, 2 mM Na_2HPO_4) (Malchow et al., 1972).

D. discoideum wild type or mutant cells were transformed with the appropriate plasmids by electroporation. 2 x 10^7 cells were extensively washed in cold Soerensen buffer and electroporation buffer pH 6.0 (50 mM sucrose, 10 mM KH_2PO_4), resuspended in 1 ml cold electroporation buffer, and then electroporated in the presence of about 25 µg DNA in a 4 mm electroporation cuvette using a Gene Pulser XCell (Biorad) and the standard settings (square wave, V= 1.0 kV, 1 ms pulse length, two pulses, 5 seconds pulse interval). Subsequently the cells were transferred to a cell culture dish and after gentle shaking (50 rpm, room temperature, 15 minutes) 2 µM $CaCl_2$ and 2 µM $MgCl_2$ were added. After another 15 minutes incubation, HL5 medium was added and the cells were allowed to recover for about 24 hours before the respective antibiotic (either 10 µg/ml G418 or 5 µg/ml blasticidin) was added to select the transformants. Single clones were obtained by spreader dilution on *K. aerogenes* lawns. Successfully isolated single clone

transformants were checked by microscopy and Western blot analysis using the appropriate antibodies.

Overexpression mutants were transformed with constructs for the expression of fluorescently labelled proteins (with C- or N-terminal GFP tags). All GFP-constructs were expressed under the actin15 promoter. To generate knock-out mutants, gene replacement constructs with a blasticidin resistance cassette were transformed and successful transformants were checked by PCR analysis.

4.2.3.2 Growth curve

Routinely $2x10^5$ cells were seeded in 30 ml of HL5 medium in a 100 ml flask and incubated at 21°C and 150 rpm on a shaker. The number of cells was determined using a Neubauer chamber at least once a day for the next 1-2 weeks. For each cell type, three independent cultures were counted in parallel.

4.2.3.3 Analysis of cell development

To induce development, cells were washed twice in Soerensen buffer pH 6.0 and adjusted to a density of 10^7 cells per ml in the buffer. Subsequently the cells were transferred to nutrient-free phosphate agar plates. Developmental stages were documented by time-lapse photography.

Lysates of cells were taken every three hours over a period of 24 h to determine protein expression during development by Western blot analysis employing specific antibodies.

4.2.3.4 Phototaxis assay

Phototactic behaviour of wild type and mutants was tested as described previously (Darcy et al., 1994) with minor modifications. Cells from the edges of colonies growing on *K. aerogenes* lawns were transferred with a sterile inoculation loop to water agar plates to form slugs. The plates were transferred into a dark box with a 2 mm wide opening for the entry of light. Plates were incubated at 21°C for at least 48 h. To visualise the slugs and their tracks, cells were transferred onto a nitrocellulose membrane and were stained

with 0.1% amidoblack in 25% 2-propanol and 10% acidic acid for 10 min and destained in water.

4.2.3.5 Immunofluorescence

To study subcellular localisation of proteins within the cell, indirect immunofluorescence was performed. Exponentially growing cells were applied on coverslips which were previously washed with 3.6% HCl and rinsed with H_2O. After allowing the cells to settle on the coverslips the medium was removed and the cells were fixed with -20°C methanol unless otherwise noted. After a 10-15 minute incubation at -20°C, the coverslips were washed several times with PBS (137 mM NaCl, 2.7 mM KCl, 8.1 mM Na_2HPO_4, 1.5 mM KH_2PO_4, pH 7.4) supplemented with 100 mM glycin. Subsequently, the fixed samples were washed with PBG (PBS + 0.5% BSA, 0.045% fish gelatin) and incubated with the primary monoclonal antibody overnight at 4°C. The fixed preparations were washed with PBG and incubated for 60 minutes with the appropriate secondary antibody (goat-anti-mouse IgG Cy3-conjugated, unless otherwise mentioned). DNA was stained with either TO-PRO-3 iodide or DAPI. The stained samples were quickly rinsed with ddH_2O, embedded in gelvatol and stored in the dark at 4°C (Hagedorn et al., 2006).

4.2.3.6 Osmotic shock and determination of cell survival

D. discoideum cells were grown to a density of $3 – 4 \times 10^6$ cells/ml in Erlenmeyer flasks. The cells were centrifuged, and washed in cold Soerensen. Subsequently, the cells were starved in Soerensen under constant shaking at 22°C. 2M sorbitol was added to the culture for a final concentration of 0.8 M sorbitol. One sample was collected before, the other samples were collected after treatment with sorbitol at time points 0, 20, 40, 60 and 120 min. To measure cell survival, a serial dilution was performed and approximately 100 *D. discoideum* cells were plated onto SM agar plates with a non-pathogenic *K. aerogenes strain*. *D. discoideum* plaques were counted after 2 – 3 days of incubation at 21°C (Na et al., 2007).

5 Results

5.1 Ste20-like kinase signalling and cytoskeletal proteins in *D. discoideum* and *R. filosa*

Ste20-like kinases are a group of serine/threonine-kinases that are ubiquitous in all eukaryotic species (Arasada et al., 2006). The name is derived from the Ste20 kinase in *S. cerevisiae.* Ste20-like kinases play an important role in many pathways, for instance the MAP-kinase signal transduction pathways. Other Ste20-like kinases are involved in processes such as apoptosis and morphogenesis (Dan et al., 2002), and can also interact with cytoskeletal proteins. The Ste20-like kinome of *D. discoideum* comprises a total of 17 kinases. These are divided into two subfamilies, the germinal centre kinases (GCK; 13 members) and the p21-activated kinases (PAK; 4 members) (Figure 9). The investigated kinases Fray1, Fray2 and DstC from *D. discoideum* and the newly discovered Ste20 from *R. filosa* all belong to the GCK-family (Figure 6).

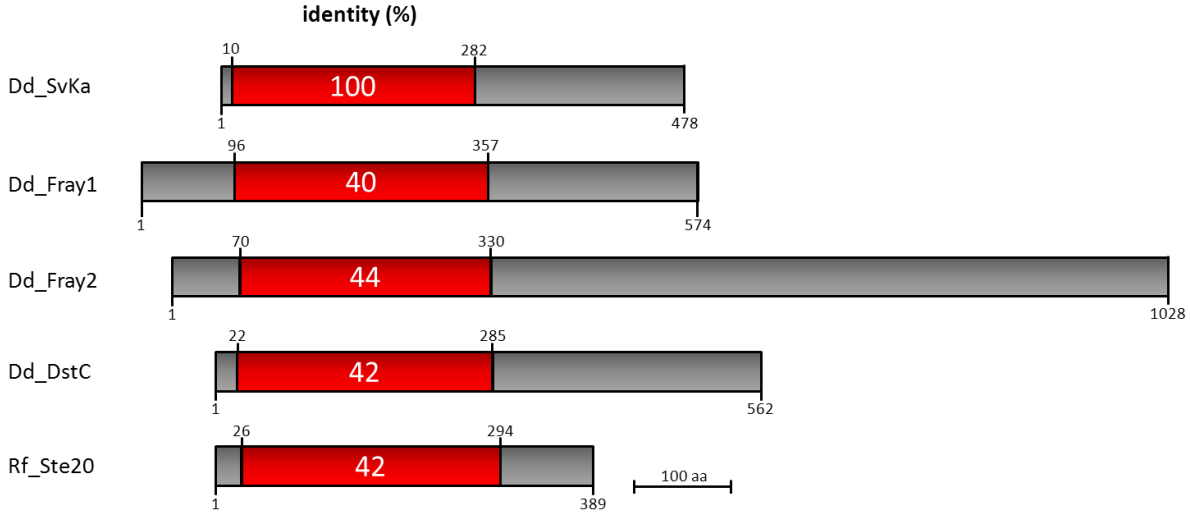

Figure 6: The Ste20-like kinases of this work compared to SvkA from *D. discoideum*
Position and percent identity of the serine/threonine-kinase domains in the investigated kinases Fray1 (Dd_Fray1), Fray2 (Dd_Fray2), DstC (Dd_DstC) from *D. discoideum* and the Ste20-like kinase (Rf_Ste20) from *R. filosa* are depicted in comparison to severin kinase (Dd_SvkA). SvkA was the first Ste20-like kinase that was described in *D. discoideum*. The catalytic domain is highlighted in red and the white numbers display the identity of the catalytic sites to SvkA.

Severin kinase (SvkA) was the first member of the Ste20-like kinases to be described in *D. discoideum. In vitro*, SvkA phosphorylates the actin binding protein severin (Eichinger

et al., 1998). Further on, SvkA is an important regulator for the late stages of cytokinesis (Rohlfs et al., 2007). By using a GFP-Trap resin we identified a novel binding partner of SvkA, the 40 kDa protein Mo25 (morula protein 25) (personal communication, Susanne Köhler). In human Mo25 is known to form a trimeric complex with a pseudokinase and a Ste20-like kinase. Disruption of this complex causes the inherited disease Peutz-Jeghers syndrome (Baas et al., 2003, Boudeau et al., 2004).

We investigated this Ste20-like kinase interacting protein in *D. discoideum* in depth due to its high conservation throughout the eukaryotes (Figure 7).

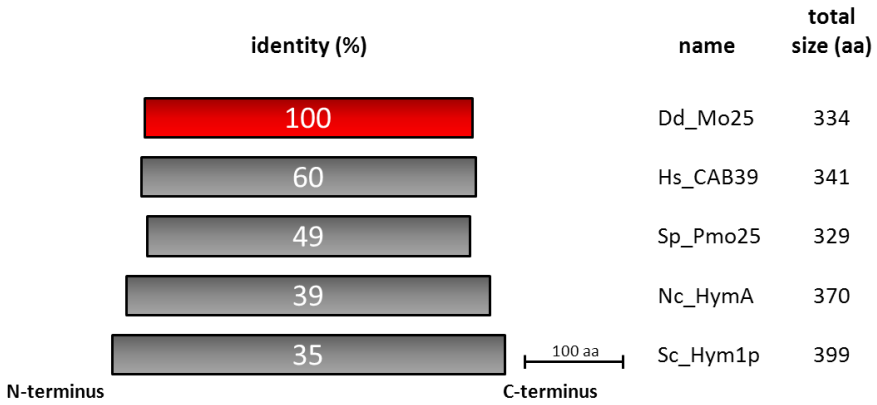

Figure 7: Comparison of the *D. discoideum* Mo25 to other species
Comparison of the full length Mo25 of *D. discoideum* with the corresponding proteins in the other species, namely *H. sapiens* (Hs_CAB39), *S. pombe* (Sp_Pmo25), *Neurospora crassa* (*N. crassa*) (Nc_HymA) and *S. cerevisiae* (Sc_Hym1). The white numbers indicate the identity compared to *D. discoideum* Mo25.

In *D. melanogaster* the Frayed knockout causes severe swelling of neuronal tissue and axonal defasciculation of the nerves (Leiserson et al., 2000a). The kinase domains of the *D. discoideum* Fray1 and Fray2 are 45% and 54% identical to their equivalents Frayed in *D. melanogaster* and OSR1 in *H. sapiens* (Figure 19). Here, we generated the knockout clones Fray1-minus, Fray2-minus, and the double knockout Fray2Fray1-minus in *D. discoideum* for phenotypical investigation.

GFP-constructs of the Ste20-like kinase DstC in *D. discoideum* have been described to localise to actin rich phagocytic cups during uptake of yeast particles (Gergana Gateva, personal communication). Additionally, these GFP-constructs also localise to acidic vesicles in the cell. Here we constructed an array of point mutation constructs that either mimic permanent phosphorylation or cannot be phosphorylated at all, to analyse the localisation of GFP-DstC in further detail.

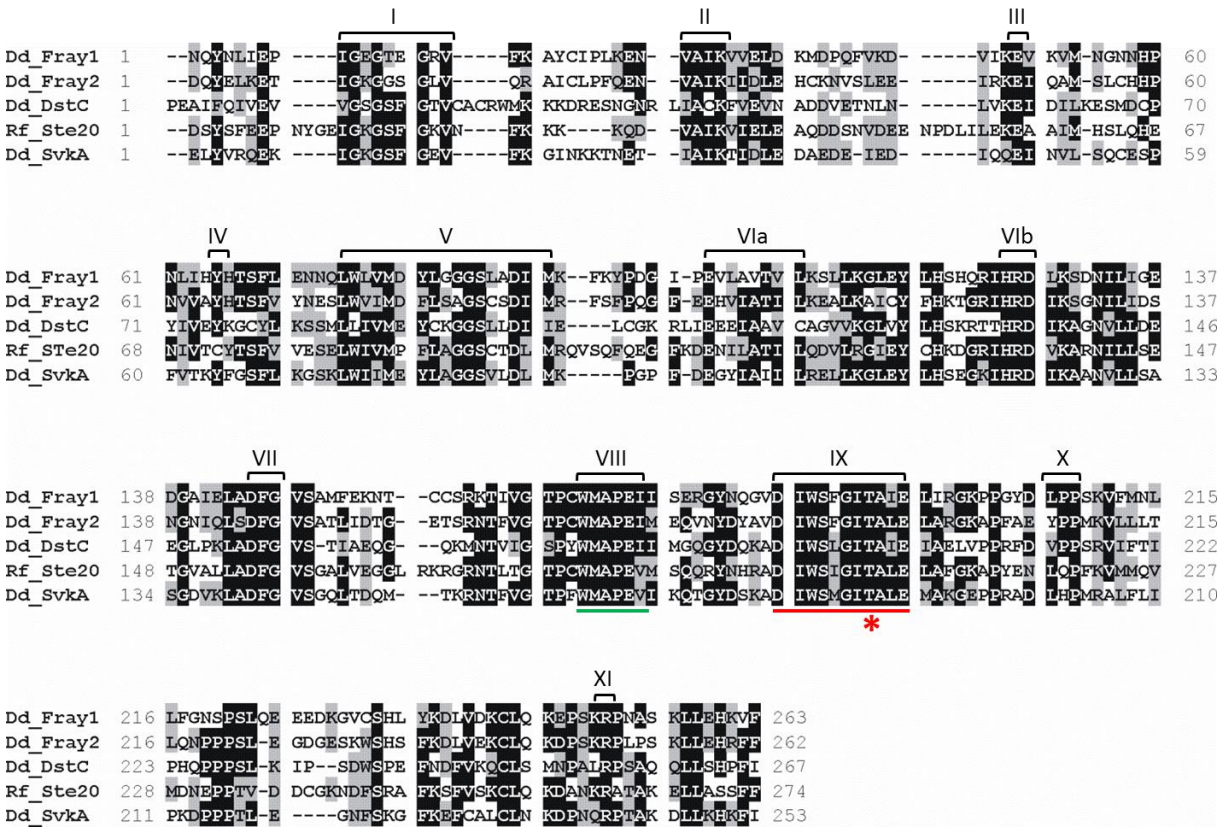

Figure 8: Sequence alignment of the Ste20-like kinases of this work

The Ste20-like kinases Fray1 (Dd_Fray1), Fray2 (Dd_Fray2), DstC (Dd_DstC) and SvkA (Dd_SvkA) of *D. discoideum* and Ste20 (Rf_Ste20) of *R. filosa* are aligned. Roman numerals above the alignment mark the 12 conserved subdomains of the Ste20-kinase group as described (Hanks and Hunter, 1995a). Identical residues have a black, conserved residues a grey background. The green bar indicates the signature motif of the protein kinases which is implicated in recognition of peptide substrates. The red bar indicates the subdomain in which the Threonine (red asterisk) needs to be phosphorylated to activate the kinases. The high level of similarity of the kinase domains is evident.

Recently the whole genome of the fresh water Foraminifera *R. filosa* was totally sequenced. It is the first foraminiferal genome to be deciphered (Glöckner et al., 2014).

In this bioinformatics project, it was the aim to identify, map and characterise potential actin and cytoskeleton-related proteins from the total sequence data. In Figure 8 a sequence alignment of the catalytic domains of the analysed Ste20-like kinases Fray1, Fray2 and DstC from *D. discoideum* and the Ste20-like kinase from *R. filosa* is depicted. The high conservation of the kinase fold and the phosphorylation site (threonine) is apparent.

A

Ste20-like kinases in *Dictyostelium discoideum*		
Dictybase No.	**Kinase**	**Type**
DDB_G0286359	SvkA	germinal-centre-kinases
DDB_G0284181	KrsA	
DDB_G0267978	KrsB	
DDB_G0278863	Fray1	
DDB_G0276577	Fray2	
DDB_G0274593	DstA	
DDB_G0267730	DstB	
DDB_G0291267	DstC	
DDB_G0288071	DstD	
DDB_G0293932	PakE	
DDB_G0274409	PakF	
DDB_G0282891	PakG	
DDB_G0273121 DDB_G0273865	PakH	
DDB_G0269166	PakA	p21-activated kinases
DDB_G0276459	PakB	
DDB_G0267450	PakC	
DDB_G0269696	PakD	

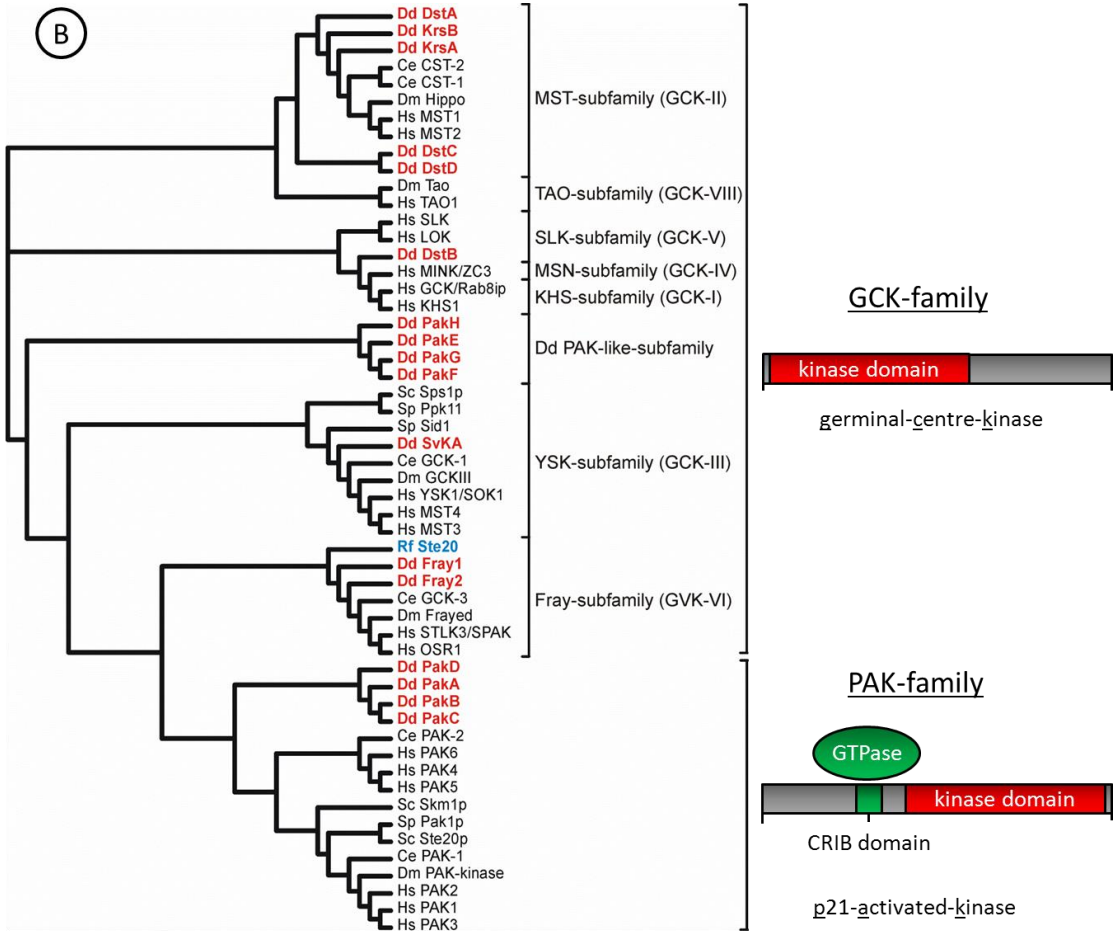

Figure 9: Ste20-like kinases in *D. discoideum* compared to kinases from other species

(A) All 17 members of the Ste20-like kinases of the *D. discoideum* kinome with their name and Dictybase number divided into the two kinase families GCK and PAK. PakH has two Dictybase numbers due to a gene duplication in the genome of *D. discoideum*. (B) Phylogenetic sequence alignment of Ste20-like kinases from *D. discoideum* (Dd) (red), *R. filosa* (Rf) (blue), *H. sapiens* (Hs), *Caenorhabditis elegans* (*C. elegans*) (Ce), *D. melanogaster* (Dm), *S. cerevisiae* (Sc) and *S. pombe* (Sp). The tree was computed using a *MUSCLE*-sequence alignment. The closely related kinases assemble into phylogenetic subgroups. The subgroups can be divided into two major kinase families, germinal-center-kinases (GCKs) and p21-activated-kinases (PAKs). PAK-kinases are characterised by the presence of a GTPase binding domain (green) additional to the Ste20-like kinase domain.

5.2 The protein Mo25 in *D. discoideum*

5.2.1 Mo25 regulates cytokinesis in *D. discoideum*

In *D. discoideum* the *mo25* (DDB_G0284307) gene on chromosome 4, codes for the Mo25 protein with 363 amino acids and a size of 42 kDa. Sequence comparison using MUSCLE showed a very high conservation throughout the eukaryotes. The phylogenetic analysis revealed a 60% identity of Mo25 from amoeba to the calcium-binding protein 39 (CAB39) from human (Figure 10). *D. discoideum* Mo25 modelled with Swiss model to CAB39 of *H. sapiens* (PDB: 2wtkA) exhibited the typical six helical repeats and the clamp-like structure of the protein (Figure 15).

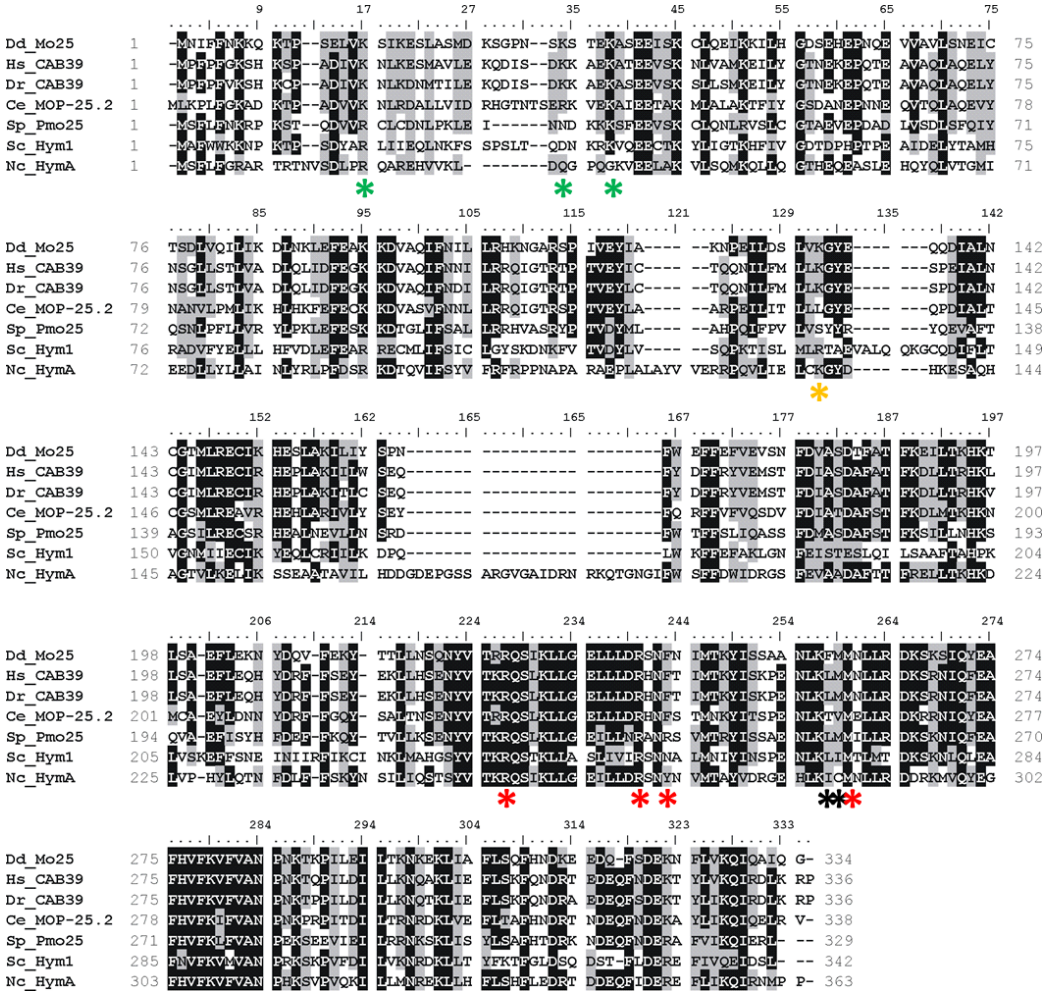

Figure 10: Sequence alignment of Mo25 with other Mo25 proteins

Sequence alignment of Mo25 from *D. discoideum* (Dd) with the corresponding proteins from *H. sapiens* (Hs), *Danio rerio*, (Dr), *C. elegans* (Ce), *S. pombe* (Sp), *S. cerevisiae* (Sc) and *N. crassa* (Nc). The coloured asterisks mark the positions of the *D. discoideum* Mo25 in which point mutations were introduced. Identical residues have a black, conserved residues a grey background. The high level of conservation throughout the eukaryotes is apparent.

5.2.2 Generation of Mo25-minus cells

To analyse the function of Mo25, Ax2 wild type cells were transformed with a gene replacement construct. The *mo25* gene was disrupted by replacing the core region with a blasticidin-S-resistance cassette by homologous recombination (Figure 11). Two independent Mo25-minus clones were generated (personal communication, Susanne Köhler).

The Mo25-minus clones were identified by polymerase chain reaction (PCR).

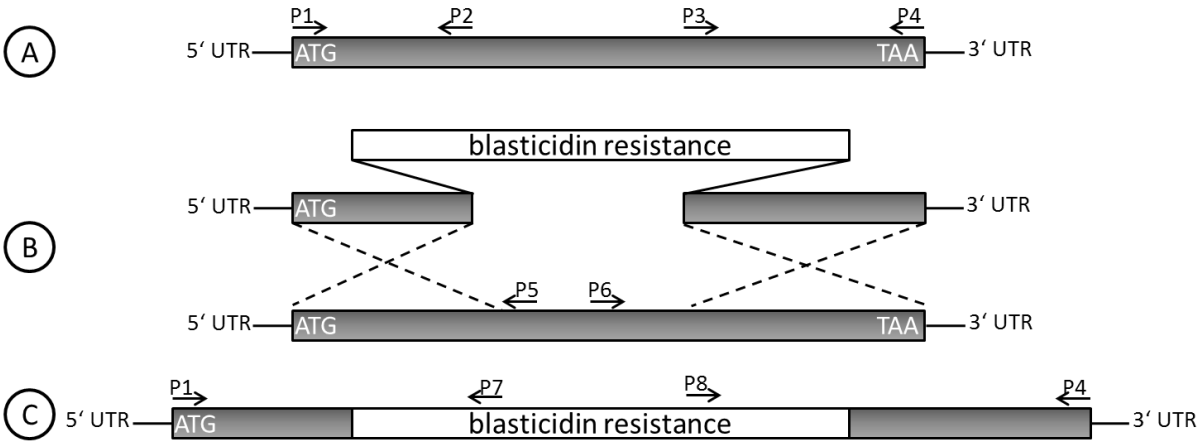

Figure 11: Generation of Mo25-minus mutants
(A) To disrupt the *mo25* gene, a 5'-prime and a 3'-prime fragment were amplified by PCR from genomic DNA and cloned into a blasticidin-S-resistance cassette containing pLPBLP vector (Faix et al., 2004). (B) The resulting construct was transformed into wild type cells. (C) The disruption of the gene was achieved through homologous recombination. The successful recombination events were verified by PCR and later confirmed by the absence of Mo25 in Western blots.

5.2.3 Mo25-minus cells exhibited a severe cytokinesis defect and an altered developmental phenotype

The initial characterisation of the phenotype of the Mo25-minus cells was carried out by Susanne Köhler during her diploma thesis in the institute (Diploma thesis, Susanne Köhler, 2009). Flourescence images showed that Mo25-minus cells were drastically larger than wild type cells (Figure 12).

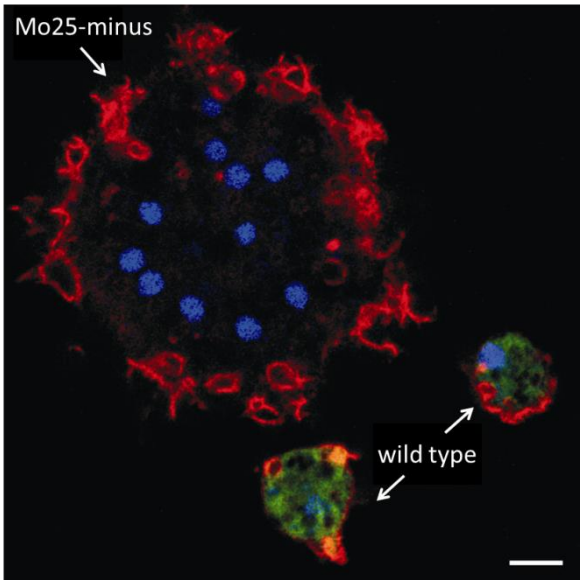

Figure 12: Mo25-minus cells exhibited a severe phenotype
Mo25-minus and wild type cells expressing GFP (green) were mixed, fixed with -30°C methanol and stained with anti-actin (red) and the DNA stain ToPro-3 (blue). The Mo25-minus cell was 10 fold bigger and multi-nucleated as compared to wild type cells (bar = 10 µm).

The quantification of nuclei showed that in Mo25-minus cells 60% of all nuclei were in cells with more than four nuclei. In contrast, in wild type cells nearly all nuclei were in cells with only one or two nuclei. Expression of the Mo25-GFP construct rescued this phenotype completely. When grown in shaking culture the Mo25-minus cells grew slower and to a lower density compared to the wild type. Also the growth rate on a bacterial lawn was delayed and colony sizes were much smaller. The starvation-induced development was delayed in cells lacking Mo25, whereas the wild type streamed and aggregated. During the developmental cycle *D. discoideum* forms an intermediate, the so called slug, comprised of several thousand cells that can move towards light, before continuing with the formation of fruiting bodies. The Mo25-minus cells were able to form these slugs, but they were largely immobile compared to the wild type.

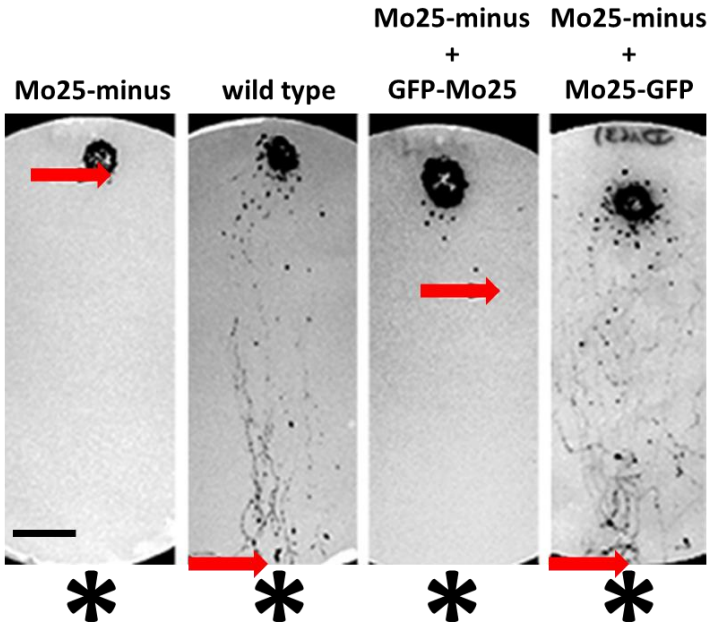

Figure 13: Mo25-minus revealed a loss of slug movement
The red arrows indicate the maximum run length of the slugs. The Mo25-minus strain was able to form slugs but they were unable to move towards the light source (black asterisks). The rescue construct with the GFP at the N-terminus was not able to revert the phenotype completely to wild type, whereas the the construct with the GFP at the C-terminus rescued the defect completely (bar = 1cm)

Interestingly, rescue experiments with GFP constructs of Mo25 showed that the N-terminal fusion could only partially rescue the slug motility defect, indicating that the GFP hindered the function of Mo25 in slug movement. On the other hand, a Mo25 construct with a C-terminal GFP tag fully rescued this motility defect (Figure 13).

5.2.4 Interaction of Mo25 with SvKA

As mentioned before, Mo25 was identified as interacting partner of the Ste20-like kinase SvkA. The structure of Mo25 seems to be so conserved, that *E. coli* expressed GST-tagged Mo25 constructs from *H. sapiens*, *Danio rerio* and *D. discoideum* interacted with SvkA from *D. discoideum* (Figure 14). This shows the tremendous conservation of the Mo25/Ste20-like kinase interface in evolution.

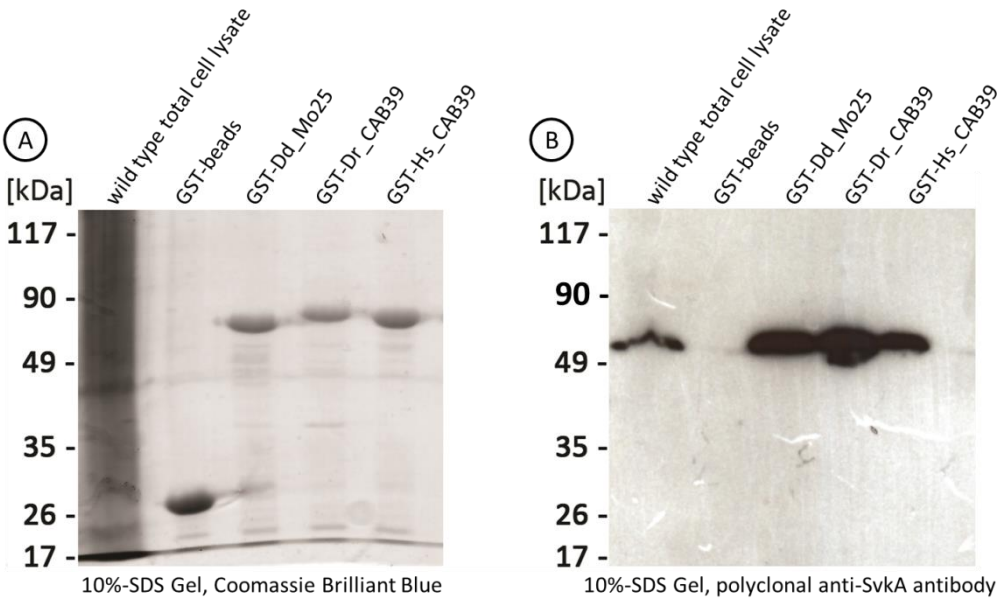

Figure 14: Mo25 from *H. sapiens*, *D. rerio* and *D. discoideum* interacted with SvkA
(A) *E.coli* expressed GST-tagged Mo25 constructs from *H. sapiens* (Hs), *D. rerio* (Dr) and *D. discoideum* (Dd) were incubated with lysate from wild type *D. discoideum* cells, separated by SDS-PAGE and stained with Coomassie Brilliant Blue. (B) Western blot analyses of the pulldown experiment using an anti-SvkA antibody. All GST-tagged Mo25 constructs were able to pull down SvkA from *D. discoideum* wild type lysate. GST was used as a control.

5.2.5 Generation of Mo25 point mutations

In order to further investigate the interaction of Mo25 and SvkA, we generated several Mo25-GFP rescue constructs with distinct point mutations. These mutations cover sequence areas already known to be essential for binding (Boudeau et al., 2003) as well as putative binding areas that were obtained from sequence and structural data analysis (Figure 15). We calculated a model of *D. discoideum* Mo25, using the three dimensional structures of human Mo25 (CAB39) co-crystallised with the Ste20-like kinases STRAD and LKB1. Areas outside the Mo25/Ste20-like kinase interface were considered as potential binding sites for so yet unknown interacting proteins and integrated into the mutational screens.

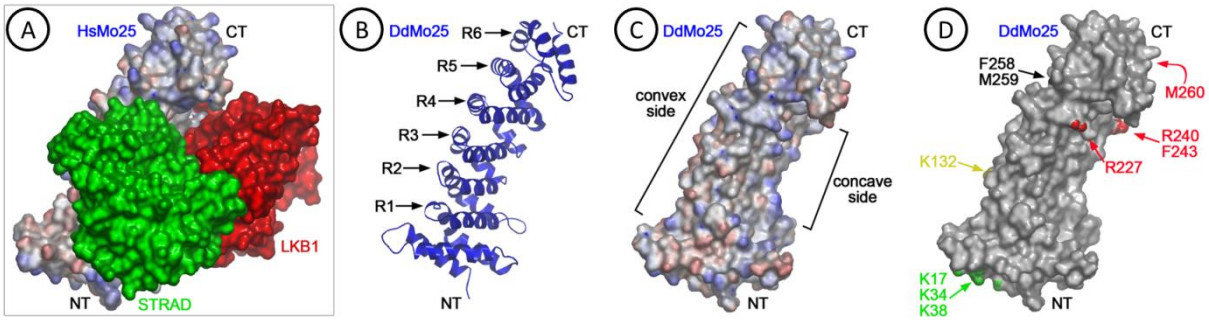

Figure 15: Mutational screen of *D. discoideum* Mo25

(A) A 3D-structure of human CAB39 paired with the two interacting proteins STRAD and LKB1. (B) The *D. discoideum* Mo25 modelled to human CAB39 (PDB: 2wtkA) exhibited the characteristic six helical repeats. (C) *D. discoideum* Mo25 could be modelled into the distinct clamp like structure with a convex and a concave side. (D) Based on the known binding sites from published sequence and structural data analyses, distinct point mutations were introduced into the Mo25 sequence.

We introduced eight different point mutation constructs, each one containing one or two distinct point mutations as summarised in Figure 15 and Figure 16.

In human Mo25 R227 and M260 are known to be key players for the binding of the pseudokinase STRAD whereas R240 and F243 are needed to bind the kinase LKB1.

As the rescue construct of Mo25 with GFP tag at the N-terminus of the protein was not able to revert the abnormal phenotype, we expected the GFP to block potential binding sites. Therefore, amino acids K17, K34 and K38 were chosen because of their prominent exposure at the N-terminus. The residue K132 was selected for being a very conserved positively charged island on the convex side of the protein amidst an otherwise negatively charged surface.

The mutations F258A and M259A, also located on the surface of the Mo25 protein, were chosen randomly as an internal control mutation to test whether a mutation itself affects the properties of the protein (Figure 16). All chosen amino acid sites were mutated to nonpolar, alanine or to polar glutamine. Every point mutation construct was introduced into a GFP expression vector (pDex-GFP-C2) with a C-terminal GFP tag and subsequently transformed into a Mo25-minus background.

Side chain	Function
R227A	humanSTRAD binding
R240A & F243A	humanLKB1 binding
M260A	humanSTRAD/WEF-domain binding
K17A	basic spikes at NT
K34A	basic spikes at NT
K34A & K38Q	basic cluster at NT
K132A	conserved positive island at convex surface
F258A & M259A	internal control mutation

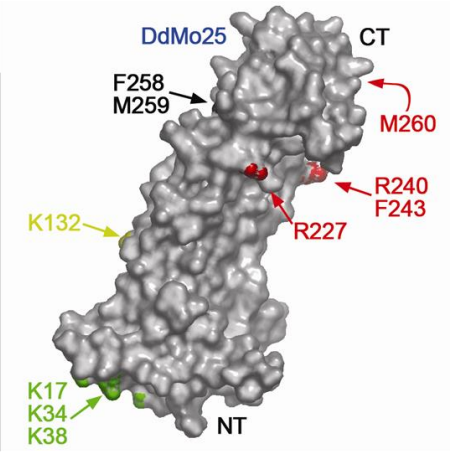

Figure 16: Location and function of the point mutations introduced into Mo25
List of the point mutations introduced into Mo25. The first three mutations (red) are the known STRAD and LKB1 binding sites. The second batch of mutations (green) on the N-terminal end of the protein was chosen from structural analyses of the protein. The only mutation (yellow) on the convex side of Mo25 was introduced due to the fact that this site is highly conserved and has an exposed position as a positively charged island amidst an otherwise negatively charged surface. Another random mutation (black) was introduced to check if a mutation in principle affected the function of the protein.

5.2.6 Mutated constructs of Mo25 have an effect on cytokinesis and slug motility

To test the effect of the point mutations on directional slug movement and cytokinesis, we performed slug motility assays and quantified the number of nuclei per cell of every mutant strain with the point-mutated construct. If one of the selected residues was necessary for either slug motility or cytokinesis or both, the Mo25-minus phenotype should not be rescued by the respective mutated construct. Whereas, if the selected residue was neither crucial for the regulation of slug motility nor cytokinesis, the introduced point mutation construct should revert the Mo25-minus phenotype to wild type behaviour. As expected, Mo25 and M260A were essential for slug dynamics and cytokinesis. Surprisingly, R227A had almost no effect on slug motility but only a severe impact on cytokinesis. The mutations R240A and F243A had no effect on cytokinesis and only a moderate influence on slug motility. All other mutations had milder effects on cytokinesis as well as on slug motility (Figure 17).

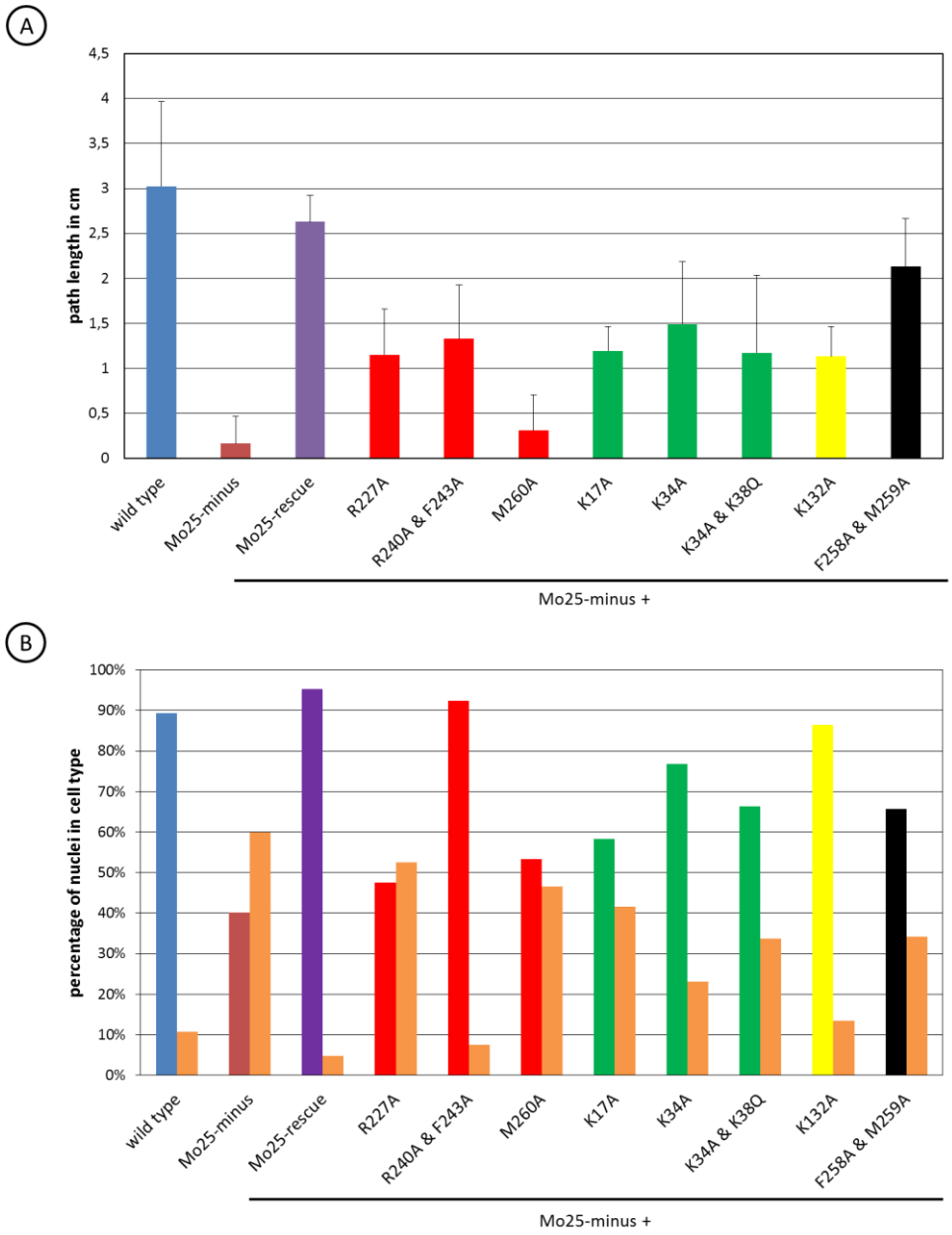

Figure 17: The different Mo25 point mutation constructs had effects on slug motility and cytokinesis

(A) Compared to the wild type, in Mo25-minus slug motility was completely abolished. Mo25 is essential for slug motility. The Mo25-rescue construct restored slug motility almost completely. Whereas M260 was absolutely crucial for Mo25 mediated slug motility, R240 & F243 and R227 played a less important role. K17, K34, K34 & K38 and K132 also had a smaller function in slug motility. The control mutations E258 & L259 did not affect directed slug motility. (B) Multicoloured bars indicate the percentage of nuclei in cells with one or two nuclei, whereas orange coloured bars depict the percentage nuclei in cells with three or more nuclei. Mo25 is essential for cytokinesis. In wild type 90% of the nuclei were in cells with one or two nuclei whereas in Mo25-minus only 40% of the nuclei were in mono- or di-nucleic cells and 60% of the nuclei were in multi-nucleic cells. Mo25-rescue restored the minus phenotype completely. R227 and M260 exhibited a phenotype comparable to the Mo25-minus, contrary to R240 & F243 which did not affect cell division at all. The sites K17, K34 and K34 & K38 also affected cytokinesis but with less impact. The modification of K132 as well as L258 & M259 did not hinder the separation of cells in any case.

5.2.7 Interaction of Mo25-point mutated constructs with SvkA

To further investigate the interaction of the Mo25 point mutated proteins with SvkA we performed glutathion-S-transferase pulldowns. Therefore, all point mutations were cloned into a GST-tag expression vector. The expressed proteins were incubated with wild type lysates. All GST-point mutation constructs interacted with Svka (Figure 18).

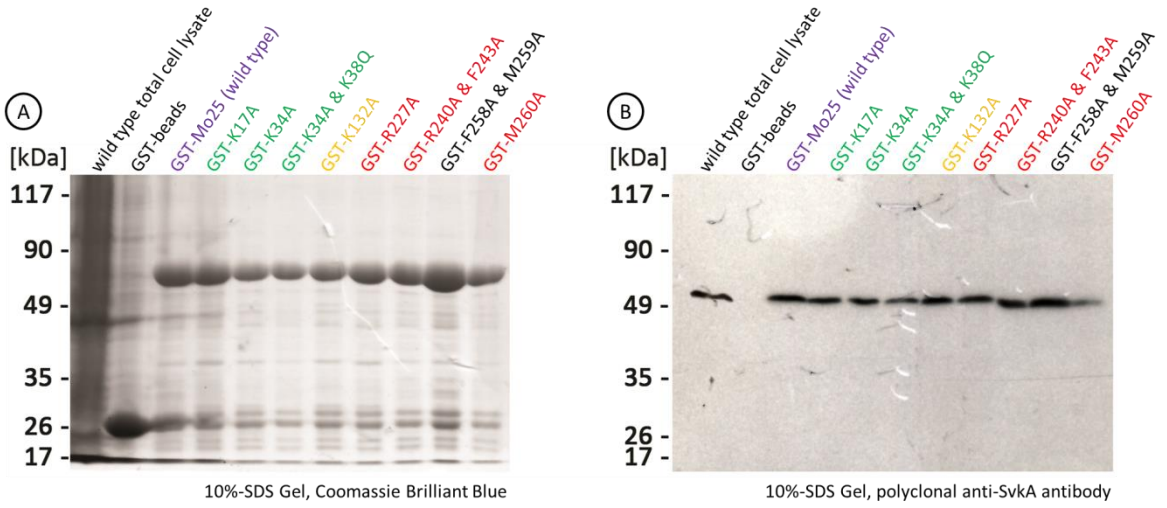

Figure 18: Recombinant expressed Mo25 point mutation constructs were able to pull down SvkA

(A) E. coli expressed GST-tagged Mo25 point mutation constructs were incubated with total cell lysate from wild type *D. discoideum* cells, separated by SDS-PAGE and stained with Coomassie Brilliant Blue. (B) The pull down of SvkA from *D. discoideum* wild type lysate with different Mo25 point mutation constructs subjected to Western blot analyses. SvkA was detected using an anti-SvkA antibody. All Mo25 point mutation constructs were able to pull down SvkA. GST was used as a control.

5.3 The Ste20-like kinases Fray1 and Fray2 of *D. discoideum*

5.3.1 Fray1 and Fray2 in *D. discoideum*

The *fray1* (DDB_G0278863) gene is located on chromosome 3, while the gene for *fray2* (DDB_G0276577) is located on chromosome 2 of the *D. discoideum* genome. These genes code for the serine/threonine kinases Fray1 with 574 aa (64 kDa) and Fray2 with 1,028 aa (116 kDa). The kinase domains of Fray1 (amino acid residue 95 to 358) and Fray2 (amino acid residue 69 to 331) contain the characteristic Ste20 group subdomains I to XI (Figure 8) as described (Hanks and Hunter, 1995a). Furthermore, they are highly homologous to the kinase domains of Frayed in *D. melanogaster* and OSR1 and SPAK (Ste20-related

proline-alanine-rich kinase) in *H. sapiens* (Delpire and Gagnon, 2008) which are known to be key players in the regulation of ion homeostasis and volume control. Identities were determined employing BLASTp (Figure 19).

A

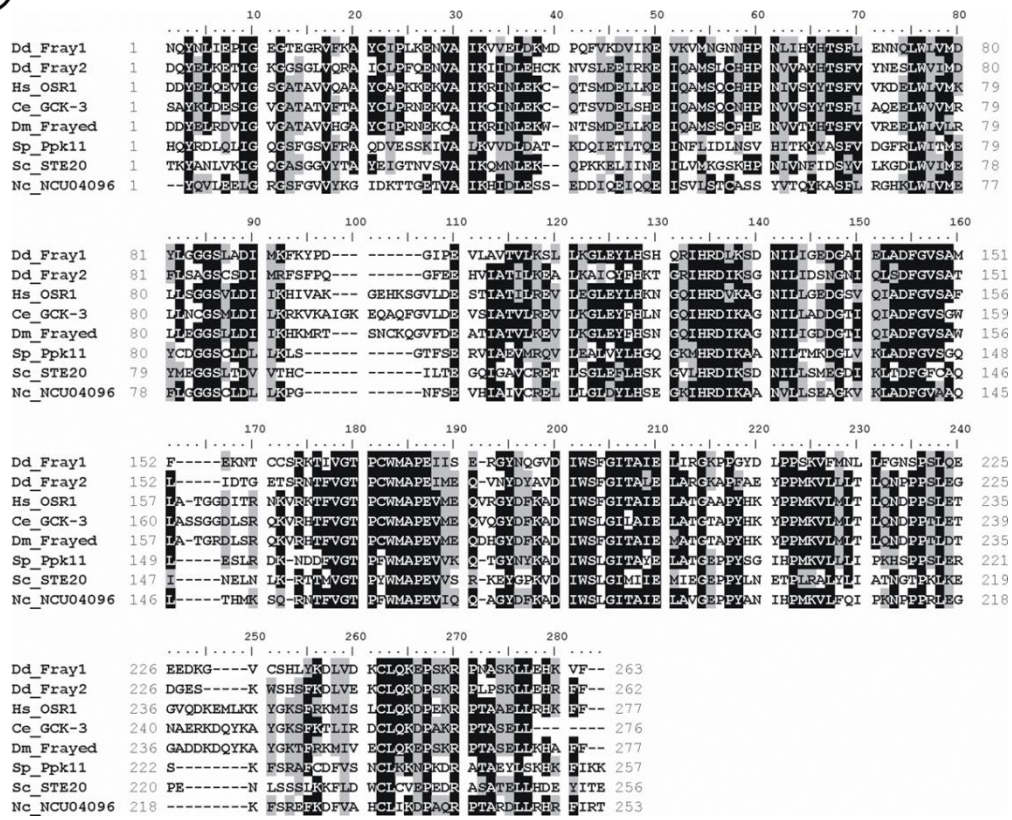

B

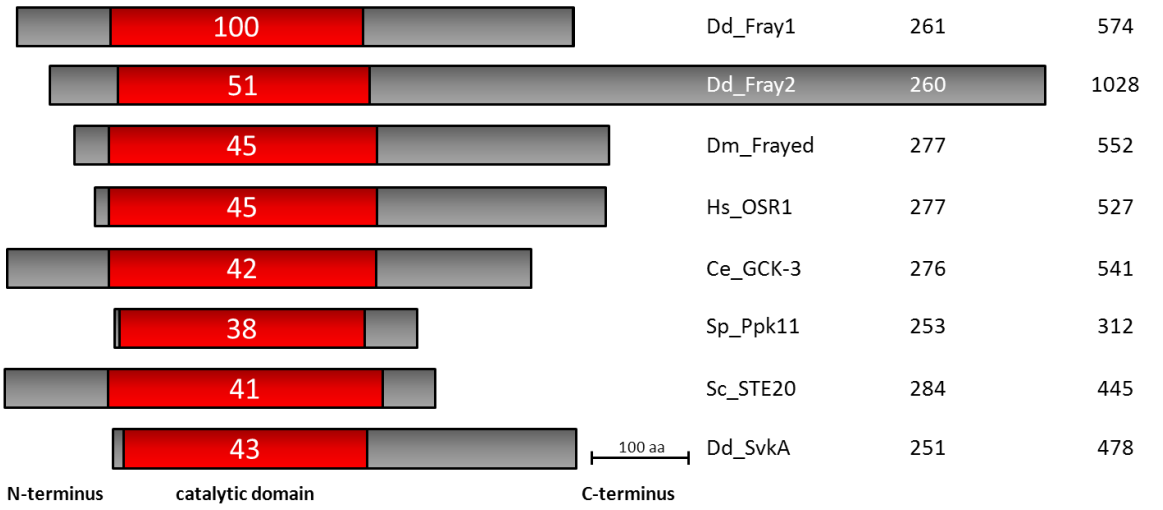

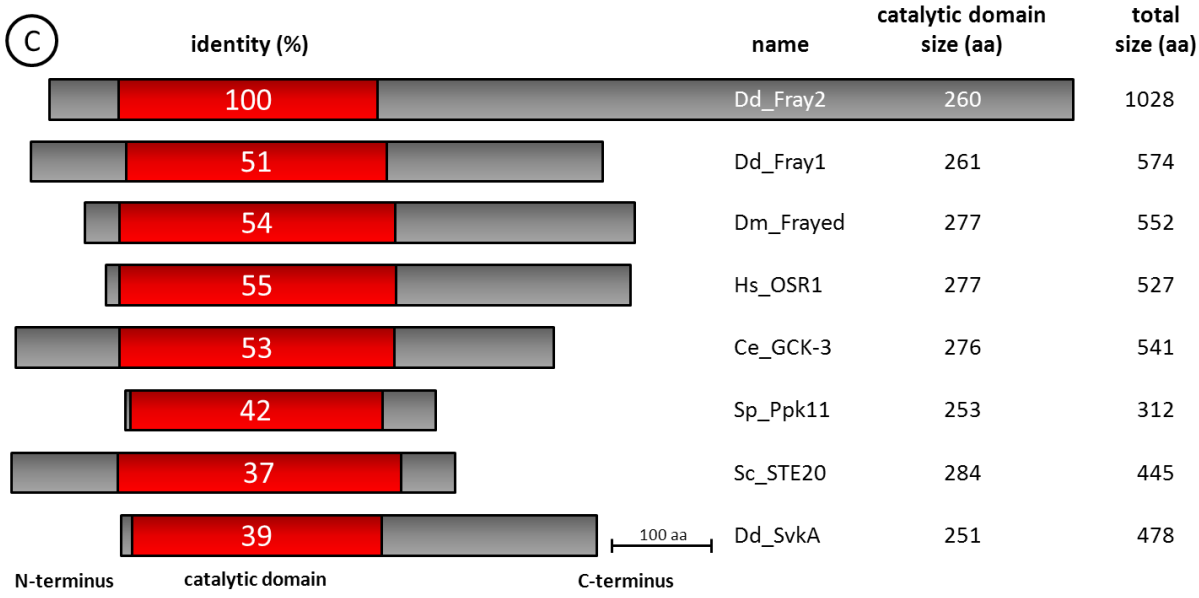

Figure 19: Kinase domains of the *D. discoideum* Fray1 and Fray2 are very similar to the corresponding domains in other species

(A) Sequence alignment of the catalytic domain of Fray1 and Fray2 from *D. discoideum* (Dd) with the corresponding proteins from *H. sapiens* (Hs), *C. elegans* (Ce), *D. melanogaster* (Dm), *S. cerevisiae* (Sc), *S. pombe* (Sp) and *N. crassa* (Nc). Identical residues have a black, conserved residues a grey background. The sequences are highly conserved. (B) Comparison of the catalytic site of Fray1 of *D. discoideum* with the corresponding proteins from other species. The white numbers indicate the identity of the domains compared to *D. discoideum* Fray1. (C) The catalytic domain of Fray2 compared to Fray analogues in different species.

5.3.2 Generation of Fray1 and Fray2-minus cells

In order to investigate the function of Fray1 and Fray2, minus mutants were generated using the procedure described in 3.2.2 (Figure 11). Thus, translation of the *fray1*-mRNA should terminate before kinase subdomain I and the *fray2*-mRNA between the subdomains VIb and VII. By this method we obtained the knockout clones Fray1-minus, Fray2-minus and the double knockout Fray2Fray1-minus. Additionally, we generated a Fray1-overexpression strain by introducing a *fray1*-DNA-construct into the pDex-GFP-N1 GFP-expression vector and subsequently transformed it into a wild type background. However, most likely due to the length of *fray2*, the construction of a GFP-*fray2* fusion was not successful. The different gene disruption events were validated using PCR (Figure 20).

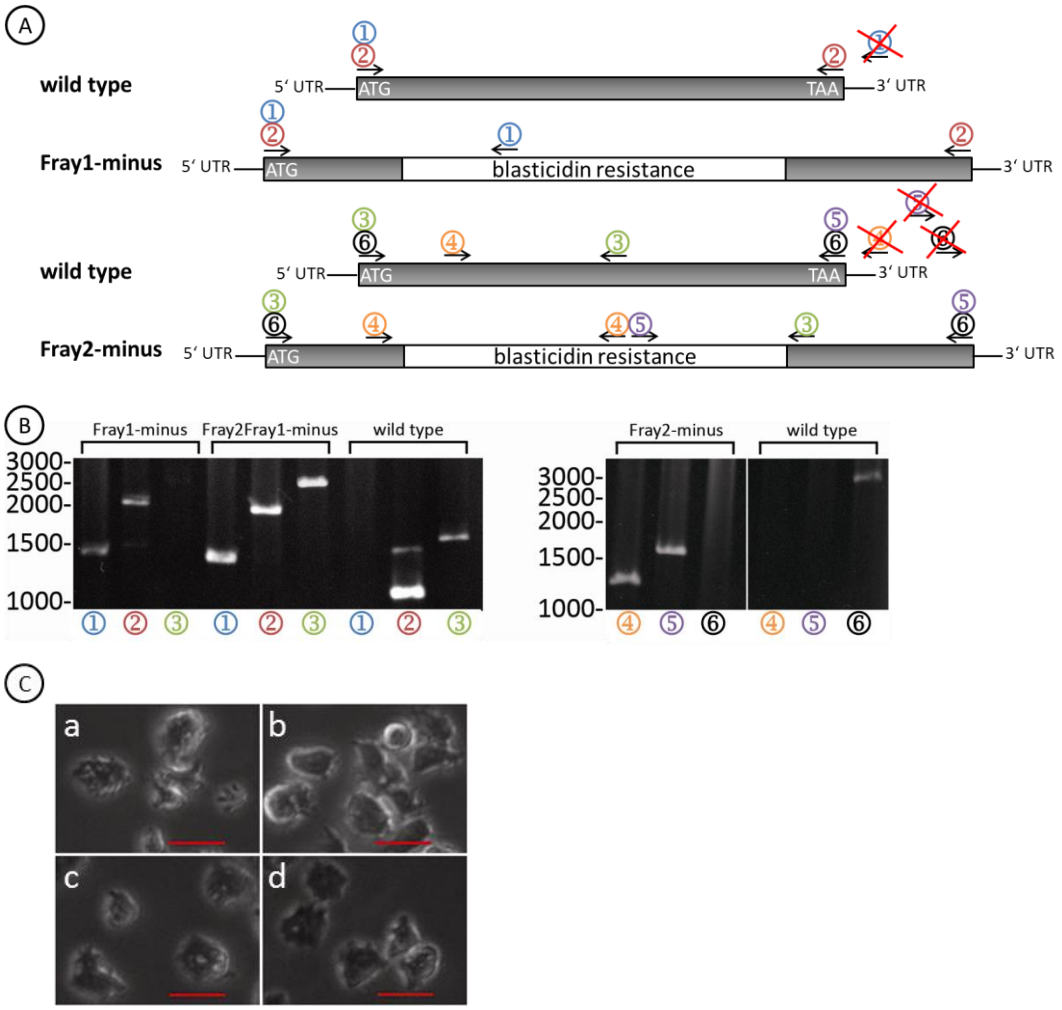

Figure 20: Generation of Fray1-, Fray2- and Fray2Fray1-minus mutants

(A) The scheme shows the fray1 and fray2 gene with the primer combinations used for the verification of the minus mutants. The coloured numbers in circles indicate the different primer combinations used. (B) Expected sizes of PCR fragments for the primer combination ① were 1.5 kbp in the fray1-minus and no amplification in the wild type. For the amplification of the primer pair ② 2.3 kbp in the fray1-minus and 1.1 kbp in the wild type were predicted. For the primer of ③ an amplification of 1.8 kbp in the fray1-minus and the wild type and 2.5 kbp for the fray2-minus was expected. For primer pair ④, a PCR-product with 1.25 kbp was calculated for the fray2-minus and none in the wild type. With primer combination ⑤ an amplification band in the 1.6 kbp region for fray2-minus should have appeared and none for the wild type. With the primer pair ⑥ no product was expected in the fray2-minus and a of 3.0 kbp PCR product in the wild type. (C) The knockout cells exhibited no phenotype that was significantly different from the wild type. (a) wild type, (b) Fray1-minus, (c) Fray2-minus and (d) Fray2Fray1-minus (bars = 20µm).

5.3.3 Fray1-GFP was distributed throughout the whole cell

To check a possible localisation of Fray1, the GFP-Fray1-overexpression strain was mixed 1:1 with the wild type. The cells were fixed with methanol and stained with polyclonal antibodies against Fray1 (red) and actin (blue). Confocal images show that Fray1 fusion

protein was distributed throughout the whole cell but could not be traced in the nucleus (Figure 21). Whereas the Fray1 overexpression construct could be stained by the antibody, an endogenous protein was not visible.

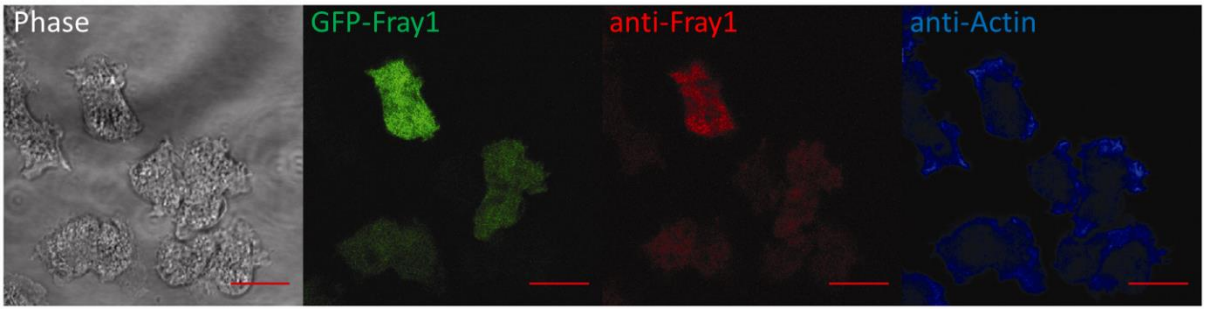

Figure 21: Fray1-GFP did not localise to distinct subcellular regions
Confocal images of a 1:1 dilution of wild type cells and a Fray1-GFP overexpressing wild type strain revealed that GFP-Fray1 (green) was distributed throughout the whole cell. Cells were fixed with -30°C methanol and stained with anti-Fray1 (red) and anti-Actin (blue) (bars = 10µm).

5.3.4 Development of Fray1, Fray2 and Fray1Fray2-minus cells was normal

In developmental studies, Fray2-minus did not show an altered phenotype, whereas Fray1-minus and Fray2Fray1-minus developed slightly slower compared to the development of wild type (Figure 22). Also the average run length of phototactic slugs of wild type, Fray1-minus, Fray2-minus and Fray2Fray1-minus was comparable (data not shown).

By using real time-PCR the mRNA transcription levels of *fray1* and *fray2* were evaluated (Figure 23). RNA samples from a 24 hour developmental time course of *D. discoideum* were taken and analysed. As presented in Figure 23, *fray1* and *fray2* had both very low transcription levels throughout the whole *D. discoideum* life cycle. Only at time point 24 hours, which represents the very last stage of development, the transcription level was slightly increased. This essay was performed in collaboration with the group of Prof. Dr. Angelika Noegel (Universität zu Köln, Germany).

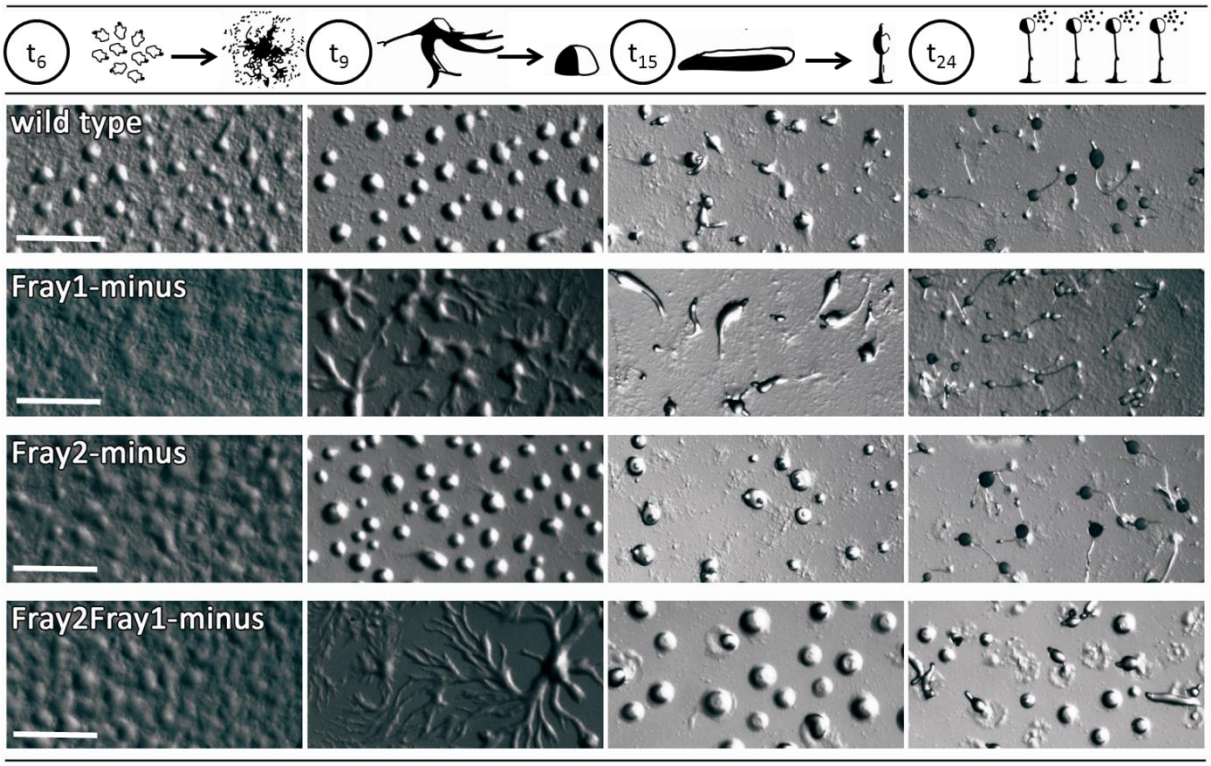

Figure 22: Development of Fray1-, Fray2- and Fray2Fray1-minus cells was normal
Wild type and Fray1-, Fray2- and Fray2Fray1-minus cells were recorded during different stages of development on phosphate agar plates. Fray2-minus cells developed comparable to the wild type, whereas Fray1- and Fray2Fray1-minus cells developed slightly slower (bars = 1cm)

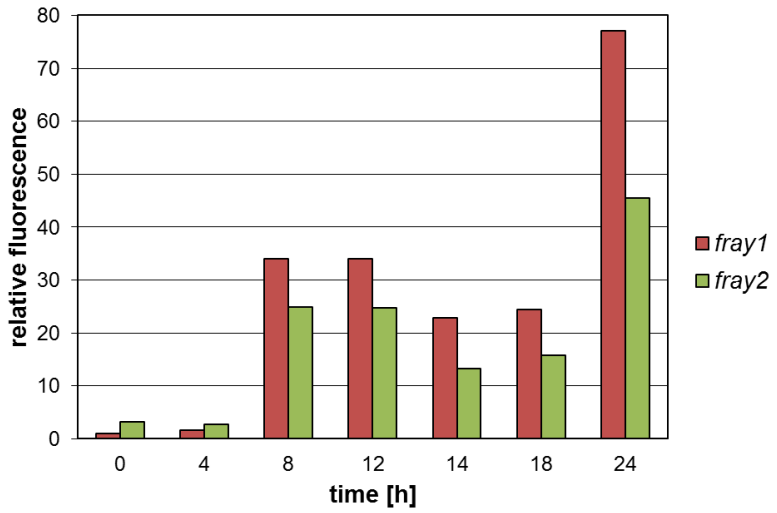

Figure 23: Transcription rate of the *fray 1* and *fray2* genes throughout the development of *D. discoideum*
Real-time -PCR of total RNA samples from defined time points during development revealed that the transcription of *fray1* and *fray2* was very low throughout. Nevertheless, transcription increased in the later stages of development.

5.3.5 Growth of Fray1, Fray2 and Fray2Fray1-minus

When grown in shaking culture, the Fray mutants reached higher densities compared to the wild type. The Fray2Fray1-minus showed a slight growth defect as it grew slower than the other cell lines but reached comparable densities (Figure 24A). Growth on bacterial lawn was not affected by the absence of Fray1, Fray2 or both (Figure 24B).

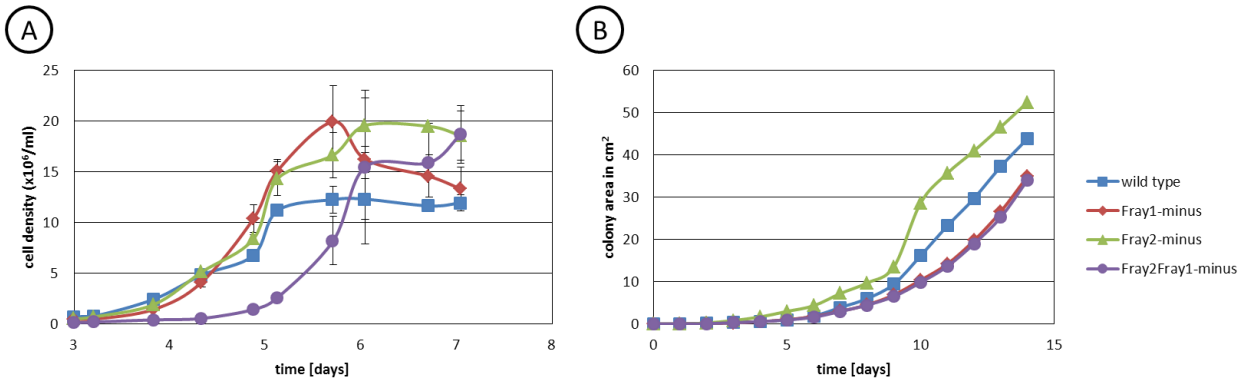

Figure 24: Deletion of Fray1, Fray2 or both did not affect growth
(A) Growth rates of wild type, Fray1-, Fray2-, and Fray2Fray1-minus cells in HL5 medium under shaking conditions. The growth of the minus strains was almost equivalent to the wild type. Although the minus strains grew to a higher density than the wild type. (B) Growth of wild type, Fray1-, Fray2-, and Fray2Fray1-minus cells on lawns of non-pathogenic *K. aerogenes*. The diameter of the different *D. discoideum* strains were measured and colony sizes were calculated. All tested strains reached almost identical sizes.

5.3.6 Osmotic shock survival

To further examine the function of the Fray proteins the minus mutants were treated with osmotic shock. Briefly, cells in shaking culture were starved for one hour and subsequently exposed to hypertonic conditions (0.8 M sorbitol). Samples were taken at defined time points and plated onto bacterial lawn, a sudden disappearance of osmotic pressure. The emerging single colonies represented the surviving cells and were counted (Figure 25).

While the wild type cells were not affected by the exposure to osmotic shock, the survival of knockout strains Fray1-minus, Fray2-minus and Fray2Fray1-minus was reduced.

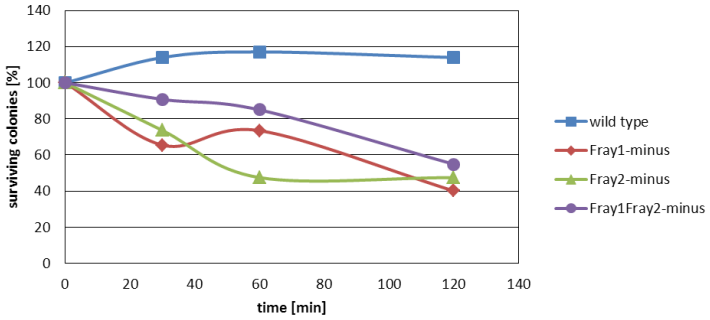

Figure 25: Osmotic shock affected Fray1-, Fray2- and Fray2Fray1-minus
Survival of wild type, Fray1-, Fray2-, and Fray2Fray1-minus cells when exposed to osmotic shock. Cells were subjected to a hypertonic environment and samples were taken every 20 minutes and plated on lawns of non-pathogenic *K. aerogenes*. Appearing colonies were counted.

5.3.7 Fray1 interacting partner FRIP

By using a GFP-Trap resin we identified a binding partner of Fray1, a yet unknown protein that we named FRIP (Fray Interacting Protein) (Figure 27). The *frip* (DDB_G0288201) gene is found on chromosome 5 in *D. discoideum* and codes for a 313 aa (35 kDa) protein. FRIP mainly consists of two CBS (cystathionine-beta-synthase) domain pairs (Figure 26) and is 30% identical to the non-catalytic gamma subunit (AMP-prkag) of the AMPK complex in *D. discoideum*.

A

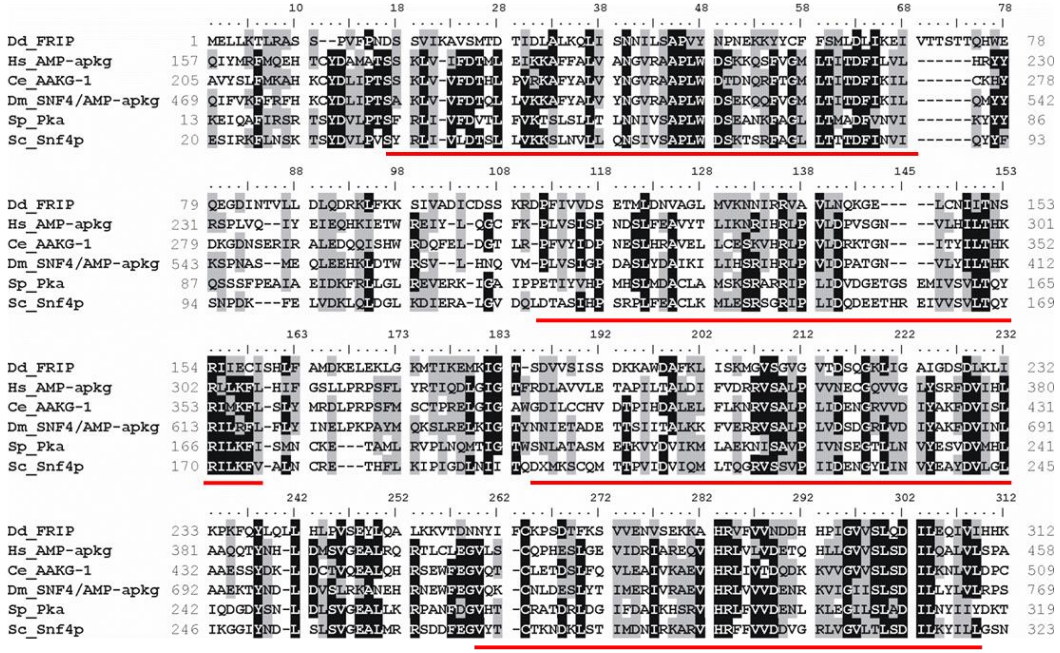

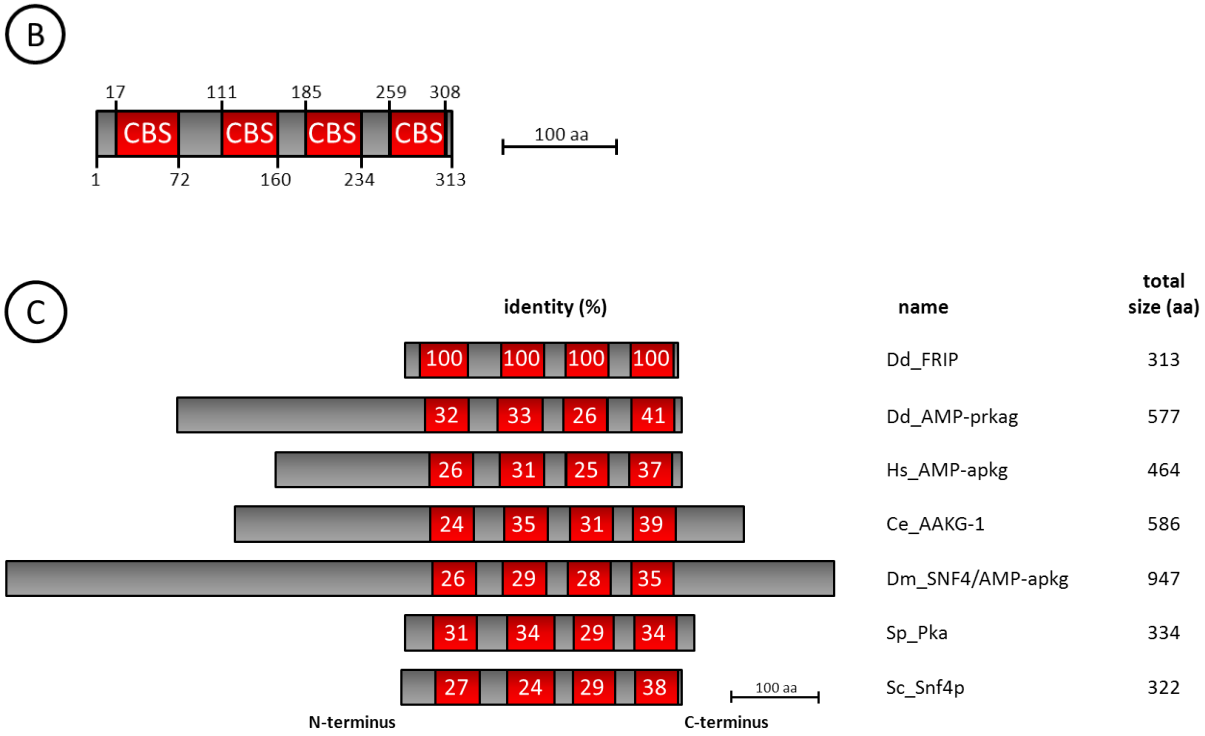

Figure 26: The structure of *D. discoideum* FRIP is conserved
(A) MUSCLE Sequence alignment of CBS domain pairs of FRIP and AMP-prkag from *D. discoideum* (Dd) with corresponding proteins from *H. sapiens* (Hs), *C. elegans* (Ce), *D. melanogaster* (Dm), *S. cerevisiae* (Sc) and *S. pombe* (Sp). The red bars indicate the CBS-domains. Identical residues have a black, conserved residues a grey background. The domain structure is conserved throughout the eukaryotes. (B) *D. discoideum* FRIP with the four CBS domains that form the distinct CBS module. (C) The CBS domains of FRIP and AMP-prkag from *D. discoideum* compared in length and identity to CBS modules from different species. The CBS domains are depicted in red and the white numbers display the identity to FRIP of *D. discoideum*.

A *frip*-minus construct was designed and transformed into wild type cells and a FRIP-minus mutant strain was obtained and verified using PCR.

The phenotype of the FRIP-minus cell line was comparable in size, shape and behaviour to the wild type. When tested for growth in shaken suspension the FRIP-minus only showed a slight retardation in growth and did not grow to the same density like the wild type. When grown on bacterial lawn, the expansion of the FRIP-minus strain colonies was reduced compared to the wild type as well as the survival rate when exposed to hypertonic conditions (0.8 M sorbitol).

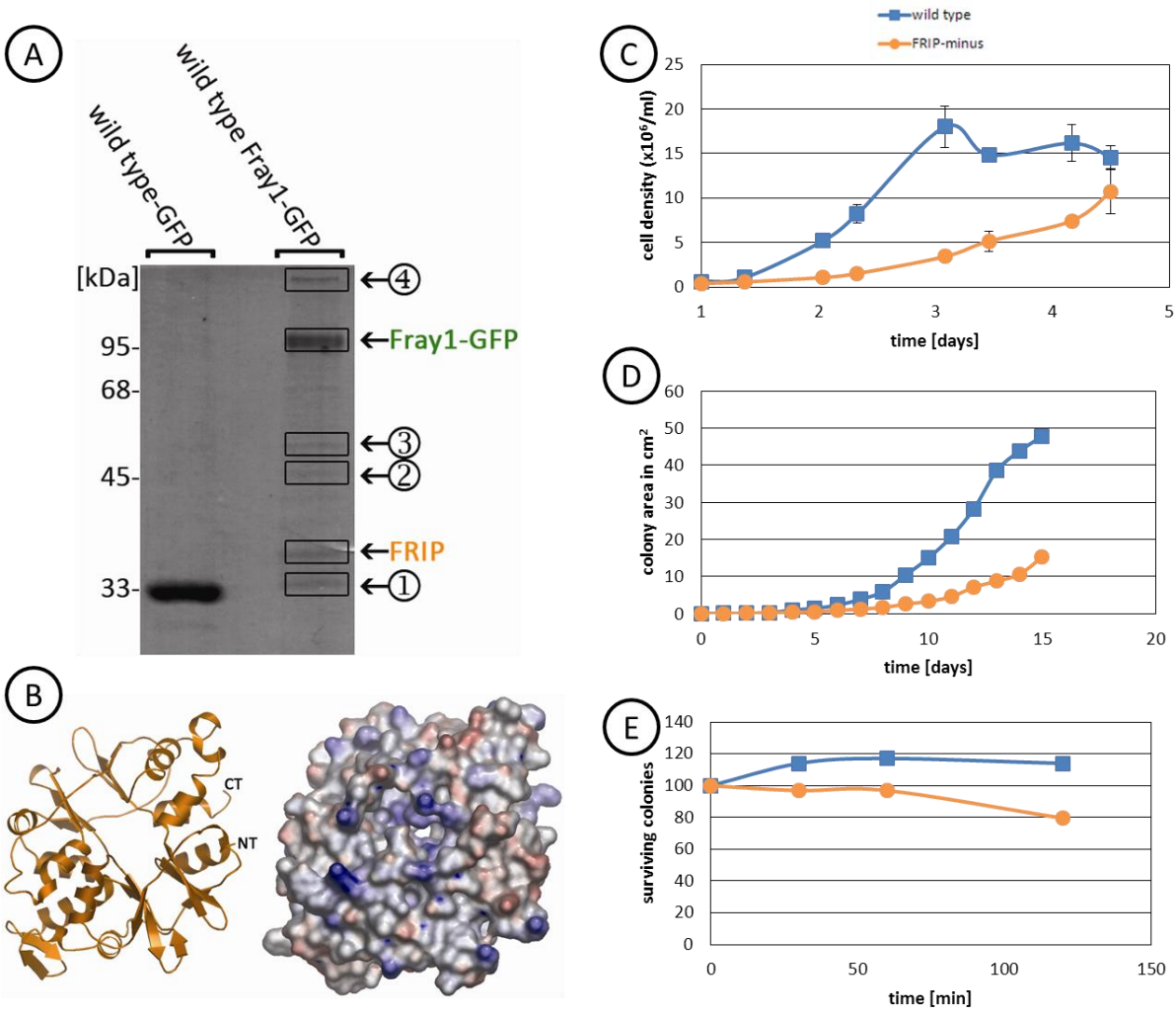

Figure 27: Characterisation of the Fray1-interacting protein FRIP

(A) To identify putative interacting proteins of Fray1 a GFP-Trap pulldown was performed. Lysates of wild type GFP and wild type Fray1-GFP strains were incubated with GFP-Trap beads and separated by SDS-PAGE, stained with Coomassie Brilliant Blue and analysed by MALDI-TOF mass spectrometry. The identified proteins are indicated on the right. ① = 14-3-3-like protein (DDB_G0269138), ② = conventional actin (DDB_G0269234), ③ = acetylornithine deacetylase (DDB_G0267380), ④ = myosin II heavy chain (DDB_G0286355) (B) The amino acid sequence of FRIP modelled to the γ-subunit of AMPK from *H. sapiens* (PDB: 4cfhE). The ribbon and the surface model both exhibit the characteristic parallel CBS module structure. (C) Growth rates of wild type and FRIP-minus cells in HL5 medium under shaking conditions. The FRIP-minus grew a little bit slower and not to the density of the wild type. (D) Growth of wild type and FRIP-minus cells on lawns of non-pathogenic *K. aerogenes*. The diameter of both strains were measured and colony sizes were calculated. The FRIP-minus strain grew slower and to smaller colony sizes than the wild type. (E) Survival of wild type and FRIP-minus cells after exposition to hypertonic environment. The cells were subjected to a 0.8 M sorbitol containing medium. Samples were taken every 20 minutes and plated on lawns of non-pathogenic *K. aerogenes*. Appearing colonies were counted.

5.4 The Ste20-like kinase DstC of *D. discoideum*

5.4.1 DstC of *D. discoideum*

Located on chromosome 6 the *dstc* (DDB_G0291267) gene codes for the 562 aa and 62 kDa protein DstC. The catalytic domain of DstC is most similar to the mammalian kinase Mst2 and Hippo in *D. melanogaster* (Figure 28) which were shown to modulate cell proliferation and apoptosis (Chan et al., 2005, Wu et al., 2003). Compared to the other Ste20-like kinases of *D. discoideum*, DstC has an unusual insertion in the N-terminal region of the kinase domain. The tail region exhibits a proline rich region which is followed by an acidic tail.

A

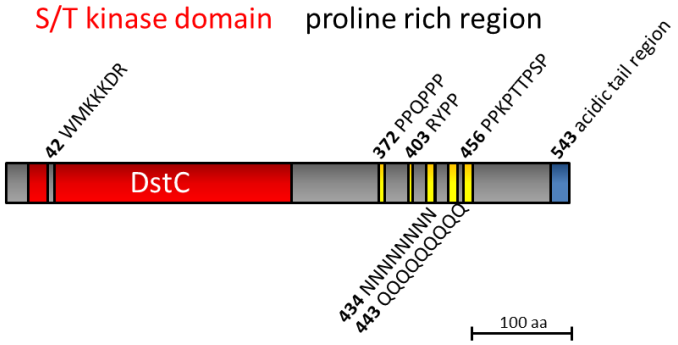

B

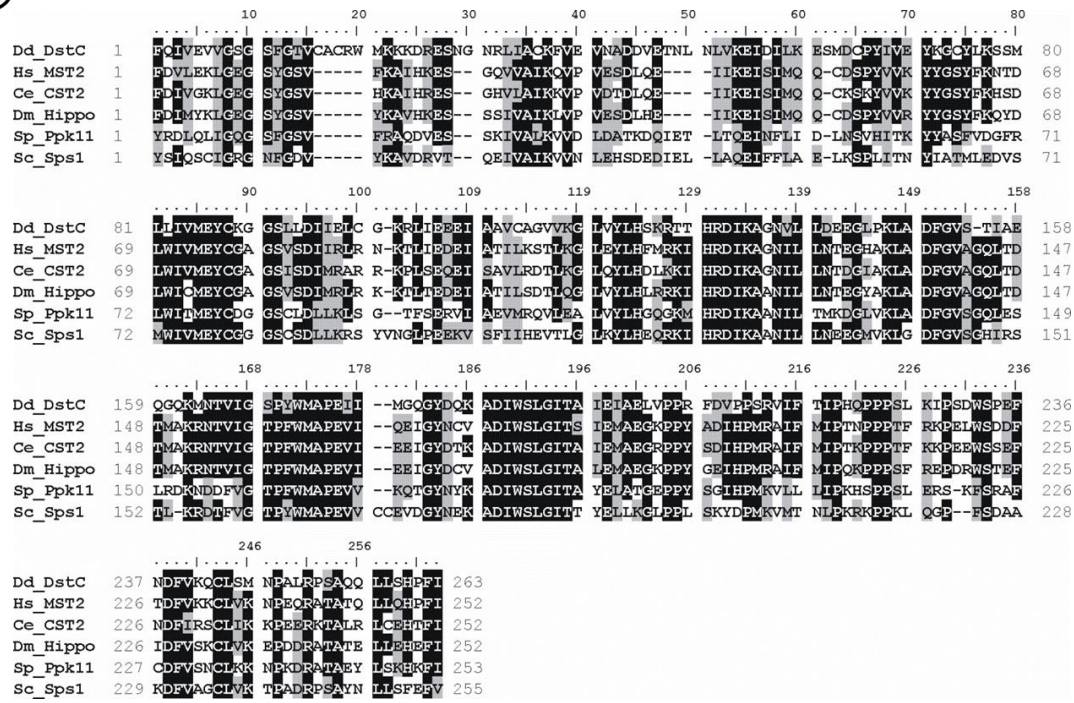

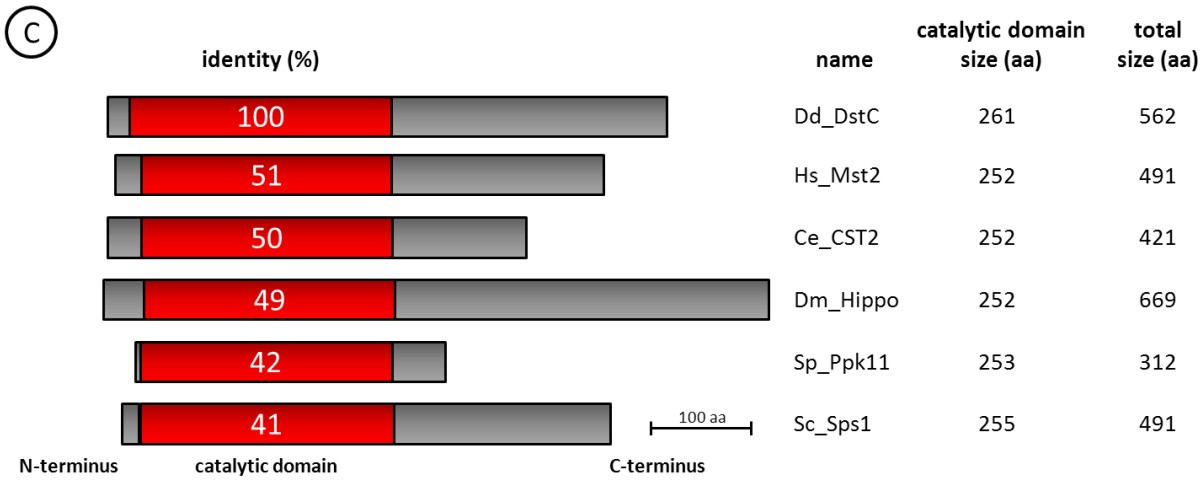

Figure 28: The catalytic domain of DstC from *D. discoideum* is conserved throughout the eukaryotes

(A) The structure of DstC. Compared to the other Ste20-like kinases of *D. discoideum*, DstC has an unusual insertion in the kinase domain. The tail region exhibits a proline rich region followed by an acidic tail. (B) Sequence alignment of the catalytic domain of DstC from *D. discoideum* (Dd) with the corresponding proteins from *H. sapiens* (Hs), *C. elegans* (Ce), *D. melanogaster* (Dm), *S. pombe* (Sp) and *S. cerevisiae* (Sc). Identical residues have a black, conserved residues a grey background. The sequences are highly conserved. (C) Comparison of the catalytic site of DstC of *D. discoideum* with corresponding Ste20-like kinases from other species. The white numbers indicate the identity of the domains compared to *D. discoideum* DstC.

5.4.2 Generation of DstC point mutation constructs

As GFP-DstC constructs were reported to localise to phagocytic cups and acidic vesicles in *D. discoideum* (Poster, Gergana Gateva, 2009) we wanted to explore this accumulation in further detail. We could narrow down the localisation signal to about 90 aa. Hence, to pinpoint the exact binding site, an array of defined shortened DstC point mutation constructs was designed. These constructs are centred around amino acids Y404, S411, T414 and S418 which have been predicted as possible phosphorylation sites at the NetPhosK server. Two sets of constructs were generated. One set of Y404E, S411D T414E and S418D that mimicked permanent phosphorylation and a second one where phosphorylation was deleted due to a conversion of all sites to alanine or phenylalanine respectively (Table 1). When brought into a DstC-minus background, the point mutation constructs will help to pinpoint the exact localisation signal.

Table 1: DstC point mutations

Two different sets of constructs of DstC were designed. One set imitated the permanent phosphorylation of serine, threonine and tyrosine while the other set abolished phosphorylation completely.

Side Chain	Construct Sequence	Phosphorylation Status
DstC S411/T414/S418	368-RNKNPQPPPPSHSSGAGGAAGSTRRVPGNKSVLNRYPPANNVSKGTIAPSPI-420	original
DstC_S411D/T414E/S418D	368-RNKNPQPPPPSHSSGAGGAAGSTRRVPGNKSVLNRYPPANNVDKGEIAPDPI-420	permanent
DstC_S411A/T414A/S418A	368-RNKNPQPPPPSHSSGAGGAAGSTRRVPGNKSVLNRYPPANNVAKGAIAPAPI-420	no
DstC_Y404	368-RNKNPQPPPPSHSSGAGGAAGSTRRVPGNKSVLNRYPPA-407	original
DstC_Y404E	368-RNKNPQPPPPSHSSGAGGAAGSTRRVPGNKSVLNREPPA-407	permanent
DstC_Y404F	368-RNKNPQPPPPSHSSGAGGAAGSTRRVPGNKSVLNRFPPA-407	no
DstC_Y404_s	394-VPGNKSVLNRYPPA-407	original
DstC_Y404E_s	394-VPGNKSVLNREPPA-407	permanent
DstC_Y404F_s	394-VPGNKSVLNRFPPA-407	no

5.5 Bioinformatical characterisation of cytoskeletal proteins in *R. filosa*

An *in silico* study was carried out to find, characterise and map the actin and actin related genes in the genome of *R. filosa* which was totally sequenced just recently. *R. filosa* is a fresh water foraminifer which belongs to the Rhizaria within the eukaryotes. In nature *R. filosa* has a very unique life cycle whereas in culture it only exists as plasmodium (Glöckner et al., 2014).

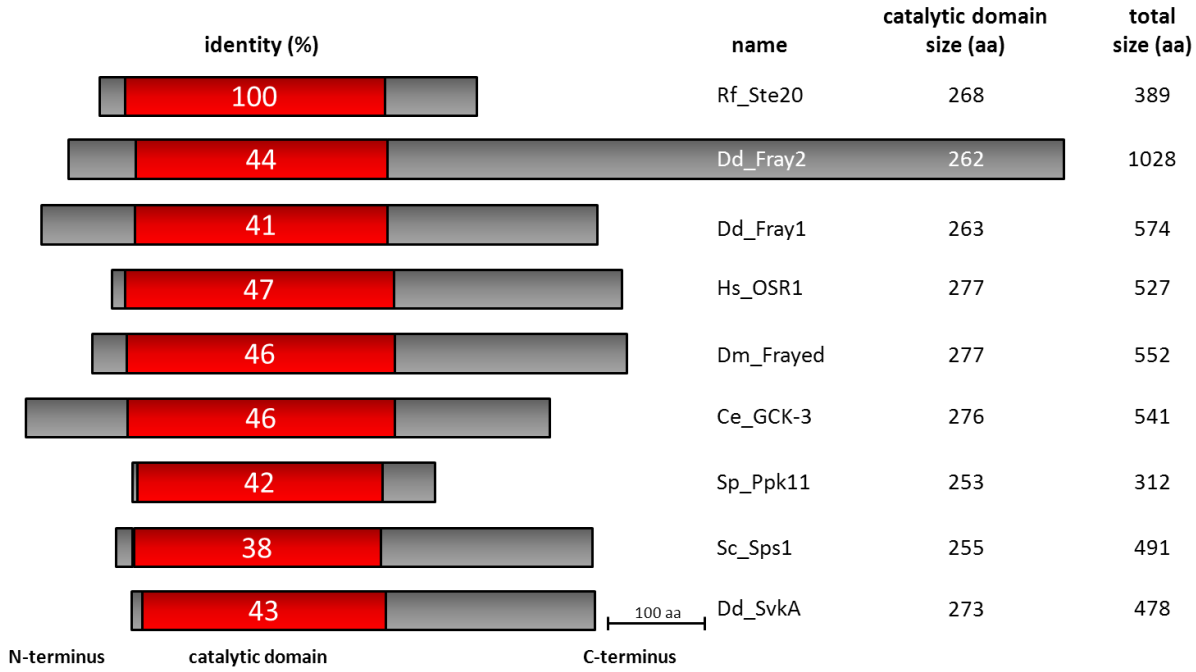

Figure 29: Solexa1552564_1.f1.exp_8 of *R. filosa* is a Ste20-like kinase
Comparison of the catalytic site of Ste20 of *R. filosa* with Ste20-like kinases from *D. discoideum* (Dd), *H. sapiens* (Hs), *D. melanogaster* (Dm), *C. elegans* (Ce), *S. pombe* (Sp) and *S. cerevisiae* (Sc). The white numbers indicate the identity of the domains compared to *R. filosa* Ste20. (C) The catalytic domain of Fray2 compared to Fray analogues in different species.

The potential genes coding for cytoskeletal proteins were searched via BLAST search on the *Reticulomyxa* BLAST server. cDNA sequences as well as protein sequences from already sequenced organisms (*D. discoideum, H. sapiens, Arabidopsis thaliana*) were used as search templates. The hits of every search were first analysed if the gene was complete and subsequently for gene type specific domains and subdomains. Furthermore, the introns were separated from the exons to obtain a DNA array that could be translated into a protein sequence (Figure 30). Additionally, the sequences were tested using multiple alignments and, if templates were available, protein models were generated using a structure homology-modelling server.

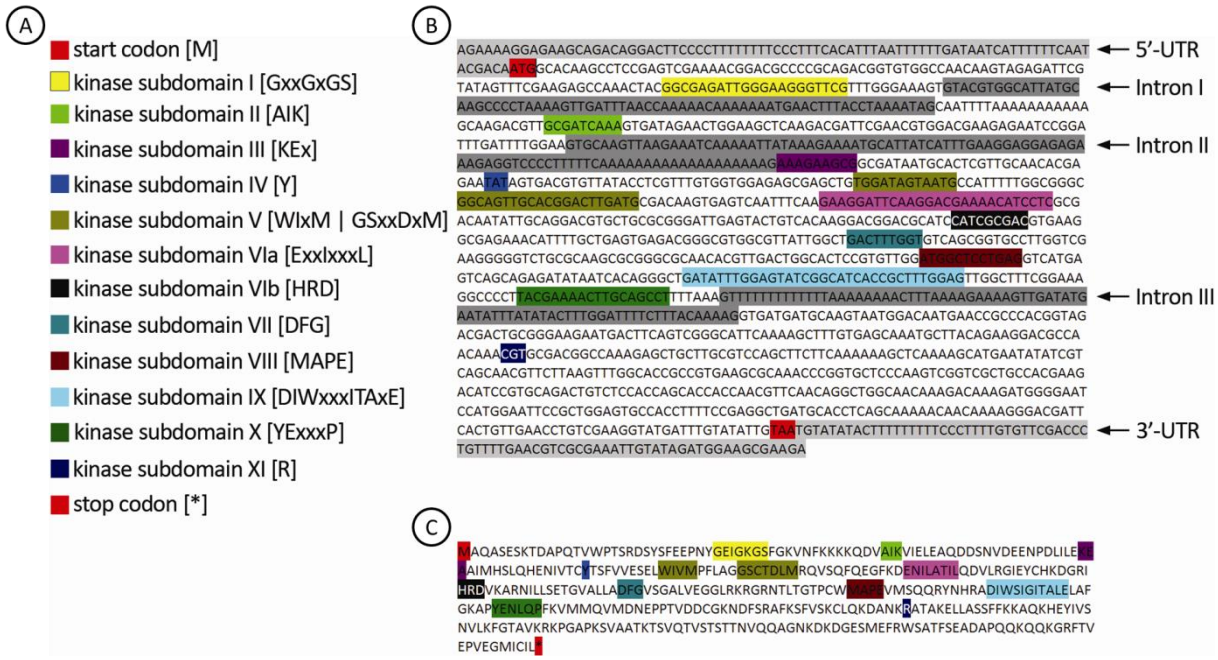

Figure 30: Bioinformatical characterisation of a Ste20-like kinase of *R. filosa*

(A) The 12 Ste20 kinase group subdomains as described (Hanks and Hunter, 1995a). Potential start and stop codons are marked in red and all the subdomains in different colours. (B) The colours of the different kinase sub domains applied to the contig solexa1552564_1.f1.exp_8 from the total sequence data of *R. filosa*. Light grey marks the 5' and 3' untranslated region. Dark grey distinguishes the introns from the exons. (C) To verify if the constructed DNA sequence was correct, it was translated into a protein sequence. Subsequently the obtained sequence was BLASTed.

Incomplete hits that could not be supplemented with a complement from the sequence data were categorised as pseudogenes, incomplete sequences that were identical to already identified genes as sequencing failures.

Applying these methods we could identify about 40 potential cytoskeletal proteins of seven different protein classes in *R. filosa* (Table 2).

Notably, we discovered 4 new actin genes in addition to the already known actin in *R. filosa* (Flakowski et al., 2005).

Table 2: Identified actin cytoskeleton proteins in *R. filosa*

Applying the afore mentioned techniques, around 40 cytoskeletal proteins could be identified.

Actin cytoskeleton proteins		
Gene Names	**No.**	**Pseudogenes**
actin	5	-
actin-related-proteins	13	22
Cap 1/2	1	16
fimbrin	4	-
formin	5	>15
Ste20-like kinase	1	-

6 Discussion

The major goal of this study was to investigate the scaffolding protein Mo25, its interactions and regulatory pathways. We could verify the Ste20-like kinase SvkA (severin kinase) as interacting partner and proved that the interaction is apparently highly conserved throughout evolution. Additionally, we introduced several point mutations into the sequence of Mo25 and investigated the influence on cytokinesis and slug motility.

Another goal was the functional characterisation of the Ste20-like kinases Fray1 and Fray2. We were able to detect a yet unknown protein as interacting partner of Fray1, which we named FRIP (Fray interacting protein).

Furthermore, we constructed several point mutation constructs of the Ste20-like kinase DstC to pinpoint the exact localisation signal to phagocytic cups and acidic vesicles.

In addition, we successfully mapped and characterised the actin and actin related genes in the genome of the recently sequenced fresh water foraminifer *R. filosa.*

6.1 Mo25, the highly conserved master regulator

The goal of this work was to investigate the role of the highly conserved eukaryotic scaffolding protein Mo25 in *D. discoideum*. In human, Mo25 facilitates and activates a trimeric complex together with the pseudokinase STRAD and the Ste20-like kinase LKB1 to act on downstream kinases. Thus, it is a master regulator of major pathways such as the mTor (Orlova et al., 2010) and the AMPK-signalling pathway (Hawley et al., 2003). Additionally, Mo25 also binds to other Ste20-like kinases like SPAK, OSR1, Mst3, Mst4 and Ysk1/Sok1 to modulate their ability to phosphorylate downstream targets (Shi et al., 2013, Filippi et al., 2011). Point mutations in the amino acid sequence of Mo25 cause the disruption of the trimeric complex and can cause in the hereditary disease Peutz-Jeghers-Syndrome (Baas et al., 2003, Boudeau et al., 2003). In organisms like yeast, fruit fly and nematode Mo25 has been described to be involved in cell polarity and cytokinesis (Boudeau et al., 2004, Kanai et al., 2005). The Mo25-minus *D. discoideum* strain exhibited a very drastic change of phenotype with a severe defect in cytokinesis and cell division. Mo25-minus cells seem to be unable to separate after chromatin duplication and

therefore accumulate dozens of nuclei in one cell. Cells with sometimes more than 60 nuclei have been observed both in shaking cultures as well as in attached cells. Additionally, Mo25-minus cells seem to be unable to produce or to follow a cAMP gradient which is essential for aggregation (Strmecki et al., 2005). Subsequently, the development also results in smaller fruiting bodies, and a disturbed ratio of spore mass to stalk cells. However, the Mo25-minus strain is able to develop into the motile intermediate slug-state, but the slugs are not able to migrate towards a light source. This resembles the AMPK over expression phenotype of *D. discoideum*, which does not have an impaired cytokinesis but exhibits a very pronounced defect in slug motility and development, very similar to Mo25-minus mutants (Bokko et al., 2007, Annesley et al., 2011). This might hint at an overlapping role for Mo25 in the regulation of AMPK signalling. Moreover, the Mo25-rescue construct with a GFP-tag at the N-terminal end was not able to cure the phenotype. Only with the GFP-tag on the C-terminal end the phenotype could be reverted to normal. This might indicate that the GFP moiety at the N-terminus blocks a necessary interaction surface for a potential interacting partner. To screen for potential interacting partners of Mo25, we coupled the GFP-tagged rescue protein to a GFP-trap resin. Employing this technique, we could verify severin kinase (SvkA) as interacting partner of Mo25. Severin kinase of *D. discoideum* is about 32% similar to STRAD and 26% similar to LKB1 from *H. sapiens*. Furthermore, SvkA additionally contains a WEF sequence motif at a similar distance to the catalytic domain as in STRAD. The WEF motif is, together with the hydrophobic VANPKT surface of the kinase domain, essential in facilitating the binding of the pseudokinase STRAD to Mo25 (Boudeau et al., 2003). This interaction of Mo25 with kinases from the Ste20-like family seems to be so conserved, that SvkA from *D. discoideum* is able to interact with Mo25 from *H. sapiens* and *D. rerio* in GST-pulldown experiments. The interaction of SvkA with Mo25 from different species clearly indicates a binding mechanism which is preserved throughout the eukaryotes. This is also emphasised by the close resemblance of the amino acid sequences of Mo25 from *D. discoideum*, *H. sapiens* and *D. rerio*, respectively. High conservations of proteins always signify the necessity of the process in which they are involved. Since the rescue construct with the GFP-tag at the N-terminus was not able to cure the Mo25-minus phenotype, we suspected that the N-terminal end of the protein

might be required for potential binding partners. Therefore, we designed an array of eight different point mutation constructs to elucidate the binding mechanisms of Mo25 in *D. discoideum*. All point mutations were inserted with the purpose to block interaction with known or unknown binding partners. Amino acids R227 and M260 are essential to bind the pseudokinase STRAD. In addition R240 and F243 are needed to bind the kinase LKB1 in human (Zeqiraj et al., 2009a). As the Mo25-rescue construct with the N-terminal GFP-tag was not able to cure the phenotype, we chose amino acids K17, K34 and K38 due to their prominent exposure at the N-terminus. Amino acid K132 is a highly conserved positively charged spot on the convex side of the protein surrounded by an otherwise negatively charged surface. To test if a mutation per se affects the behaviour of Mo25, the mutations F258A and M259A were introduced as control (Figure 16). All point mutation constructs have the GFP-tag on the C-terminus and the chosen amino acid sites converted either to nonpolar, alanine (A) or to polar uncharged glutamine (Q). Subsequently, the mutation constructs were transfected into a Mo25-minus background and tested for cytokinesis and motility. Therefore, we quantified the nuclei of every strain and performed slug motility assays. Mo25-minus and M260A are both essential for cytokinesis and slug motility, whereas R227A is also very important for cytokinesis but not for slug motility. Residues R240A & F243A seem also to play a role for slug motility but not for cytokinesis. Of the N-terminal residues only K17A seems to have a profound impact on motility and cytokinesis whereas K34A and K38Q both only have a moderate effect. Located on the convex side of Mo25, K132A also seems to impair slug motility to a certain degree but has no effect on cytokinesis. The negative control F258A & M259A is behaving almost like wild type. Taken together, two of the already known binding sites, M260 and R227, and one to date unknown K17 at the N-terminal region seem to play a role both in slug motility and cytokinesis. By contrast the sites R240 & F243 and K132 exclusively play a role in slug motility. All the other mutations seem to have milder to none effects on cytokinesis and on slug motility.

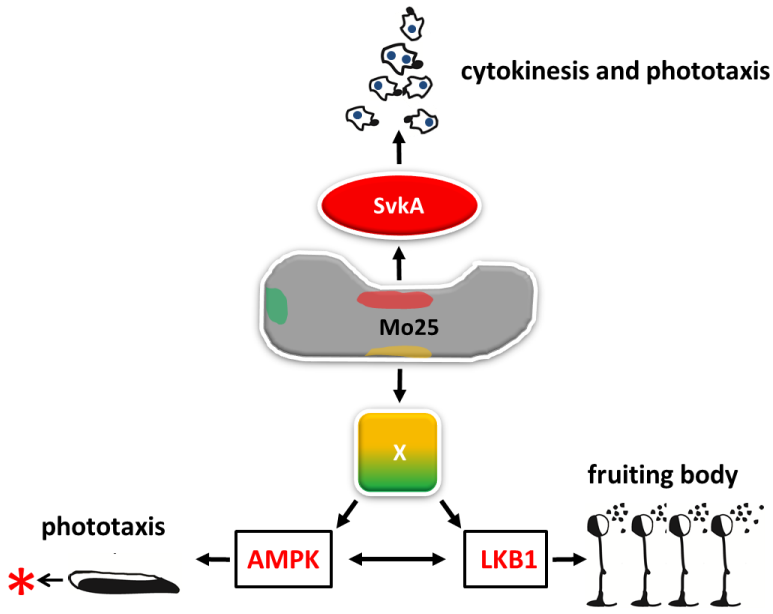

Figure 31: Hypothetic model of possible interacting partners of Mo25
Possible scenarios for interacting partners of Mo25 in *D. discoideum*. Slug movement towards a light source is impaired due to over expression of the α-subunit of AMPK (Bokko et al., 2007). Analogue, Mo25-minus mutants were not able to migrate towards a light source as well. This might indicate a potential interplay between AMPK and Mo25, mediated by a yet unknown protein. After reduction of LKB1 using RNAi-knockdown constructs, formation of stalk and sorus is heavily disturbed. LKB1 phosphorylates AMPK upon stress induction (Veeranki et al., 2011). In our experiments, Mo25-minus cells exhibited a quite similar disturbance in fruiting body formation. Nevertheless, we could only verify an interaction of Mo25 and SvkA. The exact interplay of Mo25, AMPK and LKB1 in *D. discoideum* is still unknown to date.

In human, residues R227 and M260 are essential to bind the pseudokinase STRAD (Ste20-related adapter protein) while amino acids R240 & F243 are binding partners for the Ste20-like kinase LKB1 (Zeqiraj et al., 2009a). Only, upon the assembly of these three players the Mo25/STRAD/LKB1-complex can act on downstream targets (Milburn et al., 2004). Additionally, Mo25 also regulates the activity of other Ste20-like kinases, but these bind to the adapter protein in a STRAD-like fashion (Shi et al., 2013, Filippi et al., 2011). However, the present results imply that the situation in *D. discoideum* is somewhat different compared to the human Mo25/STRAD/LKB1-complex. Intriguingly, a LKB1 homologue in *D. discoideum* exists. It has been shown that LKB1 RNAi-knockdowns in *D. discoideum* displayed severe reduction in prespore cell differentiation and early appearance of prestalk cells (Veeranki et al., 2011). It could be shown that LKB1 is the regulator of the serine/threonine kinase GSK3. GSK3 is involved in cell specification and

coordinates prespore- and prestalk-signalling. Additionally, upon stress induction, LKB1 gets activated and phosphorylates AMPK (Veeranki et al., 2011). It has also been shown that in *D. discoideum* cells which are disturbed in their AMPK-signalling cascade due to over expression of the α-subunit of AMPK, slug motility towards a light source is severely impaired (Bokko et al., 2007, Annesley et al., 2011). Both phenotypes resemble the characteristics of the here presented Mo25-minus. This led us to the most reasonable theory of an interaction of Mo25 with AMPK and LKB1, mediated by a yet unknown protein. Nevertheless, to date neither an interaction of AMPK nor of LKB1 with Mo25 in *D. discoideum* could be observed. Besides, the interaction of Mo25 and SvkA without a third protein could be sufficient for efficient cytokinesis, as mutations in the postulated Mo25/SvkA binding interface (R227A & M260A) were the only mutations that affected cytokinesis. Mutations in Mo25 that would affect the binding of a second kinase (R240A & F243A) analogue to the human Mo25/STRAD/LKB1-complex did not affect cytokinesis. So it seems that Mo25 and SvkA can jointly regulate cell division. Four findings support this notion: First, whereas human STRAD is only a pseudokinase, SvkA possesses a catalytic domain and is able to autophosphorylate, which means that SvkA can directly phosphorylate a downstream target or kinase and does not need to induce a conformational change or physical impulse as is described for STRAD and its downstream kinase LKB1 (Boudeau et al., 2003). The second reason is that we could show that Mo25 and SvkA bind to each other and that the binding mechanism is highly conserved throughout the evolution. The third argument is that the phenotype of Mo25-minus and SvkA-minus (Rohlfs et al., 2007) is of the same nature indicating a direct involvement in the same pathway. And fourth, considering the first three findings, it was not surprising that we were not able to detect any other potential interacting partner for Mo25 than SvkA. On the other hand, the need for a free NT of Mo25 and the involvement of the N-terminal residue K17 for the regulation of cytokinesis in *D. discoideum* as well as of slug motility, might indicate that there is a third interaction partner needed although at a completely different binding site. This would be a novel mode of Mo25 forming a scaffold in signalling and different to the Mo25/STRAD/LKB1-complex in human. Another surprise is the fact that the highly conserved residues R240 & F243 are not involved in the regulation of cytokinesis, they rather seem to affect slug motility, but to a somewhat

minor extent. The second residue that seems to be necessary for slug motility only is K132 on the convex side of Mo25. This discovery implies that for efficient slug motility Mo25 probably interacts with so far unknown signalling proteins that use the convex side of Mo25, together with binding of SvkA to its concave side. This adds to the findings from the mammalian system, where Mo25 is a connector and nodal point for several different pathways (Filippi et al., 2011). Concluding, these results suggest that slug motility and cytokinesis are probably regulated by two different mechanisms which overlap in certain points and are connected by Mo25. Following these findings we wanted to test if point mutation constructs of Mo25 are still able to pull down SvkA. Therefore, we used the eight Mo25 point mutations in GST-pulldown assays and tested for binding to proteins from *D. discoideum* wild type lysates. Notably, all eight point mutation constructs were able to pull down SvkA from wild type lysate. This is rather surprising, as it is described in the literature, that the point mutations of the binding sites for STRAD and LKB1 abolish the attachment of both kinases to Mo25. Taken together, we could show that of Mo25 of *D. discoideum* binds to the Ste20-like kinase SvkA. We could verify this binding mechanism and show that it is highly conserved throughout the eukaryotes, as Mo25 from fish and human is also able to pull down SvkA from amoeba. We could undertake the first steps to elucidate the different pathways that are connected through the central regulator Mo25. Nonetheless, further studies are necessary to completely unveil all the different pathways in *D. discoideum* that are regulated by the master regulator Mo25.

6.2 Ste20-like kinases Fray1, Fray2 and their partner FRIP

Ste20-like kinases are important players involved in the regulation of the cell cycle, apoptosis, stress responses, cellular volume sensing and regulation, osmotic homeostasis and link cell cycle events with cell volume (Delpire, 2009). The goal of this part was the characterisation of the Fray family kinases which belong to the Ste20-like group within the kinome of *D. discoideum*. The genome of *D. discoideum* encodes two Fray family kinases, Fray1 and Fray2 (Eichinger et al., 2005, Goldberg et al., 2006). Their kinase domains are 51% identical. Sequence alignments with the kinase domains of corresponding Fray homologues in yeast, worm, fruit fly and human reveal a very high conservation throughout the eukaryotes (Figure 19). Whereas the Ste20-like kinases of *S. cerevisiae* (STE20) and *S. pombe* (PpK11) cannot be mapped to the Fray family exclusively and the genomes of *C. elegans* (GCK-3) and *D. melanogaster* (Frayed) encode for only one kinase respectively, *D. discoideum* with two kinases of the Fray family is equivalently equipped like *H. sapiens* (Delpire, 2009). The structure of Fray1 and Fray2 reveals the typical GCK (germinal centre kinase) structure with the highly conserved N-terminal kinase domain and the less conserved C-terminal tail (Kyriakis, 1999). The tail region of Fray2 is with 698 aa remarkably longer than the one of Fray1, which makes Fray2 one of the largest Ste20-like kinases in *D. discoideum*. To investigate the function of the Ste20-like kinases Fray1 and Fray2, we isolated Fray1-minus and Fray2-minus strains. Astoundingly, neither in the Fray1-minus nor in the Fray2-minus cell line a significantly altered phenotype could be observed. We were unable to find any actin-based process which was affected by the removal of Fray1 or Fray2. Cell motility, chemotaxis, growth in liquid shaking culture, solid surface and on bacterial lawn, culmination to fruiting bodies and phototaxis at the slug stage were all principally unchanged compared to wild type cells. To avoid that either Fray1 or Fray2 substitute for each other in the respective knock out cell line, we generated a Fray2Fray1-minus strain. Also there, however no dissimilarity in any of the performed assays could be observed. The only mild phenotype we could detect in these minus mutants is a slight difference during growth in shaking culture where the minus strains always grow to higher densities than the wild type control. The initial kick off for the investigation of the Ste20-like kinases Fray1 and Fray2 in *D. discoideum* was a publication by William M. Leiserson where the serine/threonine kinase

Frayed of *D. melanogaster* was described to be essential for axonal ensheathment (Leiserson et al., 2000b). *D. melanogaster* Frayed-minus mutants have nerves with severe swelling and axonal defasciculation and die early in larval development. Moreover, the closest relatives to Fray1 and Fray2 in human are the kinases OSR1 and SPAK (Delpire, 2009). OSR1 regulates organ size during development (Zhang et al., 2011) and additionally, together with SPAK jointly regulates homeostasis in human upon stress response (Delpire and Gagnon, 2008). Hence, the blistering of the nerves in Frayed-minus clones in *D. melanogaster* and the regulation of homeostasis by SPAK/OSR1 in *H. sapiens* led us to the assumption Fray1 and Fray2 might be implicated in the regulation of cell volume. Therefore, we tested the survival of the Fray-minus strains after exposure to osmotic shock. The cells were exposed to hypertonic medium, cell samples were taken at certain time points and plated on a bacterial lawn. Subsequently, appearing plaques were counted one and two days after the start of the experiment. Unfortunately, the outcome of these experiments was extremely variable and we obtained very inconsistent data. Nevertheless, it was only during the osmotic shock survival experiment to detect a hint of a difference between the strains Fray1-minus, Fray2-minus and Fray2Fray1-minus and wild type cells. One reason, that the removal of Fray1 and Fray2 was not affecting the behaviour of the cells, might be that the kinases are probably needed in a different life stage or are regulators of responses to environmental changes of *D. discoideum*. Many of these conditions are not reproduced in the laboratory and subsequently were omitted during research. Possibly the kinases get activated by conditions only present in the natural environment of *D. discoideum*, for example in defence against predators or in the sexual reproduction cycle (Hilbi et al., 2007, O'Day and Keszei, 2012). A hint that the life cycle studied in a lab represents the wrong time frame respectively the wrong environment, are the results of the real time PCR which reveal a very low transcription level of *fray1* and *fray2* throughout. However, our results may provide first hints towards further investigations of the Fray-family kinases in *D. discoideum*. In addition, by using a GFP-trap resin we could identify a so far undescribed 35 kDa protein (DDB_G0288201) as interacting partner of Fray1, which we termed FRIP (Fray1 interacting protein). The cytoskeletal protein FRIP consists of two CBS (cystathionine-beta-synthase) domain pairs (Bateman, 1997). The structural and biophysical characterisation of CBS domain-

containing proteins is an emerging field which has recently gained much interest (Ereño-Orbea et al., 2013). The CBS domain is evolutionarily highly conserved from archaea to prokaryotes and eukaryotes (Bateman, 1997, Scott et al., 2004). In humans, CBS domains have a medical relevance as point mutations in their amino acid sequence are closely linked to hereditary diseases such as homocystinuria (Shan et al., 2001), retinitis pigmentosa (Kennan et al., 2002), hypertrophic cardiomyopathy (Blair et al., 2001), osteopetrosis (Kornak et al., 2001) and congenital myotonia (Pusch, 2002) to name a few. Moreover, CBS domains are found in a wide variety of proteins such as in the inosine monophosphate dehydrogenase (Labesse et al., 2013), voltage gated ion channels (Carr et al., 2003) and as subunits of the AMP-activated protein kinase (AMPK) (Amodeo et al., 2007). CBS domains regulate a wide variety of processes which are apparently all involved in the response to changes in Mg^{2+}-ion transport (Hattori et al., 2009), osmoregulation (Biemans-Oldehinkel et al., 2006), trafficking of chloride channels (Carr et al., 2003), nitrate transport (De Angeli et al., 2009) or pyrophosphatase activity (Jämsen et al., 2010). To date, 52 different ligands are known to bind CBS domains with AMP, ADP and ATP being the primary binding partners. FRIP of *D. discoideum* mainly consists of the four distinct CBS-domains with one pair forming a so called *Bateman domain* (Baykov et al., 2011) each. This arrangement of four CBS-domains arranged into two connected *Bateman domains* which gives the protein a disc like structure is called a *CBS module* (Mahmood et al., 2009). In principle three structures of the *CBS modules* do exist, “parallel” (~95%), “antiparallel” (~5%) and “v-shaped” (<1%) (Ereño-Orbea et al., 2013) depending on the structural organisation of the protein. The binding of a ligand causes a rearrangement of the amino acid side chains or a shift in the orientation of secondary structure elements of the protein. Upon these alterations the CBS modules adopt an “open”, “closed” or “bent” structure, which probably affects the regulatory mechanism of the protein (Tuominen et al., 2010). FRIP of *D. discoideum* seems to be a “parallel” *CBS module*, due to its clear head-to-head organisation of the CBS-domains to each other when modelled to the γ-subunit of the human AMP-kinase (PDB: 4cfhE) (Figure 27). We produced a FRIP-minus strain to further investigate the function of FRIP. Unfortunately, similar to its interaction partner Fray1, no significant phenotype upon the removal of FRIP could be detected in *D. discoideum*. We could only observe a slight growth defect in liquid

shaking culture, as the FRIP-minus strain grows slower and to lower densities compared to the wild type. Also when cultivated on bacterial lawns, FRIP-minus cells grow to smaller colony sizes than the wild type. The reduction in growth might imply an implementation of FRIP in the regulation of the energy household of the cell. Therefore, we compared FRIP to the proteins of the AMPK complex of *D. discoideum* via BLAST analysis, where FRIP is 30% identical to the non-catalytic gamma subunit (AMP-prkag). The binding of AMP to the CBS domain of the AMPK gamma subunit accounts for the energy sensing properties of the AMPK complex. Thus, an interaction of Fray1 and the CBS-module FRIP might link the Ste20-like kinases to energy homeostasis. Moreover, when exposed to a hypertonic environment, the survival rate of FRIP-minus cells drops corresponding to Fray1-minus, Fray2-minus and Fray2Fray1-minus. This also might be a further indication for the connection of the Ste20-like kinases and FRIP to the regulation of cell volume and homeostasis in *D. discoideum*. Further projects should include a detection of the ligands which activate FRIP, possible protein interactions, a clarification of the interplay of the Ste20-like kinases and FRIP, and in which pathway they are involved.

6.3 Ste20-like kinase DstC

The Ste20-like kinase DstC is one of the 17 members of the *D. discoideum* kinome (Goldberg et al., 2006). Its kinase domain contains an unusual insertion of seven basic amino acids between the Hanks and Hunter subdomains I and II. The kinase domain is 49% identical to Hippo of *D. melanogaster* and 51% identical to Mst2 of *H. sapiens*. Hippo is known to be a key player in the regulation of cell size during eye development in fruit fly (Ryoo and Steller, 2003) and Mst2 is implicated in the Hippo pathway where it regulates the tumour suppressors Lats1 and Raf-1 in human (Guo et al., 2007). However, sequence alignments of DstC from *D. discoideum* with other social amoebae indicate a very strong conservation, even outside of the kinase domain, suggesting that it is adapted to the specialised life style of the amoebae. Studies on DstC carried out by Gergana Gateva during her Diploma thesis revealed that this Ste20-like kinase plays an important role in the phagocytosis mechanism of *D. discoideum*. Whilst observing pinocytosis no localisation signal could be detected. During the uptake of bacteria, DstC seems to localise to the actin rich structures, but disappears as soon as the prey is enclosed. Only during the uptake of larger particles like yeast, GFP-constructs of DstC strongly localise to the phagocytic cup. However, upon closure of the phagocytic cup, the localisation signal disappears within seconds from the engulfed particle. The reason why DstC does not localise during pinocytosis and the intake of bacteria is unknown to date, but it might be due to size of the prey and uptake mechanism. A possible theory could be, that the uptake of liquid and smaller nutrients utilises a different import machinery in contrast to bigger particles. So far it is known that absorption of bigger particles is marked by a procedure of distinct steps: Recognition of the particle, engulfment with the membrane still in direct contact with the particle surface, sealing off the cup and finally transporting and acidifying the particle in a vesicle inside the cell (Neuhaus et al., 2002). Additionally, DstC GFP-constructs were also observed localising to acidic vesicles in the cell. During random cell movement GFP-DstC localises to the dynamic actin cortex. The minimal localisation signal of DstC could be mapped to the C-terminal region, which contains proline rich sequences. Poly-proline containing sites have been shown to be interaction domains in cytoskeleton related proteins. For example, ForminB, Abi2 (similar to Abelson

tyrosine kinase Interacting protein 2) and Abp1 (actin binding protein 1) of *D. discoideum* all contain poly-proline motifs which are implicated in binding. (Dieckmann et al., 2010, Wang and O'Halloran, 2006). The potential localisation sites in DstC have been narrowed down to two sequence motifs with 52 and 66 aa, overlapping in 27 aa. To further investigate the localisation signal and to pinpoint the actual binding sequence, we fed the two overlapping sequences into the NetPhosK server which predicted four phosphorylation sites which might be implicated in a potential binding site. According to this prediction, we constructed two different arrays of shortened point mutation constructs. The first set of constructs is designed to mimic a permanent phosphorylated state whereas in the second set all phosphorylation sites are removed due to a conversion to alanine. With these point mutation constructs we hope to have pinpointed the localisation signal. The permanent phosphorylated version of DstC should stick to the phagocytic cup and acidic vesicles whereas the constructs that are blinded for phosphorylation should not localise anywhere at all.

6.4 Unveiling the members of the actin cytoskeleton of *R. filosa*

The fresh water protist *R. filosa* belongs to the Foraminifera within the branch of the Rhizaria. The supergroup Rhizaria constitutes one of the six, respectively eight major groups of the eukaryote tree of life (Glöckner et al., 2014). However, the availability of molecular data for this main group is very sparse. Prior to the total sequencing of the genome of *R. filosa*, only the genome of the chlorarachniophyte alga *B. natans* was available for genomic studies (Curtis et al., 2012). This is due to the lack of cultivability of most of the organisms of this phylum. The clear advantage of *R. filosa* is that it can be kept it in culture and so it is possible to obtain high yields for sequencing. Thus, the genome of *R. filosa* will provide deeper insights into the molecular world of the Rhizaria and serve as a model for this eukayote crown group. Of the 320 Mb genome with approximately 40.443 protein coding genes, only 103 Mb could be assembled. Long-range amplifications and tandem repeats make it almost impossible to completely compile the genome. Albeit, the assembled segment represents the protein coding part very well as 93% of the ESTs (expressed sequence tags) and 99.5% of the RNA-sequencing data could be mapped to the genome assembly (Glöckner et al., 2014). Its structure is very diffuse and overflows with short repeats and pseudogenes. The complex organisation of multiple gene copies followed by pseudogenisation might be a way to procure sufficient expression for certain key genes. For example the genes for motor proteins and microtubules are present in multiple copies. Also members of the actin cytoskeleton family seem to be amplified. We could detect five different actin genes in *R. filosa*, which are about half as many as in *B. natans* and only one more than in human. In contrast, in *D. discoideum*, 41 copies of actin exist of which 17 are identical proteins from 17 different genes (Joseph et al., 2008). The number of actin genes of *R. filosa* clearly reflects the demands of the environment which it inhabits. In its natural habitat, *R. filosa* mainly exists as acellular syncytium with thousands of nuclei, forming giant net-like plasmodia. The thicker centre part of the plasmodium is mostly hidden in the ground, whereas the pseudopodia spread over the substrate (Hülsmann, 2006). Compared to *D. discoideum*, *R. filosa* does not exert rapid movements, directional changes or does undergo a morphological change from single cell to a multicellular stadium. As almost stationary organism, the processes where actin is crucial are confined to cortex stability,

reproduction and cell division, growth of filopodia, uptake of nutrients and encystation upon starvation (Schleicher and Jockusch, 2008, Joseph et al., 2008). Additionally, during our search for potential actin genes, we discovered quite a number of genes which were very similar to actin, but did in a calculated structure not exhibit the ATP-binding pocket. The putative gene products were subsequently classified as actin-related-proteins (Arp). Nevertheless, *in silico* studies can reveal directions but are not capable to reflect reality completely. Furthermore, considering the assembly limitations of the genome it cannot be excluded that duplications and therefore amplifications of the actin family exist. The genes for the other cytoskeletal proteins could also be detected, like the true actin-related proteins (Arp), Cap1/2, fimbrin and formin, also amplified by repeats and extensive pseudogenisation. Interestingly the Ste20-like kinase group is greatly underrepresented. The genome of *R. filosa* encodes one Ste20-like kinase, with a domain highly identical to kinases Fray1 and Fray2 of *D. discoideum*, Frayed of *D. melanogaster* and OSR1 of *H. sapiens*. Albeit, compared to 14 Ste20-like kinases in yeast, 17 in *D. discoideum* and 24 members in *H. sapiens*, only one Ste20-like kinase in *R. filosa* is very scarce (Goldberg et al., 2006, Manning et al., 2002a, Manning et al., 2002b). Also considering that in these organisms an orchestrated array of Ste20-like kinases regulates diverse cellular processes, such as budding and formation of mating projections in budding yeast (Ramer and Davis, 1993), cell division in fission yeast (Tang et al., 2003), development, cell polarity and cytokinesis in *D. discoideum* (Artemenko et al., 2012, Arasada et al., 2006, Rohlfs et al., 2007) and complex pathways like homeostasis and energy sensing in human (Strange et al., 2006) the lack of these kinases in in *R. filosa* is surprising. One reason for such sparse equipment might be that the simple life cycle of *R. filosa* does not require meticulous phosphorylation cascades. It could also be a documentation of evolution from one kinase to many, as the genome of *B. natans* too only harbours one Ste20-like kinase (Curtis et al., 2012). Nevertheless, it cannot be excluded that additional Ste20-like kinase genes are hidden in the genome of *R. filosa*. One indication for this theory might be that we found numerous bits and pieces of Ste20-like kinase domains at various positions in the genome. Due to the fact that only one third of the genome can be mapped to date, there is still a lot to discover. Also the circumstance that 93% of the ESTs (expressed sequence tags) have been be mapped to

the sequenced data does not exclude that the other two thirds of the genome are expressed in other possible life-stage of *R. filosa*, not considered in this study. Actually, findings in the genome suggest a second sexual flagellated state of *R. filosa* which has not been observed in culture or natural environment yet (Glöckner et al., 2014). Nonetheless, all the obtained *in silico* data of *R. filosa* will have to be verified by extensive biochemical and cell biological research.

7 Literature

ADAMS, J. A. 2001. Kinetic and Catalytic mechanisms of protein kinases. *Chem Rev,* 101**,** 2271-2290.

ADL, S. M., SIMPSON, A. G., LANE, C. E., LUKES, J., BASS, D., BOWSER, S. S., BROWN, M. W., BURKI, F., DUNTHORN, M., HAMPL, V., HEISS, A., HOPPENRATH, M., LARA, E., LE GALL, L., LYNN, D. H., MCMANUS, H., MITCHELL, E. A., MOZLEY-STANRIDGE, S. E., PARFREY, J., PAWLOWSKI, J., RUECKERT, S., SHADWICK, R. S., SCHOCH, C. L., SMIRNOV, A. & SPIEGEL, F. W. 2013. The revised classification of eukaryotes. *J Eukaryot Microbiol.,* 5**,** 429-493.

AMODEO, G. A., RUDOLPH, M. J. & TONG, L. 2007. Crystal structure of the heterotrimer core of Saccharomyces cerevisiae AMPK homologue SNF1. *Nature,* 449**,** 492-495.

ANNESLEY, S. J., BAGO, R., MEHTA, A. & FISCHER, P. R. 2011. A genetic interaction between NDPK and AMPK in Dictyostelium discoideum that affects motility, growth and development. *Naunyn Schmiedebergs Arch Pharmacol. ,* 384**,** 341-349.

ARASADA, R., SON, H., RAMALINGAM, N., EICHINGER, L., SCHLEICHER, M. & ROHLFS, M. 2006. Characterization of the Ste20-like kinase Krs1 of Dictyostelium discoideum. *Eur J Cell Biol.,* 85**,** 1059-1068.

ARTEMENKO, Y., BATSIOS, P., BORLEIS, J., GAGNON, Z., LEE, J., ROHLFS, M., SANSÉAU, D., WILLARD, S. S., SCHLEICHER, M. & DEVREOTES, P. N. 2012. Tumor suppressor Hippo/MST1 kinase mediates chemotaxis by regulating spreading and adhesion. *Proc Natl Acad Sci U S A,* 109**,** 13632–13637.

ASHKIN, A., SCHÜTZE, K., DZIEDZIC, J. M., EUTENEUER, U. & SCHLIWA, M. 1990. Force generation of organelle transport measured in vivo by an infrared laser trap. *Nature,* 348**,** 346-348.

ASHWORTH, J. M. & WATTS, D. J. 1970. Metabolism of the cellular slime mould Dictyostelium discoideum grown in axenic culture. *Biochem J,* 119**,** 175-82.

AVRUCH, J., ZHOU, D., FITAMANT, J. & BARDEESY, N. 2011. Mst1/2 signalling to Yap: gatekeeper for liver size and tumour development. *Br J Cancer,* 104**,** 24-32.

BAAS, A. F., BOUDEAU, J., SAPKOTA, G. P., SMIT, L., MEDEMA, R., MORRICE, N. A., ALESSI, D. R. & CLEVERS, H. C. 2003. Activation of the tumour suppressor kinase LKB1 by the STE20-like pseudokinase STRAD. *EMBO J,* 22**,** 3062-72.

BAAS, A. F., KUIPERS, J., VAN DER WEL, N. N., BATLLE, E., KOERTEN, H. K., PETERS, P. J. & CLEVERS, H. C. 2004a. Complete polarization of single intestinal epithelial cells upon activation of LKB1 by STRAD. *Cell,* 116**,** 457-66.

BAAS, A. F., SMIT, L. & CLEVERS, H. 2004b. LKB1 tumor suppressor protein: PARtaker in cell polarity. *Trends Cell Biol,* 14**,** 312-9.

BALDAUF, S. L., ROGER, A. J., WENK-SIEFERT, I. & DOOLITTLE, W. F. 2000. A kingdom-level phylogeny of eukaryotes based on combined protein data. *Science,* 290**,** 972-977.

BATEMAN, A. 1997. The structure of a domain common to archaebacteria and the homocystinuria disease protein. *Trends Biochem Sci,* 22**,** 12-13.

BAYKOV, A. A., TUOMINEN, H. K. & LAHTI, R. 2011. The CBS Domain: A Protein Module with an Emerging Prominent Role in Regulation. *ACS Chem Biol.,* 6**,** 1156-1163.

BECCARI, D. F. 1745. De Bononiensi Scientiarum et Artium Institute atque Acedemia Commentarii,. *Proceedings of the Bologna Academy,* 2**,** 122.

BIDLINGMAIER, S., WEISS, E. L., SEIDEL, C., DRUBIN, D. G. & SNYDER, M. 2001. The Cbk1p pathway is important for polarized cell growth and cell separation in Saccharomyces cerevisiae. *Mol Cell Biol,* 21**,** 2449-62.

BIEMANS-OLDEHINKEL, E., MAHMOOD, N. A. & POOLMAN, B. 2006. A sensor for intracellular ionic strength. *Proc Natl Acad Sci U S A,* 103**,** 10624-10629.

BLAIR, E., REDWOOD, C., ASHRAFIAN, H., OLIVEIRA, M., BROXHOLME, J., KERR, B., SALMON, A., OSTMAN-SMITH, I. & WATKINS, H. 2001. Mutations in the gamma(2) subunit of AMP-activated protein kinase cause familial hypertrophic cardiomyopathy: evidence for the central role of energy compromise in disease pathogenesis. *Hum Mol Genet,* 10**,** 1215-1220.

BLOW, J. J. & TANAKA, T. U. 2005. The chromosome cycle: coordinating replication and segregation. *EMBO Rep,* 6**,** 1028-1034.

BOGOMOLNAYA, L. M., PATHAK, R., GUO, J., CHAM, R., ARAMAYO, R. & POLYMENIS, M. 2004. Hym1p affects cell cycle progression in Saccharomyces cerevisiae. *Curr Genet,* 46**,** 183-92.

BOKKO, P. B., FRANCIONE, L., BANDALA-SANCHEZ, E., AHMED, A. U., ANNESLEY, S. J., HUANG, X., KHURANA, T., KIMMEL, A. R. & FISHER, P. R. 2007. Diverse cytopathologies in mitochondrial disease are caused by AMP-activated protein kinase signaling. *Mol Biol Cell,* 18**,** 1874-86.

BOUDEAU, J., BAAS, A. F., DEAK, M., MORRICE, N. A., KIELOCH, A., SCHUTKOWSKI, M., PRESCOTT, A. R., CLEVERS, H. C. & ALESSI, D. R. 2003. MO25alpha/beta interact with STRADalpha/beta enhancing their ability to bind, activate and localize LKB1 in the cytoplasm. *EMBO J,* 22**,** 5102-14.

BOUDEAU, J., SCOTT, J. W., RESTA, N., DEAK, M., KIELOCH, A., KOMANDER, D., HARDIE, D. G., PRESCOTT, A. R., VAN AALTEN, D. M. & ALESSI, D. R. 2004. Analysis of the LKB1-STRAD-MO25 complex. *J Cell Sci,* 117**,** 6365-75.

BRACONNOT, H. 1820. Sur la Conversion des matieres animales en nouvelles substances par le moyen de Vacide sulfurique. *Ann. de Chim. et de Phys.,* 13**,** 113-125.

BRAJENOVIC, M., JOBERTY, G., KUSTER, B., BOUWMEESTER, T. & DREWES, G. 2004. Comprehensive proteomic analysis of human Par protein complexes reveals an interconnected protein network. *J Biol Chem,* 279**,** 12804-11.

BREFELD, J. O. 1869. Dictyostelium mucoroides. Ein neuer Organismus aus der verwandtschaft der Myxomyceten. *Abhandlung en der Senckenbergischen Naturforschenden Gesellschaft Frankfurt***,** 85-107.

BURNETT, G. & KENNEDY, E. P. 1954. The enzymatic phosphorylation of proteins. *J. Biol. Chem.,* 211.

CANTLEY, L. 2002. The phosphoinositide 3-kinase pathway. *Science,* 296**,** 1655-1657.

CARR, G., SIMMONS, N. & SAYER, J. 2003. A role for CBS domain 2 in trafficking of chloride channel CLC-5. *Biochem Biophys Res Commun,* 310**,** 600-605.

CHAN, E. H., NOUSIAINEN, M., CHALAMALASETTY, R. B., SCHAFER, A., NIGG, E. A. & SILLJE, H. H. 2005. The Ste20-like kinase Mst2 activates the human large tumor suppressor kinase Lats1. *Oncogene,* 24**,** 2076-86.

CHARETTE, S. J. & COSSON, P. 2004. Preparation of genomic DNA from Dictyostelium discoideum for PCR analysis. *Biotechniques,* 36**,** 574-5.

CHISHOLM, R. L. & FIRTEL, R. A. 2004. Insights into morphogenesis from a simple developmental system. *Nat Rev Mol Cell Biol,* 5**,** 531-41.

COHEN, P. 2002. The origins of protein phosphorylation. *Nat Cell Biol,* 4**,** E127-E130.

COOPER, G. M. & HAUSMAN, R. E. 2013. Part IV, Chapter 16: The Eukaryotic Cell Cycle. *ASM Press,* 6th ed.**,** 641-647.

COZZONE, A. J. 1988. Protein phosphorylation in prokaryotes. *Annu. Rev. Microbiol.,* 42**,** 97-125.

CRICK, F. H. C. 1957. On protein synthesis. *Symp. Soc. Exp. Biol.,* 12**,** 138-163.

CURTIS, B. A., TANIFUIJI, G., BURKI, F., GRUBER, A., IRIMIA, M., MARUYAMA, S., ARIAS, M. C., BALL, S. G., GILE, G. H., HIRAKAWA, Y., HOPKINS, J. F., KUO, A., RENSING, S. A., SCHMUTZ, J., SYMEONIDI, A., ELIAS, M., EVELEIGH, R. J., HERMAN, E. K., KLUTE, M. J., NAKAYAMA, T., OBORNÍK, M., REYES-PRIETO, A., ARMBRUST, E. V., AVES, S. J., BEIKO, R. G., COUTINHO, P., DACKS, J. B., DURNFORD, D. G., FAST, N. M., GREEN, B. R., GRISDALE, C. J., HEMPEL, F., HENRISSAT, B., HÖPPNER, M. P., ISHIDA, K., KIM, E., KOŘENÝ, L., KROTH, P. G., LIU, Y., MALIK, S. B., MAIER, U. G., MCROSE, D., MOCK, T., NEILSON, J. A., ONODERA, N. T., POOLE, A. M., PRITHAM, E. J., RICHARDS, T. A., ROCAP, G., ROY, S. W., SARAI, C., SCHAACK, S., SHIRATO, S., SLAMOVITS, C. H., SPENCER, D. F., SUZUKI, S., WORDEN, A. Z., ZAUNER, S., BARRY, K., BELL, C., BHARTI, A. K., CROW, J. A., GRIMWOOD, J., KRAMER, R., LINDQUIST, E., LUCAS, S., SALAMOV, A., MCFADDEN, G. I., LANE, C. E., KEELING, P. J., GRAY, M. W., GRIGORIEV, I. V. & ARCHIBALD, J. M. 2012. Algal genomes reveal evolutionary mosaicism and the fate of nucleomorphs. *Nature,* 492**,** 59-65.

D'ORBIGNY, A. D. 1826. Tableau méthodique de la classe des Céphalopodes. *Annals des Sciences Naturelles,* 7**,** 245-314.

D'ORBIGNY, A. D. 1840. Mémoire sur les Foraminiféres de la Craie blanche du Bassin de Paris. *Mém. Soc. Géol. France,* 4**,** 1-51.

DAGERT, M. & EHRLICH, S. D. 1979. Prolonged incubation in calcium chloride improves the competence of Escherichia coli cells. *Gene,* 6**,** 23-8.

DAN, I., ONG, S., WATANABE, N., BLAGOEV, B., NIELSEN, M., KAJIKAWA, E., KRISTIANSEN, T., MANN, M. & PANDEY, A. 2002. Cloning of MASK, a novel member of the mammalian germinal center kinase III subfamily, with apoptosis-inducing properties. *J Biol Chem***,** 5929-5939.

DAN, I., WATANABE, N. M. & KUSUMI, A. 2001. The Ste20 group kinases as regulators of MAP kinase cascades. *Trends Cell Biol,* 11**,** 220-30.

DARCY, P. K., WILCZYNSKA, Z. & FISHER, P. R. 1994. Genetic analysis of Dictyostelium slug phototaxis. *Genetics,* 134**,** 977-985.

DE ANGELI, A., MORAN, O., WEGE, S., FILLEUR, S., EPHRITIKHINE, G., THOMINE, S., BARBIER-BRYGOO, H. & GAMBALE, F. 2009. ATP Binding to the C Terminus of the Arabidopsis thaliana Nitrate/Proton Antiporter, AtCLCa, Regulates Nitrate Transport into Plant Vacuoles. *J Biol Chem,* 284**,** 26526-26532.

DE SOUZA, C. P. & OSMANI, S. A. 2007. Mitosis, not just open or closed. *Eukaryot Cell,* 6**,** 1521-1527.

DELPIRE, E. 2009. The mammalian family of sterile 20p-like protein kinases. *Pflugers Arch,* 458**,** 953-67.

DELPIRE, E. & GAGNON, K. B. 2008. SPAK and OSR1: STE20 kinases involved in the regulation of ion homoeostasis and volume control in mammalian cells. *Biochem J,* 409**,** 321-31.

DIECKMANN, R., VON HEYDEN, Y., KISTLER, C., GOPALDASS, N., HAUSHERR, S., CRAWLEY, S. W., SCHWARZ, E. C., DIENSTHUBER, R. P., COTE, G. P., TSIAVALIARIS, G. & SOLDATI, T. 2010. A myosin IK-Abp1-PakB circuit acts as a switch to regulate phagocytosis efficiency. *Mol Biol Cell,* 21**,** 1505-18.

DOBELL, C. 1932. Antony van Leeuwenhoek and his Little Animals. *Harcourt, Brace and Company, New York,* 1st ed.**,** 261-264.

DORLAND, S., DEEGENAARS, M. L. & STILLMAN, D. J. 2000. Roles for the Saccharomyces cerevisiae SDS3, CBK1 and HYM1 genes in transcriptional repression by SIN3. *Genetics,* 154**,** 573-86.

EDGAR, B. A. 2006. From cell structure to transcription: Hippo forges a new path. *Cell,* 124**,** 267-73.

EFFLER, J. C., KEE, Y. S., BERK, J. M., TRAN, M. N., IGLESIAS, P. A. & ROBINSON, D. N. 2006. Mitosis-specific mechanosensing and contractile-protein redistribution control cell shape. *Curr Biol,* 16**,** 1962-1967.

EGGERT, U. S., MITCHISON, T. J. & FIELD, C. M. 2006. ANIMAL CYTOKINESIS: From Parts List to Mechanisms. *Annu Rev Biochem,* 75**,** 543-566.

EICHINGER, L., BÄHLER, M., DIETZ, M., ECKERSKORN, C. & SCHLEICHER, M. 1998. Characterization and cloning of a Dictyostelium Ste20-like protein kinase that phosphorylates the actin-binding protein severin. *J Biol Chem***,** 12952-12959.

EICHINGER, L., PACHEBAT, J. A., GLOCKNER, G., RAJANDREAM, M. A., SUCGANG, R., BERRIMAN, M., SONG, J., OLSEN, R., SZAFRANSKI, K., XU, Q., TUNGGAL, B., KUMMERFELD, S., MADERA, M., KONFORTOV, B. A., RIVERO, F., BANKIER, A. T., LEHMANN, R., HAMLIN, N., DAVIES, R., GAUDET, P., FEY, P., PILCHER, K., CHEN, G., SAUNDERS, D., SODERGREN, E., DAVIS, P., KERHORNOU, A., NIE, X., HALL, N., ANJARD, C., HEMPHILL, L., BASON, N., FARBROTHER, P., DESANY, B., JUST, E., MORIO, T., ROST, R., CHURCHER, C., COOPER, J., HAYDOCK, S., VAN DRIESSCHE, N., CRONIN, A., GOODHEAD, I., MUZNY, D., MOURIER, T., PAIN, A., LU, M., HARPER, D., LINDSAY, R., HAUSER, H., JAMES, K., QUILES, M., MADAN BABU, M., SAITO, T., BUCHRIESER, C., WARDROPER, A., FELDER, M., THANGAVELU, M., JOHNSON, D., KNIGHTS, A., LOULSEGED, H., MUNGALL, K., OLIVER, K., PRICE, C., QUAIL, M. A., URUSHIHARA, H., HERNANDEZ, J., RABBINOWITSCH, E., STEFFEN, D., SANDERS, M., MA, J., KOHARA, Y., SHARP, S., SIMMONDS, M., SPIEGLER, S., TIVEY, A., SUGANO, S., WHITE, B., WALKER, D., WOODWARD, J., WINCKLER, T., TANAKA, Y., SHAULSKY, G., SCHLEICHER, M., WEINSTOCK, G., ROSENTHAL, A., COX, E. C., CHISHOLM, R. L., GIBBS, R., LOOMIS, W. F., PLATZER, M., KAY, R. R., WILLIAMS, J., DEAR, P. H., NOEGEL, A. A., BARRELL, B. & KUSPA, A. 2005. The genome of the social amoeba Dictyostelium discoideum. *Nature,* 435**,** 43-57.

EREÑO-ORBEA, J., OYENARTE, I. & MARTÍNEZ-CRUZ, L. A. 2013. CBS domains: Ligand binding sites and conformational variability. *Arch Biochem Biophys,* 54**,** 70-81.

FAIX, J., KREPPEL, L., SHAULSKY, G., SCHLEICHER, M. & KIMMEL, A. R. 2004. A rapid and efficient method to generate multiple gene disruptions in Dictyostelium discoideum using a single selectable marker and the Cre-loxP system. *Nucleic Acids Res,* 32**,** e143.

FARBROTHER, P., WAGNER, C., NA, J., TUNGGAL, B., MORIO, T., URUSHIHARA, H., TANAKA, Y., SCHLEICHER, M., STEINERT, M. & EICHINGER, L. 2006. Dictyostelium transcriptional host cell response upon infection with Legionella. *Cell Microbiol,* 8**,** 438-56.

FILIPPI, B. M., DE LOS HEROS, P., MEHELLOU, Y., NAVRATILOVA, I., GOURLAY, R., DEAK, M., PLATER, L., TOTH, R., ZEQIRAJ, E. & ALESSI, D. R. 2011. MO25 is a master regulator of SPAK/OSR1 and MST3/MST4/YSK1 protein kinases. *Embo J,* 30**,** 1730-1741.

FILOSA, M. F. & DENGLER, R. E. 1972. Ultrastructure of macrocyst formation in the cellular slime mold, Dictyostelium mucoroides: extensive phagocytosis of amoebae by a specialized cell. *Dev Biol,* 29**,** 1-16.

FLAKOWSKI, J., BOLIVAR, I., FAHRINI, J. & PAWLOWSKI, J. 2005. Actin Phylogeny Of Foraminifera. *Journal of Foraminferal Research,* 35**,** 93-102.

GERISCH, G., FAIX, J., KOHLER, J. & MULLER-TAUBENBERGER, A. 2004. Actin-binding proteins required for reliable chromosome segregation in mitosis. *Cell Motil Cytoskeleton,* 57**,** 18-25.

GIGLIONE, C., BOULAROT, A. & MEINNEL, T. 2004. Protein N-terminal methionine excision. *Cell Mol. Life Sci.,* 61**,** 1455-1474.

GLÖCKNER, G., HÜLSMANN, N., SCHLEICHER, M., NOEGEL, A. A., EICHINGER, L., GALLINGER, C., PAWLOWSKI, J., SIERRA, R., EUTENEUER, U., PILLET, L., MOUSTAFA, A., PLATZER, M., GROTH, M., SZAFRANSKI, K. & SCHLIWA, M. 2014. The genome of the foraminiferan Reticulomyxa filosa. *Curr Biol.,* 24**,** 11-18.

GLOTZER, M. 2001. Animal cell cytokinesis. *Annu Rev Cell Dev Biol,* 17**,** 351-86.

GOLDBERG, J. M., MANNING, G., LIU, A., FEY, P., PILCHER, K. E., XU, Y. & SMITH, J. L. 2006. The dictyostelium kinome--analysis of the protein kinases from a simple model organism. *PLoS Genet,* 2**,** e38.

GOSHIMA, T., KUME, K., KOYANO, T., OHYA, Y., TODA, T. & HIRATA, D. 2010. Fission yeast germinal center (GC) kinase Ppk11 interacts with Pmo25 and plays an auxiliary role in concert with the morphogenesis Orb6 network (MOR) in cell morphogenesis. *J Biol Chem,* 285**,** 35196-35205.

GUO, C., TOMMASI, S., LIU, L., YEE, J. K., DAMMANN, R. & PFEIFER, G. P. 2007. RASSF1A Is Part of a Complex Similar to the Drosophila Hippo/Salvador/Lats Tumor-Suppressor Network. *Curr Biol*.

HAGEDORN, M., NEUHAUS, E. M. & SOLDATI, T. 2006. Optimized fixation and immunofluorescence staining methods for Dictyostelium cells. *Methods Mol Biol,* 346**,** 327-38.

HANKS, S. & HUNTER, T. 1995a. Protein kinases 6. The eukaryotic protein kinase superfamily: kinase (catalytic) domain structure and classification. *FASEB J,* 9**,** 576-596.

HANKS, S. K. & HUNTER, T. 1995b. The eukaryotic protein kinase superfamily: kinase (catalytic) domain structure and classification. *Faseb J,* 9**,** 576-96.

HARPER, R. A. 1926. Morphogenesis in Dictyostelium. *Bull. Torrey Bot. Club***,** 229-268.

HARPER, R. A. 1932. Organization and light relations in Polyshondylium. *Bull. Torrey Bot. Club***,** 49-84.

HATTORI, M., IWASE, N., FURUYA, N., TANAKA, Y., TSUKAZAKI, T., ISHITANI, R., MAGUIRE, M. E., ITO, K., MATURANA, A. & NUREKI, O. 2009. Mg(2+)-dependent gating of bacterial MgtE channel underlies Mg(2+) homeostasis. *Embo J,* 28**,** 3602-3612.

HAWLEY, S. A., BOUDEAU, J., REID, J. L., MUSTARD, K. J., UDD, L., MAKELA, T. P., ALESSI, D. R. & HARDIE, D. G. 2003. Complexes between the LKB1 tumor suppressor, STRAD alpha/beta and MO25 alpha/beta are upstream kinases in the AMP-activated protein kinase cascade. *J Biol,* 2**,** 28.

HAYLES, J. & NURSE, P. 1989. A review of mitosis in the fission yeast Schizosaccharomyces pombe. *Exp Cell Res,* 184**,** 273-286.

HILBI, H., WEBER, S., RAGAZ, C., NYFELDER, Y. & URWYLER, S. 2007. Environmental predators as models for bacterial pathogenesis. *Environ Microbiol,* 9**,** 563-575.

HOAGLAND, M. B. 1955. An enzymatic mechanism for amino acid activation in animal tissues. *Biochim Biophys Acta,* 16**,** 288-289.

HOAGLAND, M. B., KELLER, E. B. & ZAMECNIK, P. C. 1956. Enzymatic activation of amino acids. *J. Biol. Chem,* 231**,** 345-358.

HOLZER, H. & DUNTZE, W. 1971. Metabolic regulation by chemical modification of enzymes. *Annu Rev Biochem,* 40**,** 345-374.

HÜLSMANN, N. 2006. Bewegung, Nahrungsaufnahme und Fortpflanzung bei Reticulomyxa filosa (Rhizopodia). *Begleitpublikation zum Film C 1639*.

HWANG, E., RYU, K. S., PAAKKONEN, K., GÜNTERT, P., CHEONG, H. K., LIM, D. S., LEE, J. O., JEON, Y. H. & CHEONG, C. 2007. Structural insight into dimeric interaction of the SARAH domains from Mst1 and RASSF family proteins in the apoptosis pathway. *Proc Natl Acad Sci U S A,* 104**,** 9236-9241.

JAFFER, Z. M. & CHERNOFF, J. 2002. p21-Activated kinases: three more join the Pak. *The International Journal of Biochemistry & Cell Biology,* 34**,** 713-717.

JALEEL, M., MCBRIDE, A., LIZCANO, J. M., DEAK, M., TOTH, R., MORRICE, N. A. & ALESSI, D. R. 2005. Identification of the sucrose non-fermenting related kinase SNRK, as a novel LKB1 substrate. *FEBS Lett,* 579**,** 1417-23.

JÄMSEN, J., BAYKOV, A. A. & LAHTI, R. 2010. Nucleotide- and Substrate-Induced Conformational Transitions in the CBS Domain-Containing Pyrophosphatase of Moorella thermoacetica. *Biochemistry,* 49**,** 1005-1013.

JANSEN, M., TEN KLOOSTER, J. P., OFFERHAUS, G. J. & CLEVERS, H. 2009. LKB1 and AMPK family signaling: the intimate link between cell polarity and energy metabolism. *Physiol Rev,* 89**,** 777-98.

JOSEPH, J. M., FEY, P., RAMALINGAM, N., LIU, X. I., ROHLFS, M., NOEGEL, A. A., MULLER-TAUBENBERGER, A., GLOCKNER, G. & SCHLEICHER, M. 2008. The actinome of Dictyostelium discoideum in comparison to actins and actin-related proteins from other organisms. *PLoS ONE,* 3**,** e2654.

KANAI, M., KUME, K., MIYAHARA, K., SAKAI, K., NAKAMURA, K., LEONHARD, K., WILEY, D. J., VERDE, F., TODA, T. & HIRATA, D. 2005. Fission yeast MO25 protein is localized at SPB and septum and is essential for cell morphogenesis. *EMBO J,* 24**,** 3012-25.

KANNAN, N. & TAYLOR, S. S. 2008. Rethinking pseudokinases. *Cell,* 133**,** 204-5.

KAROS, M. & FISCHER, R. 1996. hymA (hypha-like metulae), a new developmental mutant of Aspergillus nidulans. *Microbiology,* 142 (Pt 11)**,** 3211-8.

KAROS, M. & FISCHER, R. 1999. Molecular characterization of HymA, an evolutionarily highly conserved and highly expressed protein of Aspergillus nidulans. *Mol Gen Genet,* 260**,** 510-21.

KENDREW, J. C., BODO, G., DINTZIS, H. M., PARRISH, R. G., WYCKOFF, H. & PHILLIPS, D. C. 1958. A three-dimensional model of the myoglobin molecule obtained by x-ray analysis. *Nature,* 181**,** 662-666.

KENNAN, A., AHERNE, A., PALFI, A., HUMPHRIES, M., MCKEE, A., STITT, A., SIMPSON, D. A., DEMTRODER, K., ORNTOFT, T., AYUSO, C., KENNA, P. F., FARRAR, G. J. & HUMPHRIES, P. 2002. Identification of an IMPDH1 mutation in autosomal dominant retinitis pigmentosa (RP10) revealed following comparative microarray

analysis of transcripts derived from retinas of wild-type and Rho(-/-) mice. *Hum Mol Genet,* 11**,** 547-557.

KORNAK, U., KASPER, D., BOSL, M. R., KAISER, E., SCHWEIZER, M., SCHULZ, A., FRIEDRICH, W., DELLING, G. & JENTSCH, T. J. 2001. Loss of the ClC-7 chloride channel leads to osteopetrosis in mice and man. *Cell,* 104**,** 205-215.

KOSSEL, A. 1898. Ueber die Constitution der einfachsten Eiweissstoffe. *Zeit. physiol. Chem.,* 25**,** 165-189.

KREBS, E. G. & FISCHER, F. H. 1956. The phosphorylase b to a converting enzyme of rabbit skeletal muscle. *Biochim Biophys Acta.,* 20**,** 811-820.

KYRIAKIS, J. M. 1999. Signaling by the germinal center kinase family of protein kinases. *J Biol Chem,* 274**,** 5259-62.

KYRIAKIS, J. M. 2014. In the Beginning, There Was Protein Phosphorylation. *J. Biol. Chem.***,** 1-4.

LABESSE, G., ALEXANDRE, T., VAUPRÉ, L., SALARD-ARNAUD, I., HIM, J. L., RAYNAL, B., BRON, P. & MUNIER-LEHMANN, H. 2013. MgATP regulates allostery and fiber formation in IMPDHs. *Structure,* 21**,** 975-985.

LAEMMLI, U. K. 1970. Cleavage of structural proteins during the assembly of the head of bacteriophage T4. *Nature,* 227**,** 680-5.

LEE, S. J., COBB, M. H. & GOLDSMITH, E. J. 2009. Crystal structure of domain-swapped STE20 OSR1 kinase domain. *Protein Sci,* 18**,** 304-313.

LEISERSON, W., HARKINS, E. & KESHISHIAN, H. 2000a. Fray, a Drosophila serine/threonine kinase homologous to mammalian PASK, is required for axonal ensheathment. *Neuron***,** 793-806.

LEISERSON, W. M., HARKINS, E. W. & KESHISHIAN, H. 2000b. Fray, a Drosophila serine/threonine kinase homologous to mammalian PASK, is required for axonal ensheathment. *Neuron,* 28**,** 793-806.

LEVENE, P. A. & ALSBERG, C. L. 1906. The cleavage products of vitellin. *J. Biol. Chem.,* 2**,** 127-133.

LING, P., LU, T. J., YUAN, C. J. & LAI, M. D. 2008. Biosignaling of mammalian Ste20-related kinases. *Cell Signal,* 20**,** 1237-47.

LIU, G., SHI, Z., JIAO, S., ZHANG, Z., WANG, W., CHEN, C., HAO, Q., ZHANG, M., FENG, M., XU, L., ZHANG, Z., ZHOU, Z. & ZHANG, M. 2014. Structure of MST2 SARAH domain provides insights into its interaction with RAPL. *J Struct Biol,* 185**,** 366-374.

LIZCANO, J. M., GORANSSON, O., TOTH, R., DEAK, M., MORRICE, N. A., BOUDEAU, J., HAWLEY, S. A., UDD, L., MAKELA, T. P., HARDIE, D. G. & ALESSI, D. R. 2004. LKB1 is a master kinase that activates 13 kinases of the AMPK subfamily, including MARK/PAR-1. *EMBO J,* 23**,** 833-43.

MAHMOOD, N. A., BIEMANS-OLDEHINKEL, E. & POOLMAN, B. 2009. Engineering of Ion Sensing by the Cystathionine β-Synthase Module of the ABC Transporter OpuA. *J Biol Chem,* 284**,** 14368-14376.

MAHMOUDI, M., AZAMANESH, K., SHOKRGOZAR, M. A., JOURNEAY, W. S. & LAURENT, S. 2011. Effect of nanoparticles on the cell life cycle. *Chem Rev,* 111**,** 3407-3432.

MALCHOW, D., NAGELE, B., SCHWARZ, H. & GERISCH, G. 1972. Membrane-bound cyclic AMP phosphodiesterase in chemotactically responding cells of Dictyostelium discoideum. *Eur J Biochem,* 28**,** 136-42.

MANNING, G., PLOWMAN, G. D., HUNTER, T. & SUDARSANAM, S. 2002a. Evolution of protein kinase signaling from yeast to man. *Trends Biochem Sci,* 27**,** 514-20.

MANNING, G., WHYTE, D. B., MARTINEZ, R., HUNTER, T. & SUDARSANAM, S. 2002b. The protein kinase complement of the human genome. *Science,* 298**,** 1912-34.

MAYA-MENDOZA, A., TANG, C. W., POMBO, A. & JACKSON, D. A. 2009. Mechanisms regulating S phase progression in mammalian cells. *Front Biosci.,* 14**,** 4199-4213.

MEHELLOU, Y., ALESSI, D. R., MACARTNEY, T. J., SZKLARZ, M., KNAPP, S. & ELKINS, J. M. 2013. Structural insights into the activation of MST3 by MO25. *Biochem Biophys Res Commun.,* 431**,** 604-609.

MENDOZA, M., REDEMANN, S. & BRUNNER, D. 2005. The fission yeast MO25 protein functions in polar growth and cell separation. *Eur J Cell Biol,* 84**,** 915-26.

MILBURN, C. C., BOUDEAU, J., DEAK, M., ALESSI, D. R. & VAN AALTEN, D. M. 2004. Crystal structure of MO25 alpha in complex with the C terminus of the pseudo kinase STE20-related adaptor. *Nat Struct Mol Biol,* 11**,** 193-200.

MIYAMOTO, H., MATSUSHIRO, A. & NOZAKI, M. 1993. Molecular cloning of a novel mRNA sequence expressed in cleavage stage mouse embryos. *Mol Reprod Dev,* 34**,** 1-7.

MULDER, G. J. 1839. Ueber die Zusammensetzung einiger thierischen Substanzen. *Journal für praktische Chemie***,** 129-152.

MURAMOTO, T., KUWAYAMA, H., KOBAYASHI, K. & URUSHIHARA, H. 2007. A stress response kinase, KrsA, controls cAMP relay during the early development of Dictyostelium discoideum. *Developmental Biology,* In Press**,** doi: 10.1016/j.ydbio.2007.01.039.

NA, J., TUNGGAL, B. & EICHINGER, L. 2007. STATc is a key regulator of the transcriptional response to hyperosmotic shock. *BMC Genomics,* 8**,** 123.

NAGASAKI, A., KANADA, M. & UYEDA, T. Q. 2009. Cell adhesion molecules regulate contractile ring-independent cytokinesis in Dictyostelium discoideum. *Cell Res,* 19**,** 236-46.

NAUSS, R. N. 1949. Reticulomyxa filosa gen. et spec. nov., a new primitive plasmodium. *Bull. Torrey Bot. Club,* 76**,** 161-173.

NELSON, B., KURISCHKO, C., HORECKA, J., MODY, M., NAIR, P., PRATT, L., ZOUGMAN, A., MCBROOM, L. D., HUGHES, T. R., BOONE, C. & LUCA, F. C. 2003. RAM: a conserved signaling network that regulates Ace2p transcriptional activity and polarized morphogenesis. *Mol Biol Cell,* 14**,** 3782-803.

NEUHAUS, E. M., ALMERS, W. & SOLDATI, T. 2002. Morphology and dynamics of the endocytic pathway in Dictyostelium discoideum. *Mol Biol Cell,* 13**,** 1390-1407.

NEUJAHR, R., HEIZER, C. & GERISCH, G. 1997. Myosin II-independent processes in mitotic cells of Dictyostelium discoideum: redistribution of the nuclei, re-arrangement of the actin system and formation of the cleavage furrow. *J Cell Sci,* 110 (Pt 2)**,** 123-37.

NOZAKI, M., ONISHI, Y., TOGASHI, S. & MIYAMOTO, H. 1996. Molecular characterization of the Drosophila Mo25 gene, which is conserved among Drosophila, mouse, and yeast. *DNA Cell Biol,* 15**,** 505-9.

O'CONNELL, K. L. & STULTS, J. T. 1997. Identification of mouse liver proteins on two-dimensional electrophoresis gels by matrix-assisted laser desorption/ionization mass spectrometry of in situ enzymatic digests. *Electrophoresis,* 18**,** 349-59.

O'DAY, D. & KESZEI, A. 2012. Signalling and sex in the social amoebozoans. *Biol Rev Camb Philos Soc,* 87**,** 313-329.

O'NEILL, E. E., MATALLANAS, D. & KOLCH, W. 2005. Mammalian sterile 20-like kinases in tumor suppression: an emerging pathway. *Cancer Res,* 65**,** 5485-7.

ORLOVA, K. A., PARKER, W. E., HEUER, G. G., TSAI, V., YOON, J., BAYBIS, M., FENNING, R. S., STRAUSS, K. & CRINO, P. B. 2010. STRADalpha deficiency results in aberrant mTORC1 signaling during corticogenesis in humans and mice. *J Clin Invest,* 120**,** 1591-602.

OROKOS, D. D., COLE, R. W. & TRAVIS, J. L. 2000. Organelles Are Transported on Sliding Microtubules in Reticulomyxa In: Cell Motility and the Cytoskeleton. *Cell Motil Cytoskeleton,* 47**,** 296-306.

PERUTZ, M. F., ROSSMANN, M. G., CULLIS, M. G., MUIRHEAD, H., WILL, G. & NORTH, A. C. 1960. Structure of haemoglobin: a three-dimensional Fourier synthesis at 5.5-A. resolution, obtained by X-ray analysis. *Nature,* 185**,** 416-422.

PIECHOTTA, K., GARBARINI, N., ENGLAND, R. & DELPIRE, E. 2003. Characterization of the interaction of the stress kinase SPAK with the Na+-K+-2Cl- cotransporter in the nervous system: evidence for a scaffolding role of the kinase. *J Biol Chem,* 278**,** 52848-56.

PUSCH, M. 2002. Myotonia caused by mutations in the muscle chloride channel gene CLCN1. *Hum Mutat,* 19**,** 423-434.

RADU, M. & CHERNOFF, J. 2009. The DeMSTification of mammalian Ste20 kinases. *Curr Biol,* 19**,** R421-5.

RAJAKULENDRAN, T. & SICHERI, F. 2010. Allosteric protein kinase regulation by pseudokinases: insights from STRAD. *Sci Signal,* 3**,** pe8.

RAMER, S. W. & DAVIS, R. W. 1993. A dominant truncation allele identifies a gene, STE20, that encodes a putative protein kinase necessary for mating in Saccharomyces cerevisiae. *Proc Natl Acad Sci U S A,* 90**,** 452-456.

RAPER, K. B. 1935. Dictyostelium discoideum, a new species of slime mold from decaying forest leaves. *J. Agric. Res.,* 50**,** 135-147.

RAPER, K. B. 1984. The Dictyostelids. *Princeton University Press, Princeton, NJ.*

ROBINSON, D. N., GIRARD, K. D., OCTTAVIANI, E. & REICHL, E. M. 2002. Dictyostelium cytokinesis: from molecules to mechanics. *J Muscle Res Cell Motil,* 23**,** 719-27.

ROBINSON, D. N. & SPUDICH, J. A. 2004. Mechanics and regulation of cytokinesis. *Curr Opin Cell Biol,* 16**,** 182-8.

ROHLFS, M., ARASADA, R., BATSIOS, P., JANZEN, J. & SCHLEICHER, M. 2007. The Ste20-like kinase SvkA of Dictyostelium discoideum is essential for late stages of cytokinesis. *Journal of Cell Science,* 120**,** 4345-4354.

ROTHBAUER, U., ZOLGHADR, K., MUYLDERMANS, S., SCHEPERS, A., CARDOSO, M. C. & LEONHARDT, H. 2008. A versatile nanotrap for biochemical and functional studies with fluorescent fusion proteins. *Mol Cell Proteomics,* 7**,** 282-9.

RYOO, H. D. & STELLER, H. 2003. Hippo and its mission for growth control. *Nat Cell Biol,* 5**,** 853-5.

SADOUL, K., BOYAULT, C., PABION, M. & KHOCHBIN, S. 2008. Regulation of protein turnover by acetyltransferases and deacetylases. *Biochimie,* 90**,** 306-312.

SAMBROOK, J. & RUSSEL, D. W. 2001. *Molecular Cloning,* New York, Cold Spring Harbour Laboratory.

SANGER, F. 1949. The terminal peptides of Insulin. *Biochem J,* 45**,** 563-574.

SCHLEICHER, M. & JOCKUSCH, B. M. 2008. Actin: its cumbersome pilgrimage through cellular compartments. *Histochem Cell Biol,* 129**,** 695-704.

SCHLIWA, M., SHIMIZU, T., R.D., V. & EUTENEUER, U. 1991. Nucleotide Specificities of Anterograde and Retrograde Organelle Transport in Reticulomyxa Are Indistinguishable. *Journal of Cell Biology,* 6**,** 1199-1203.

SCOTT, J. W., HAWLEY, S. A., GREEN, K. A., ANIS, M., STEWART, G., SCULLION, G. A., NORMAN, D. G. & HARDIE, D. G. 2004. CBS domains form energy-sensing modules whose binding of adenosine ligands is disrupted by disease mutations. *J Clin Invest,* 113**,** 274-284.

SHAN, X., DUNBRACK, R. L. J., CHRISTOPHER, S. A. & KRUGER, W. D. 2001. Mutations in the regulatory domain of cystathionine β-synthase can functionally suppress patient-derived mutations in cis. *Hum Mol Genet,* 10**,** 635-643.

SHI, Z., JIAO, S., ZHANG, Z., MA, M., ZHANG, Z., CHEN, C., WANG, K., WANG, H., WANG, W., ZHANG, L., ZHAO, Y. & ZHOU, Z. 2013. Structure of the MST4 in complex with MO25 provides insights into its activation mechanism. *Structure,* 21**,** 449-461.

SOBEL, S. G. 1997. Mini review: mitosis and the spindle pole body in Saccharomyces cerevisiae. *J Exp Zool,* 277**,** 120-138.

SPICER, J., RAYTER, S., YOUNG, N., ELLIOTT, R., ASHWORTH, A. & SMITH, D. 2003. Regulation of the Wnt signalling component PAR1A by the Peutz-Jeghers syndrome kinase LKB1. *Oncogene,* 22**,** 4752-6.

STRANGE, K., DENTON, J. & NEHRKE, K. 2006. Ste20-type kinases: evolutionarily conserved regulators of ion transport and cell volume. *Physiology (Bethesda),* 21**,** 61-8.

STRMECKI, L., GREENE, D. M. & PEARS, C. J. 2005. Developmental decisions in Dictyostelium discoideum. *Dev Biol,* 284**,** 25-36.

SURCEL, A., KEE, Y. S., LUO, T. & ROBINSON, D. N. 2010. Cytokinesis through biochemical-mechanical feedback loops. *Semin Cell Dev Biol,* 21**,** 866-873.

TANG, Z., MANDEL, L. L., YEAN, S. L., LIN, C. X., CHEN, T., YANAGIDA, M. & LIN, R. J. 2003. The kic1 kinase of schizosaccharomyces pombe is a CLK/STY orthologue that regulates cell-cell separation. *Exp Cell Res,* 283**,** 101-15.

TEN KLOOSTER, J. P., JANSEN, M., YUAN, J., OORSCHOT, V., BEGTHEL, H., DI GIACOMO, V., COLLAND, F., DE KONING, J., MAURICE, M. M., HORNBECK, P. & CLEVERS, H. 2009. Mst4 and Ezrin induce brush borders downstream of the Lkb1/Strad/Mo25 polarization complex. *Dev Cell,* 16**,** 551-62.

TIAINEN, M., VAAHTOMERI, K., YLIKORKALA, A. & MAKELA, T. P. 2002. Growth arrest by the LKB1 tumor suppressor: induction of p21(WAF1/CIP1). *Hum Mol Genet,* 11**,** 1497-504.

TOWBIN, H., STAEHELIN, T. & GORDON, J. 1979. Electrophoretic transfer of proteins from polyacrylamide gels to nitrocellulose sheets: procedure and some applications. *Proc Natl Acad Sci U S A,* 76**,** 4350-4.

TRAVIS, J. F. & BOWSER, S. S. 1991. The motility of Foraminifera, Chapter in The Biology of the Foraminifera, (Lee, J.J. and O.R. Anderson, Eds.). *Academic Press, London.***,** 91-155.

TUOMINEN, H., SALMINEN, A., OKSANEN, E., JÄMSEN, J., HEIKKILÄ, O., LEHTIÖ, L., MAGRETOVA, N. N., GOLDMAN, A., BAYKOV, A. A. & LAHTI, R. 2010. Crystal Structures of the CBS and DRTGG Domains of the Regulatory Region of Clostridiumperfringens Pyrophosphatase Complexed with the Inhibitor, AMP, and Activator, Diadenosine Tetraphosphate. 398**,** 400-413.

URUSHIHARA, H. 2006. Cultivation, spore production, and mating. *Methods Mol Biol,* 346**,** 113-24.

URUSHIHARA, H. 2008. Developmental biology of the social amoeba: history, current knowledge and prospects. *Dev Growth Differ,* 50 Suppl 1**,** S277-81.

VEERANKI, S., HWANG, S. H., SUN, T., KIM, B. & KIM, L. 2011. LKB1 regulates development and the stress response in Dictyostelium. *Dev Biol,* 360**,** 351-357.

VELEVA-ROTSE, B. O., SMART, J. L., BAAS, A. F., EDMONDS, B., ZHAO, Z. M., BROWN, A., KLUG, L. R., HANSEN, K., REILLY, G., GARDNER, A. P., SUBBIAH, K., GAUCHER, E. A., CLEVERS, H. & BARNES, A. P. 2014. STRAD pseudokinases regulate axogenesis and LKB1 stability. *Neural Dev.,* [in process]

VUILLEMIN, P. 1903. Un Acrasiée bactériophage. *C. R. Acad. Sci. Paris,* 137**,** 387-389.

WALSH, C. 2006. *Posttranslational Modification of Proteins: Expanding Nature's Inventory*, Roberts and Company Publishers.

WANG, Y. & O'HALLORAN, T. J. 2006. Abp1 regulates pseudopodium number in chemotaxing Dictyostelium cells. *J Cell Sci,* 119**,** 702-10.

WEBER, I., GERISCH, G., HEIZER, C., MURPHY, J., BADELT, K., STOCK, A., SCHWARTZ, J. M. & FAIX, J. 1999. Cytokinesis mediated through the recruitment of cortexillins into the cleavage furrow. *Embo J,* 18**,** 586-94.

WEIJER, C. J. 2004. Dictyostelium morphogenesis. *Curr Opin Genet Dev,* 14**,** 392-8.

WOLF, W. A., CHEW, T. L. & CHISHOLM, R. L. 1999. Regulation of cytokinesis. *Cell Mol. Life Sci.,* 55**,** 108-120.

WU, S., HUANG, J., DONG, J. & PAN, D. 2003. hippo encodes a Ste-20 family protein kinase that restricts cell proliferation and promotes apoptosis in conjunction with salvador and warts. *Cell,* 114**,** 445-56.

YAMAMOTO, Y., IZUMI, Y. & MATSUZAKI, F. 2008. The GC kinase Fray and Mo25 regulate Drosophila asymmetric divisions. *Biochem Biophys Res Commun,* 366**,** 212-8.

YU, B., FEY, P., KESTIN-PILCHER, K. E., FEDOROV, A., PRAKASH, A., CHISHOLM, R. L. & WU, J. Y. 2011. Spliceosomal genes in the D. discoideum genome: a comparison with those in H. sapiens, D. melanogaster, A. thaliana and S. cerevisiae. *Protein Cell,* 2**,** 395-409.

ZEQIRAJ, E., FILIPPI, B. M., DEAK, M., ALESSI, D. R. & VAN AALTEN, D. M. 2009a. Structure of the LKB1-STRAD-MO25 complex reveals an allosteric mechanism of kinase activation. *Science,* 326**,** 1707-11.

ZEQIRAJ, E., FILIPPI, B. M., GOLDIE, S., NAVRATILOVA, I., BOUDEAU, J., DEAK, M., ALESSI, D. R. & VAN AALTEN, D. M. 2009b. ATP and MO25alpha regulate the conformational state of the STRADalpha pseudokinase and activation of the LKB1 tumour suppressor. *PLoS Biol,* 7**,** e1000126.

ZHANG, Z., IGLESIAS, D., ELIOPOULOS, N., EL KARES, R., CHU, L., ROMAGNANI, P. & GOODYER, P. 2011. A variant OSR1 allele which disturbs OSR1 mRNA expression in renal progenitor cells is associated with reduction of newborn kidney size and function. *Hum Mol Genet,* 20**,** 4167-4174.

ZHAO, B., LEI, Q. Y. & GUAN, K. L. 2008. The Hippo-YAP pathway: new connections between regulation of organ size and cancer. *Curr Opin Cell Biol,* 20**,** 638-346.

ZHOU, T., RAMAN, M., GAO, Y., EARNEST, S., CHEN, Z., MACHIUS, M., COBB, M. H. & GOLDSMITH, E. J. 2004. Crystal structure of the TAO2 kinase domain: activation and specificity of a Ste20p MAP3K. *Structure (Camb),* 12**,** 1891-900.

8 Acknowledgements

First of all, I thank *Prof. Dr. Michael Schleicher* for admitting me to his laboratory and for providing me with the interesting topics which led to the completion of this work. I thank you very much for your caring support, your great mentoring, your unlimited scientific and non-scientific knowledge and your unique way of looking at things from different angles. You are really an outstanding professor, a thoroughly decent person, a precious colleague and a friend. To me, you represent the classic picture of the humanist. Thank you very much, indeed!

Secondly, I thank *Dr. Meino Rohlfs*. Without you, this thesis would not have been possible. Thanks for your guidance, the fruitful discussions on proteins and experiments and your proof reading. I really learned a lot from you. Even more I thank you for being a real friend!

Many thanks also go to *Prof. Dr. Angelika Noegel*, *PD Dr. Gernot Glöckner* and *Prof. Dr. Ludwig Eichinger* for sharing knowledge, work and lab equipment.

I also want to thank all lab colleagues for the great working environment with all sorts of help, support, motivation, fun and friendship. Special thanks to *Daniela Rieger*, who cared for me like for a son. I sincerely thank *Dr. Peter Kastner*, *Dr. Matthias Samereier*, *Dr. Nagendran Ramalingam*, *Dr. Petros Batsios*, *Dr. Dennis Zimmermann*, *Dr. Marija Vukajlovic*, *Dr. Annette Müller-Taubenberger*, *Linda Sanftenberg*, *Heike Roth*, *Süleyman Kösem*, *Gergana Gateva*, *Susanne Köhler*, *Thi-Hieu Ho*, *Maria Beer*, *Stefanie Lindholz*, *Gudrun Trommler* and *Marlis Fürbringer* for their scientific and moral support.

I thank *Dr. Penelope Strittmatter* for proof reading my thesis and for moral support.

Very special thanks go out to my sister *Dr. Julia Gallinger*. You've been my most precious colleague of the past few years. You are the reason why all this started and now gets finished. I owe you a lot! You are simply the best! Thank you!

I thank the Elite Network of Bavaria for generous support and providing the possibility to be an active part of the innovative graduate program 'Protein Dynamics in Health and Disease'. Thanks to all the members for the great time.

Finally, very special thanks go to my parents, who always supported me. Thanks for all your love, trust and patience throughout all the years. You are the best! Thank you!